

UiT – The Arctic University of Norway

Faculty of Science and Technology

Department of Geosciences

Morphological analysis of mass-transport deposits in Cenozoic sediments at the Southern Vøring Margin

Péter Béla Pálóczy

Master's Thesis in Geology [GEO-3900], August 2024



I. Foreword

First and foremost, I would like to offer my gratitude to my supervisor, Professor Stefan Bünz for his help, and immense patience.

From my first tentative request for advice throughout the entire long process, he aided my efforts with utmost commitment.

Furthermore, my heartfelt appreciation to the entire faculty of the Department of Geosciences at the University of Tromsø.

Without the work of these capable and dedicated people, I would not have arrived at this stage.

I would like to also offer recognition to the Student Welfare Organization of UiT, for helping to create a wonderful environment for our studies.

Last, but not least, I must thank my parents who have supported me all my life and all my friends, present and departed, for joining in on the fun(?) somewhere along the way.

Contents

I.	Foreword	2
II.	Introduction	5
III.	Background	8
1)	Geological Setting	8
A.	General Introduction to the Norwegian Continental Shelf.....	9
B.	North Sea.....	11
C.	Western Barents Sea	12
D.	Mid-Norwegian Margin	13
2)	Formative processes and associated features	18
A.	Submarine slope failures	18
B.	Polygonal faulting	28
IV.	Methodology	31
1)	Acquisition of WIN19M02	31
2)	Seismic processing	33
3)	Seismic interpretation.....	35
V.	Results	37
1)	HORIZON 03	39
A.	Horizon 03 – Offset: 50.....	42
B.	Horizon 03 – Offset:70.....	44
C.	Horizon 03 – Offset: 85.....	50
D.	Horizon 03 – Offset: 100.....	52
E.	Unit X.....	53
2)	HORIZON 02	54
A.	UNIT-2	56
B.	UNIT-3:	60
C.	UNIT 4	64
D.	UNIT 5	70
E.	UNIT X.....	76
3)	HORIZON 01 & SEAFLOOR	77
A.	UNIT 6	78
B.	SEAFLOOR	80
VI.	Discussion	81
1)	Lithostratigraphical boundaries in the study area	81
A.	Supplementary.....	84

2)	Identifying the slide deposits – fitting the characteristics	85
A.	Horizon 03-02	85
B.	Horizon 02-01	86
3)	Traits of chosen sedimentary structures	88
4)	Summary	92
VII.	Conclusion.....	96
VIII.	References	97
8)	Illustrations.....	99

II. Introduction

With the global population expanding at an accelerating rate, more and more people will inevitably inhabit coastal areas, and maybe eventually large-scale offshore settlements, if and when they become feasible.

This results in an increase in potential exposure to the risks associated with a life near, or at sea, for humans and infrastructure alike.

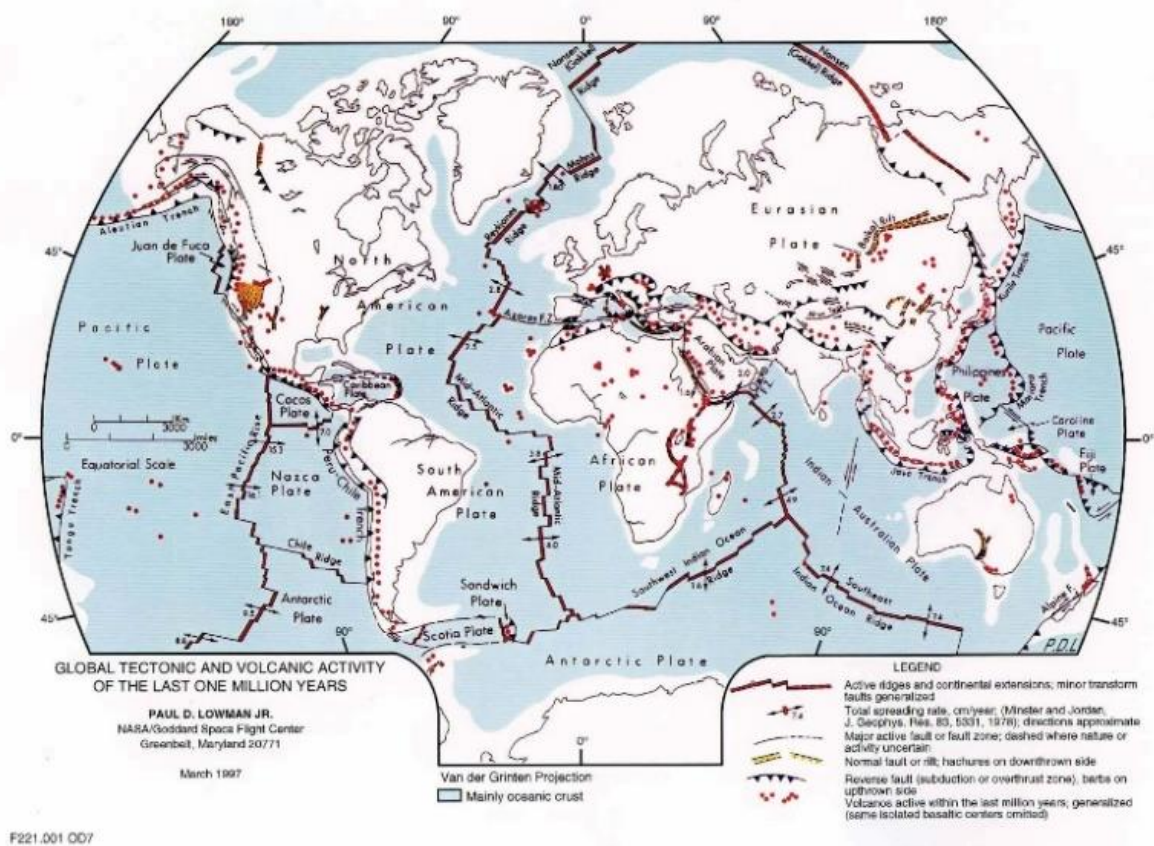


Figure II-1A global map of the major tectonic plate boundaries

For this reason marine architecture has been becoming the focus of ever increasing attention in recent decades and this tendency will almost certainly continue in the foreseeable future. (Mastrantonis and Dubininkas 2022)

For example, it is not an exaggeration to say that submarine internet cables are holding much of our modern world together, not to mention the economical and (and political, as recent world events illustrate) significance of hydrocarbon transport pipelines and offshore

extraction platforms – the growing prevalence of offshore wind farms also warrants a mention.

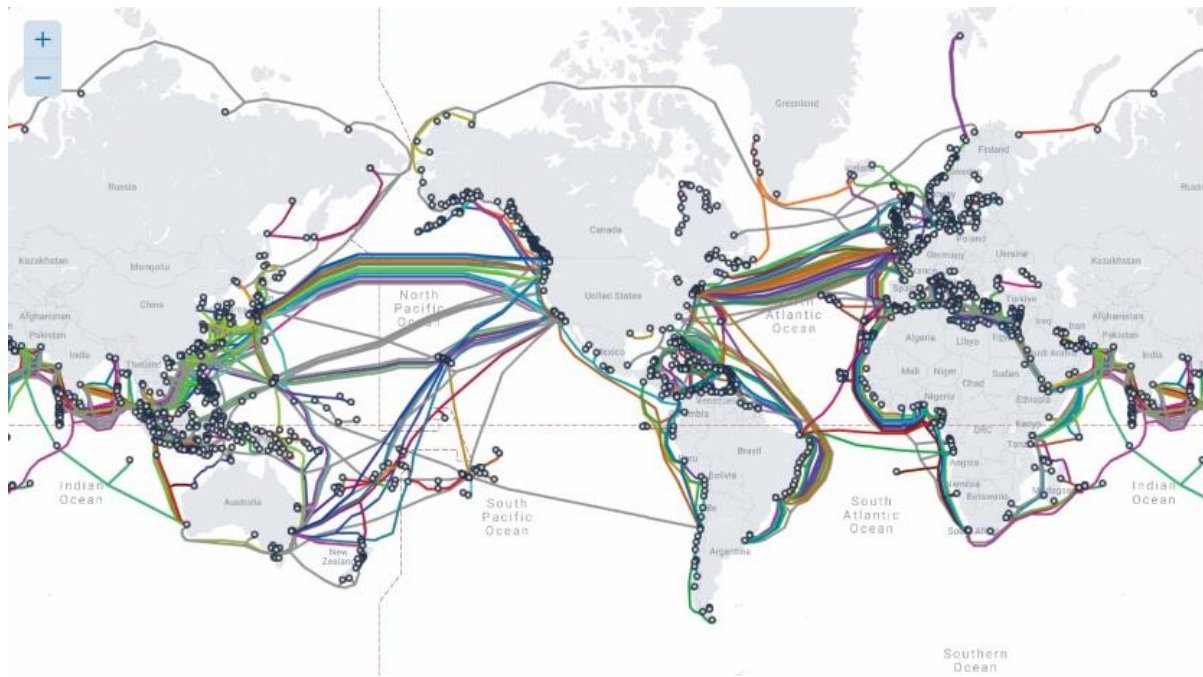


Figure II-2 Rough map of the submarine internet cables running across the seafloor

A comparison of *Figures II-1 and II-2* reveals that these cables must often travel through areas of instability, such as the Mid-Atlantic Ridge, or the eponymous Ring of Fire, and there are other risk factors that might not yet be a part of the collective consciousness, such as submarine landslides.

These events have been the cause of many local apocalypses throughout the history of our species, and before that.

A prerequisite of responsible development in such environments is the careful evaluation of the seafloor and what lies beneath, from the the littoral- through the neritic zone and all the way to the continental shelf.

The magnitude of the task and the intransigent nature of the former makes this a challenge, but a necessary one.

It is well known just how little of the seafloor has been mapped, less than a quarter of it globally, and science has only recently reached the double digits.

Even compared to that, the amount we have discovered of the subseafloor is woefully small.

The choice of topic was motivated by a desire to learn about marine geohazards, and this work focuses on a seismic dataset recorded from the southwestern Vøring margin in 2019, designated WIN19M02 – this specific study area was offered because preliminary inspection of the dataset revealed sediment masses that are probably originated from landslide events.

One of the cardinal methods for seeking out risks buried under the sea is the triptych of seismic data acquisition, -processing and -interpretation, in that order of progress.

The practical part of this thesis used the third, seismic interpretation via Schlumberger Limited's Petrel Subsurface Software package.

Based on (*Knut Bjørlykke, Jan Inge Faleide et al. 2015*), there is some debate over the compressional deformation in the sediments of the Vøring margin – such forces have been documented as a known influence in the local sediment record, but precise age and effect of these sequences have not yet been conclusively identified.

Initial examination of the seismic reflectors in the study area suggested signs of this phenomenon as well.

If the assumption is proven to be correct, ideally this thesis might also contribute to the broader discussion in some small way.

III. Background

This chapter will provide a brief record on the turbulent geohistory of the Vøring Marginal High and environs, with some details on the overall setting of the Norwegian Continental Shelf to establish a framework in which WIN19M02 might be placed.

The primary resource for the first subchapter of the thesis is a chapter of Petroleum Geoscience (*Knut Bjørlykke, Jan Inge Faleide et al. 2015*), unless specifically indicated otherwise.

Two preceding theses focusing on nearby locations were used as guidelines and for comparison.

The first, submitted by Runar Johansen in 2010, examined two seismic blocks, one of which partially overlaps *WIN19M02* on the west – this would be *SH0402* – and the second, larger block is located slightly to the northeast (*SH0701*).

The reason for this overlap is explained in Chapter IV. Methodology – 1) Acquisition of *WIN19M02*.

1) Geological Setting

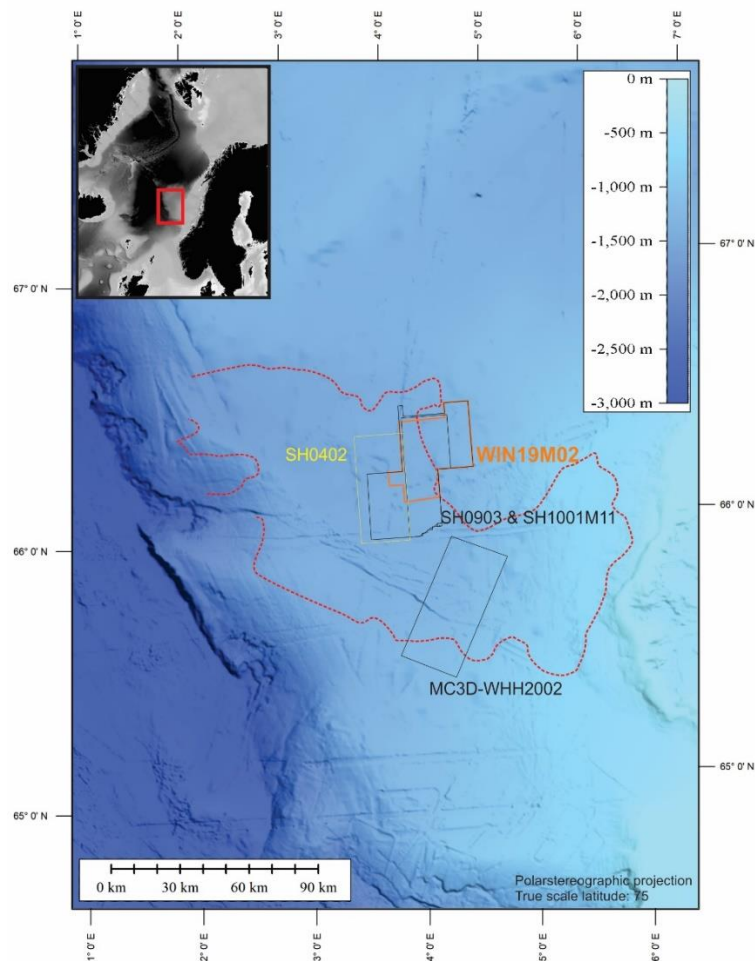


Figure III-1 Location of the study area in relation to Continental Norway and sites of previous studies

WIN19M02 is located between 66°N-66,5 °N and 4°E- and 5°E.

After measuring the dimensions of the the study area in Petrel, it has been is calculated as approximately 900 square kilometres in total (no precise measurement due to its irregular shape and angles, furthermore some sections were deemed unusable due to data acquisition errors and subsequently removed).

Similarly, taking two-way travel time values from two extreme ends of the block in the software, average water depth estimated to be 1300 metres (using an average seawater velocity of 1500 ms) and the general dip of the region is towards due west.

The seafloor surface appears relatively featureless, with only faint hints of notable relief, mostly in the west-northwestern portion – more on this in the „results” chapter.

(Knut Bjørlykke, Jan Inge Faleide et al. 2015)

The aforementioned overlap covers the western boundary of *WIN19M02* and a smaller half-rectangular extension of it further intruding westward into *SH0402*.

Following R. Johansen, for the next reference-thesis, Torgeir Fjellaksel’s chosen subject in 2012 was the seismic block *MC3D-WHH2002* slightly further to the south.

Figure III-1 shows the location of *WIN19M02* and other datasets mentioned above.

The dotted red line marks the run-off area of the Sklinnadjupet slide, an event from approximately 250.000 years ago. (Rise, Ottesen et al. 2006)

A. General Introduction to the Norwegian Continental Shelf

In the later stages of the continental breakup of Pangea, approximately 55 million years ago, what is today the Norwegian Continental Shelf was covered by a shallow epicontinental sea.

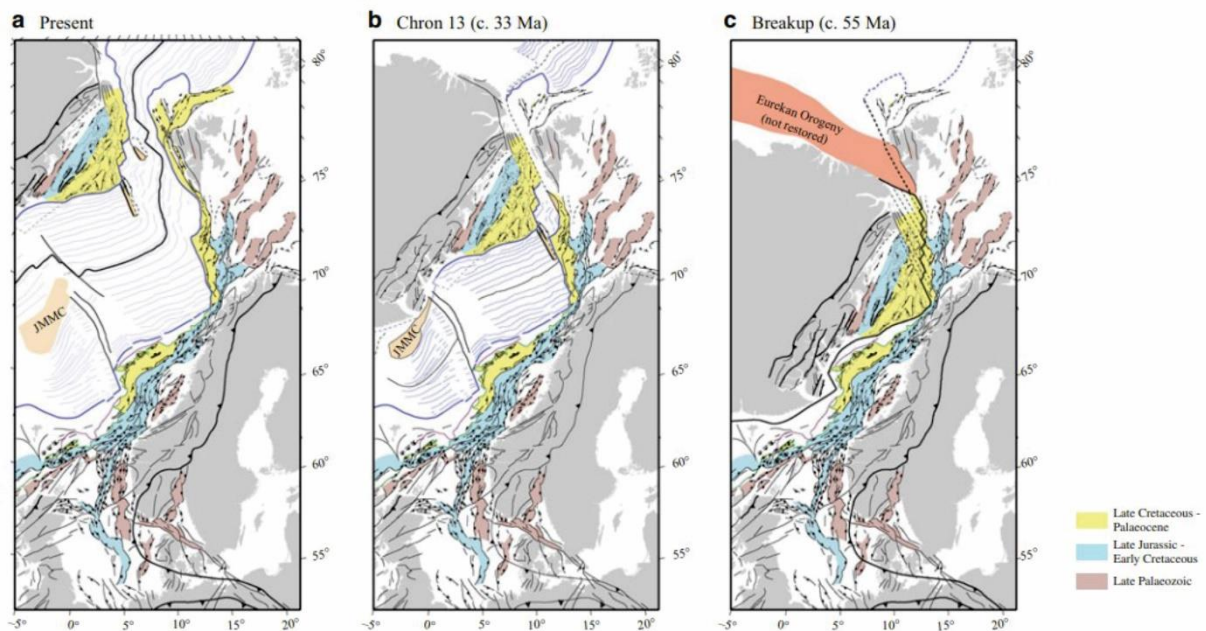


Figure III-2 Large-scale evolution of the Norwegian Continental Shelf

Through a series of rifting events, shown on *Figure III-2* above, the formerly connecting Greenland tectonic plate and the Eurasian plate spread apart in a roughly NW-SE direction; to a lesser extent, the Svalbard Platform also moved.

While the distance between the Svalbard archipelago and Fennoscandia didn't change significantly, the opening of the Norwegian-Greenland sea (separating Greenland and Fennoscandia) and the opening of the Eurasian Basin between Greenland and Svalbard happened almost simultaneously.

Today, the following three are the main provinces of the Norwegian Continental Margin, starting from the south:

- North Sea - roughly between 50°N by the french coastline, 60°N by the scottish shores, and also ~60°N at Norway.
- The Mid-Norwegian Margin – following the norwegian shoreline between 62-70°N
- The Western Barents Sea – further along the coast of Norway, then north to Svalbard (~70-82°N)

For the sake of thoroughness, introductions will be given for all three but for the purposes of this thesis only the Mid-Norwegian margin warrants detailed description – information on the North Sea and the Barents Sea will be provided using a single source.

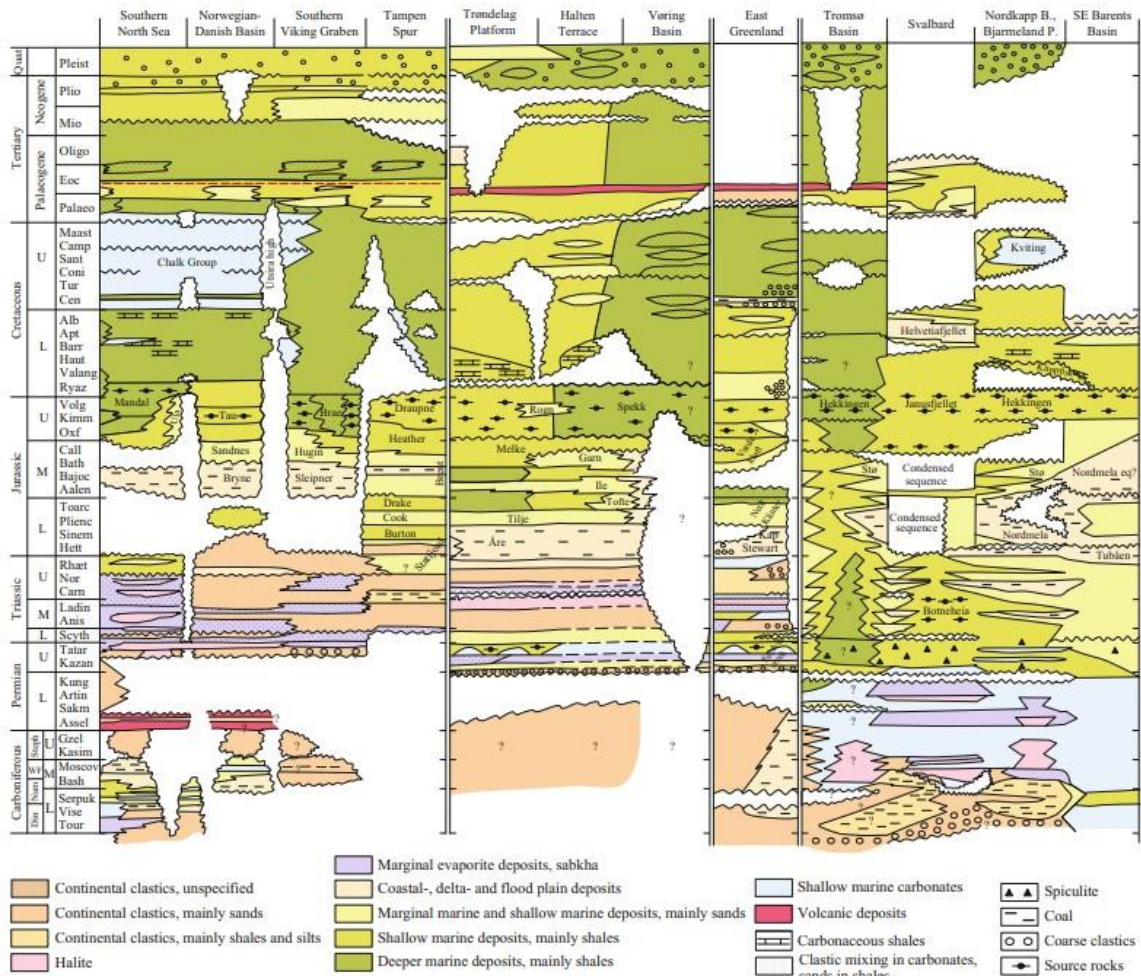


Figure III-3 Lithostratigraphy of the Norwegian Continental Shelf

(Knut Bjørlykke, Jan Inge Faleide et al. 2015)

B. North Sea

The North Sea is a sedimentary basin that formed through intermittent rifting-, stretching- and subsidence events, most of which happened during the Mesozoic.

It's development was guided by multiple persistent rifting events, and a number of uplifting- and subsidence episodes.

Multiple periods of volcanism also occurred.

In the sediment record, Triassic salts, carbonates and clastic rocks give way to Jurassic black shales and iron-rich sediments of fluvial origins.

The Cretaceous marks a reemergence of carbonates and the gradual cessation of hydrocarbon-formation.

In much of the Cenozoic, generally less-compacted shales and sandstones dominate and eventually, in recent times, glacial deposits started to become prevalent in intermittent sequences. (see Fig. III-3)

(Knut Bjørlykke, Jan Inge Faleide et al. 2015)

C. Western Barents Sea

The northernmost part of the Norwegian Continental Shelf is the Barents sea, specifically the western portion of it.

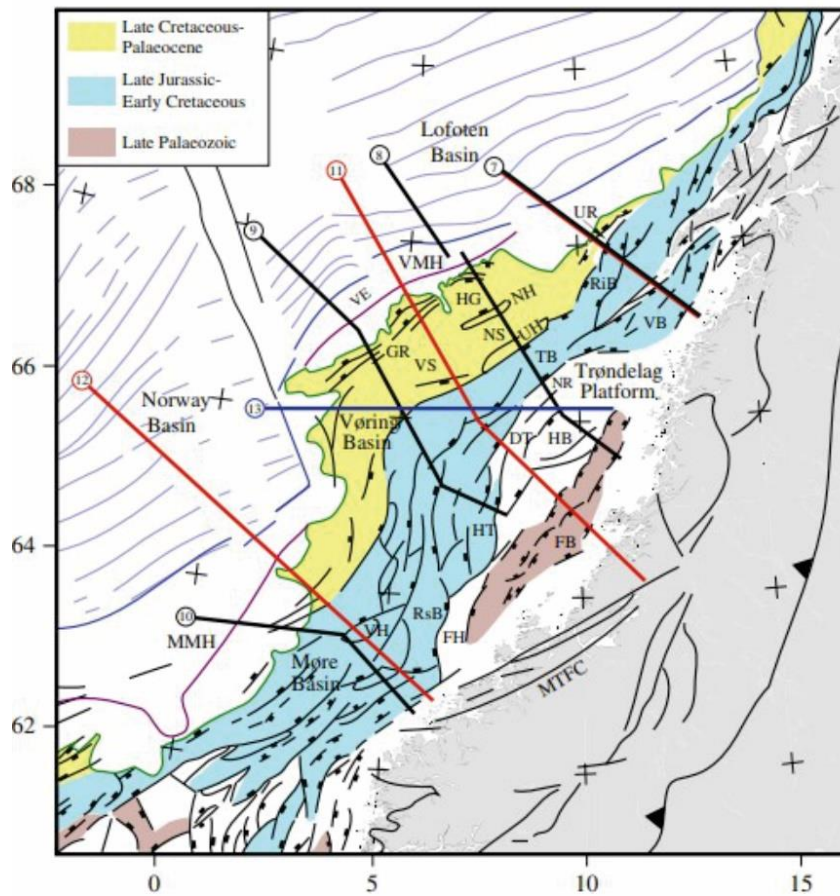
As mentioned at the beginning of this chapter, the sea originated from two major rifting events, and is located between the resultant passive margins.

Afterwards, tectonic activity and erosion were the main formative forces that have apparently eliminated a significant part of the sediment record.

Shales and sands are the most common, with significant amount of (mostly) Jurassic carbonates and fluvial deposits present, but some traces of volcanism can also be found. As everywhere else in the Norwegian Continental Shelf, the extant deposits of the Quaternary are glacial here as well.

(Knut Bjørlykke, Jan Inge Faleide et al. 2015)

D. Mid-Norwegian Margin



DT = Dønna Terrace, FB = Froan Basin, FH = Frøya High,
 GR = Gjallar Ridge, HT = Halten Terrace, HB = Helgeland Basin,
 HG = Hel Graben, MMH = Møre Marginal High,
 MTFC = Møre-Trøndelag Fault Complex, NH = Nyk High,
 NR = Nordland Ridge, NS = Någrind Syncline,
 RiB = Ribban Basin, RsB = Rås Basin, TB = Træna Basin,
 UH = Utgard High, UR = Utrøst Ridge, VE = Vøring Escarpment,
 VH = Vigra High, VB = Vestfjorden Basin,
 VMH = Vøring Marginal High, VS = Vigrid Syncline

Figure III-4 Elements of the Mid-Norwegian Margin

The central part of the Norwegian Continental margin is divided into three major units (starting from the south in sequence) – the Møre-, Vøring- and Lofoten-Vesterålen margins; forming the boundaries of the Vøring margin we find the Jan Mayen Fracture Zone to the south, and the Bivrost Fracture Zone to the north.

These components, and more are shown on *Figure III-4* above.

This thesis focuses on the seismic block designated WIN19M02, which was recorded of a submarine region near the Southwest termination of the Vøring Marginal High, just north-northeast of the Jan Mayen Fracture Zone/Jan Mayen Lineament.

The specifics of the region's evolution before the Late Permian are uncertain, but known to have been governed by rifting between Norway and Greenland. Signs of faulting can be seen in parts of the Trøndelag platform (southeastern boundary of the Vøring margin) until the Early Triassic which, in turn, gave way to subsidence and a major influx of sediments as a formative force during the Mid- and Late Triassic. In the Early to Mid-Jurassic, the sandstone-rich record suggests shallow marine conditions (see Fig. III-3) until the onset of an episode of the Atlantic rifting caused a significant change in environment – the Møre- and Vøring-basins formed of tectonic forces linked to this sequence of events (crustal extension and -thinning and subsidence). (Knut Bjørlykke, Jan Inge Faleide et al. 2015)

Naturally, the development of these depressions did not happen uniformly – the seafloor was distorted by internal forces and created a highly varied relief resulting in multiple internal sub-basins.(Johansen 2010)

Both the Møre- and Vøring-basin filled up relatively quickly and have subsequently been covered by clastics of varying fraction sizes.

The earlier rifting episodes created an exceptionally fragile geological environment which led to powerful brittle faulting during the late Cretaceous. This rifting event lasted well into the Palaeocene and is documented from the sothern Vigrid Syncline, a subregion of the Vøring margin located just NE of *WIN19M02*. The record of this time is characterized by lava deposits, with some terrigenous sediment from the west also. (see Fig. III-3)

The subsequent development of the Mid-Norwegian Margin would remain quite violent for a time.

Although the tectonic plates would continue to diverge to this day, Greenland and Eurasia completely separated during the Palaeocene-Eocene transition. This came about amidst intense tectonic activity and magmatism and a large number of lava intrusions mark this episode in the material of the Northeast-Atlantic margin. Those of the Møre- and Vøring-basins are no exceptions. (Possibly associated sills and vent structures can be seen on the seismic data from *WIN19M02*, but this points beyond the scope of this thesis).

Following this period the margin became passive in the middle Eocene, and the region has been affected by multiple smaller subsidence events. (Knut Bjørlykke, Jan Inge Faleide et al. 2015)

Seafloor development was governed by deposition from bottom currents and the sediment record from this time shows contourites which, although not exactly dominating, would remain prevalent throughout the Oligocene and the Miocene, until the ocean current patterns were altered (Fjellaksel 2012) as a consequence of the Fram Strait's opening, and the Greenland-Scotland Ridge's subsiding. (Johansen 2010)

These deposits have also been strongly affected by compressional forces in the Vøring basin. The Late Eocene uplifting of Fennoscandia was felt in this region as well and terrigenous muds cover the area by the Late Miocene, with glacial material gaining prominence in the Pliocene-Pleistocene. (Knut Bjørlykke, Jan Inge Faleide et al. 2015)

Ice sheet oscillations transported massive amounts of sediment from the terrestrial areas to the west all the way to the edge of the continental shelf. (see Fig. III-3)

The ice also heavily scarred the seafloor, carving sizeable troughs signifying differential ice

velocities. (Fjellaksel 2012)

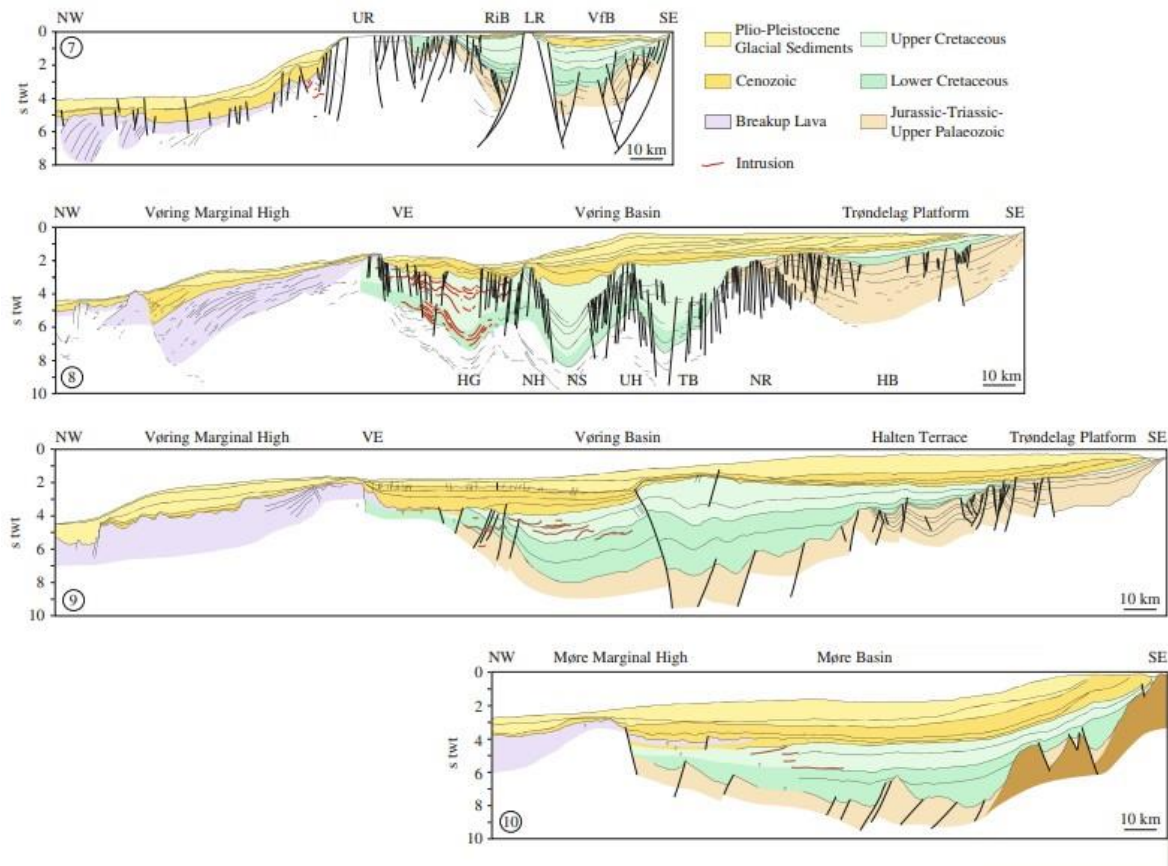


Figure III-5 Selected sedimentary profiles from the region

Figure III-5 above shows four cross-sections of the Mid-Norwegian Margin. The sections correspond to the numbered black lines on Figure III-4.

With the exception of Profile 9, all of them start at near-shore areas; number „7” runs between Vestfjorden Basin and the Utrøst High and terminates in the Lofoten basin, the longer, but interrupted „8” between the Nordland Ridge and the Helgeland basin through the Hel graben into once again, the Lofoten basin, „9” starts by the outer boundary of the Trøndelag platform, passing through the Halten terrace and then the Gjallar ridge and beyond, and finally, profile „10” again begins near-shore, cutting through the Møre basin, and heading almost due west across the Møre Marginal High.

a) Lithostratigraphy

In the subchapter „Development of the Vøring Margin” above, multiple shifts in sedimentation patterns and conditions during the Cenozoic were briefly mentioned. Based on data from the website of the Norwegian Offshore directorate, the closest location where cores have been recovered from is Wellbore 6604/10-1 at the time of writing this thesis. WIN19M02 itself has not yet been directly sampled at this time. 6604/10-1 is a now plugged and abandoned, wildcat exploratory well from the early 2010s which has a total depth of 3715 metres below the seafloor. Depth data from this well shows the RKB depths of the Brygge FM. from 2075 metres, the Kai FM. from 1578 metres and the Naust FM. from 1385 metres. (*source: Factpages*) Once again, the theses of R. Johansen and T. Fjellaksel were also used as references, along with the noted articles. There is also a fourth significant sequence in the region called the Molo formation that has been deposited close to concurrently with the Kai formation, but it is present only near the eastern boundary of the Vøring margin, far from *WIN19M02*.

Brygge Formation

The earliest constituents of the Brygge formation were deposited in the early Eocene, approximately 55 million years ago, and it has continued to develop over the next 37 million years. (Chand, Rise et al. 2011)

The oldest sediments are defined by sands, some from terrestrial sources from before the opening of the Norwegian-Greenland Sea, and later from shallow marine environments. As the opening progressed further, these gave way to biogenic oozes composed mostly of fine-grained silica. (Johansen 2010) & (Chand, Rise et al. 2011)

There are regional differences in the formation, but at the Vøring Margin these deposits formed clays and are host to polygonal faulting.

Compressional forces created large-scale deformation, which formed the Modgunn- and Helling-Hansen Arches, and also resulted in a hiatus in the mid-Miocene. (Chand, Rise et al. 2011)

Kai formation

Above the mid-Miocene unconformity, the sediments of the Vøring basin dated to the Oligocen-early Pliocene (14-4 million years ago) (Johansen 2010) are a mixture of calcareous and siliceous oozes from indicating deep marine conditions with some shales present. (Chand, Rise et al. 2011)

The previously mentioned two arches are surrounded by contourites (Chand, Rise et al. 2011) and their presence and patterns of deposition point to shifting ocean currents. (Fjellaksel 2012) & (Chand, Rise et al. 2011)

Similarly to the Brygge formation, polygonal faulting has also been described in the sediments of the Kai formation. (Chand, Rise et al. 2011)

NAUST formation

During the last ~2.8 million years, the average rate of sedimentation was approximately 25 centimetres every thousand years, which is considerably faster than either Brygge- or Kai-times.

At certain areas, this adds up to a thickness of over 1000 metres.

To reference Chapter III – 1/D, this increase is owed largely to the glaciation events of this period, and an uplift of Scandinavia.

The sediments of this time also show evidence of having been locally reworked by multiple mass-transport events.

The formation shows a westward-thinning tendency, and has been dated using biostratigraphic correlation.

The name „Naust” is an acronym, which stand for the five subunits making up the formation – these, in a decreasing sequence of age (and depth) are N, A, U, S, and T.

- Naust N: Approximately 2.8-1.5 million years old wedge-formed massive deposits extend westward mainly by gravity currents and mass transport. Naust N's deposition was affected by bottom currents and slide scars and craters have been documented.
- Naust A: Dated ~1.5-0.8 Ma, continuing the westward progradation. Its material and deposition is mostly analogous to that of Naust N, but stratified sediments occur locally. Some of the material may have originated from glacial debris flows.
- Naust U: The age of Naust U ranges ~0.8-0.4 Ma, characterised by glacial debris and its largest thickness is approximately 500 metres, although locally it has been completely removed by a mass wasting event. In parts of the region, the topography was altered and massive sediment units formed, one of which has an acoustic signature resembling that of slide deposits but no related slide scar has been found.
- Naust S: Between 0.4-0.2 million years ago, the westerly progradation reached its largest extent, built largely by glacial debris. (Rise, Chand et al. 2010) At the end of the Elsterian glaciation, earthquakes may have resulted from isostatic rebound leading to the initiation of the Sklinnadjupet slide, significantly reworking the massive sediments. (Rise, Ottesen et al. 2006) Following this event, the remainder of Naust S time is characterised by hemipelagic stratified sediments, with some contourite-filled craters.
- Naust T: In the last 0.2 million years the hemipelagic deposits remain most prominent, along with two massive glacial deposits of the Saalian and Weichselian glaciations. The material is a combination of glacial and glacial marine deposit and stratified, fine-grained sediment.

(Rise, Chand et al. 2010)

2) Formative processes and associated features

This subchapter will give a brief description of the geological processes dominating the upper layers of WIN19M02.

In addition to landslide deposits, some explanation will be given for kinematic indicators – sedimentary structures whose properties indicate the general progress of a mass transport complex.

Preliminary observation also revealed two polygonal faulting zones, one of which has considerably influenced much of the sediments this thesis focuses on.

Massive fluid flow expressions are visible in the dataset, but only at greater depths which fall beyond the scope of this thesis.

A. Submarine slope failures

The term „slope failure” refers to the rapid displacement of sediments settled on an angled surface.

After the initial failure, the material is transported through gravity-driven processes. (Shanmugam 2018)

Although terrestrial mass wasting has been a near constant companion of our species, similar events occurring in a marine environment are less familiar.

In fact, they have never been observed as they occur, and their studies are largely based on how they affect seafloor- and subseafloor development. (Piper, Mosher et al. 2012)

This is done through direct observation, (which is limited by the water mass), velocity calculations with remote sensing methods such as seismic measurements and sometimes by drilling, but sample recovery from submarine sediment deposits is a difficult and costly endeavour. (Shanmugam 2018)

Numerical- and practical modeling methods are also utilised, and understanding terrestrial analogues is a good foundation for research.

We know now that they can happen often on the slopes of the seafloor and everywhere there is tectonic activity.

The different types of mass movement processes are the same on the continent as in the water. A detailed list will be provided later on.

The two environments also show some differences, however: undersea sedimentation generally affects large areas in contrast to the more „guided” terrestrial equivalent which causes less compaction, and also that significant amounts of water might be incorporated in the slope failure material, meaning a less dense load, and thus vastly longer run-off distances. (Piper, Mosher et al. 2012)

Two different classification are used for slope failures: velocity-based terms and mechanics-based terms.

Since there is no precise way to measure the moving speed of already settled deposits in the sediment record, and it hasn't yet been established what qualifies as „fast” or „slow” when it comes to sediment masses, the first type can be somewhat arbitrary.

Velocity-based terms:

Free-falling: rock fall

Fast-moving: flow slide, rock slide, debris avalanche, mud flow and sturzstorm

Slow-moving: debris slide and creep

In the mechanics-based classification, we differentiate between mass transport and sediment flow (with further divisions based on the material and the characteristic of movement, seen on *Table 1*, just below).

A classification of subaqueous gravity-driven processes

Major type	Nature of moving material	Nature of movement	Sediment concentration (vol.%)	Fluid rheology and flow state	Depositional process
Mass transport (also known as mass movement, mass wasting, or landslide)	Coherent mass without internal deformation	Translational motion between stable ground and moving mass	Not applicable	Not applicable	Slide
	Coherent mass with internal deformation	Rotational motion between stable ground and moving mass			Slump
Sediment flow (in cases, mass transport)	Incoherent body (sediment-water slurry)	Movement of sediment-water slurry <i>en masse</i>	High (25–95)	Plastic rheology and laminar state	Debris flow (mass flow)
Sediment flow	Incoherent body (water-supported particles in suspension)	Movement of individual particles within the flow	Low (1 – 23)	Newtonian rheology and turbulent state	Turbidity current

Table 1 The properties differentiating mass transport processes

Mass transport might mean to any type of gravity-driven movement of sediments, and can happen in any environment, whereas sediment flow in this case refers only to slope failures where significant amount of water is mixed in the displaced material, as shown on *Figure III-6*. (Shanmugam 2018)

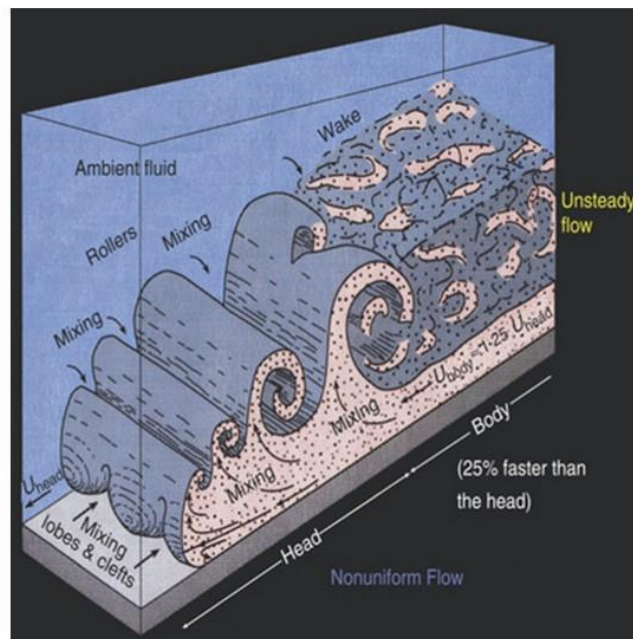


Figure III-6 Water mixing into a turbidity current

The different types of submarine mass wasting processes deserve a more detailed description:

- Creep: when stratified sediments lose cohesion between layers and the separated mass travels downslope (over the glide plane) in an unbroken unit. As mentioned above, the movement is slow, and there is no significant fragmentation.
- Rock- or debris falls: hardened material from a vertical, or near-vertical slope loses support and detaches from the surface. The blocks travel in free-fall, and accumulate at the base – major fragmentation may occur from the impact, but larger fractions are prevalent. (Gravels or even solitary boulders)
- Debris- or rock avalanches: the amount of displaced material is considerably higher, but the process is almost identical to rock falls. The difference in quantity means more opportunities for collisions, which causes the debris to fragment further. Settles as breccias and conglomerates. (Piper et al. mentions a „jigsaw texture” in one such deposit).
- Slides and slumps: similar to creep, but at higher velocities. These processes are largely the same, but are differentiated based on the ratio physical dimensions of the displaced mass (depth of the landslide times the inverse of total length) – these characteristics translate into the texture of the resultant deposits. A higher value (slumps) indicates the presence of larger, intact fractions.
 - o Debris flows: if the internal structure of slide- or slump deposits is notably deformed.

(Piper, Mosher et al. 2012)

It is difficult to measure the likelihood of a collapse, but sometimes a slope is only stable through a very delicate balance of physical properties and there are a number of external forces that may easily cause, or contribute to a sudden loss of equilibrium.

Potential triggers for mass wasting events:

- Earthquakes: The subsurface movements caused by earthquakes can increase the shear stress
- Oversteepening (tectonic or depositional): altering the angle of a slope may lead to increased stress affecting the slope’s support
- Sediment loading (depositional, hydrostatic or glacial): increase in the overlying mass will likewise heighten stress
- Tsunamis and tropical cyclones: rapid movement in the water column may damage and destabilise the slope
- Submarine volcanism: see both „Earthquakes” and „Tsunamis and tropical cyclones”
- Salt movements, biological erosion and gas hydrate decomposition: Processes that introduce or alter the underlying material or the structure of the slope itself might also cause a collapse

(Shanmugam 2018)

To facilitate the mapping of mass-wasting events, it is necessary to distinguish between areas of the mass-wasting event and parts of the resultant deposits. This becomes important in later sections of this thesis. Three different regions can be established with the central region further subdivided:

Headwall domain – the upslope boundary of the slope failure

Translational domain – the main body of the mass-transport complex

Lateral margins – along-slope boundaries of the wasting event

Basal shear surface – detachment surface formerly underlying the slide material

Internal translational domain – the settled material of the slope failure

Top slide surface – self-explanatory, the surface of the slide material

Toe domain – downslope termination area

(Bull, Cartwright et al. 2009)

It was deemed prudent to showcase the appearance of a sediment mass deposited by a mass wasting event on seismic data for later comparison.

The following seismic section was taken from (Bull, Cartwright et al. 2009) and shows a boundary of the Storegga Slide – submarine mass wasting complexes are characterised by generally low-very low amplitude material and high frequency discontinuous internal reflections.

Local deviations might occur as some larger blocks might not have been destroyed during transport.

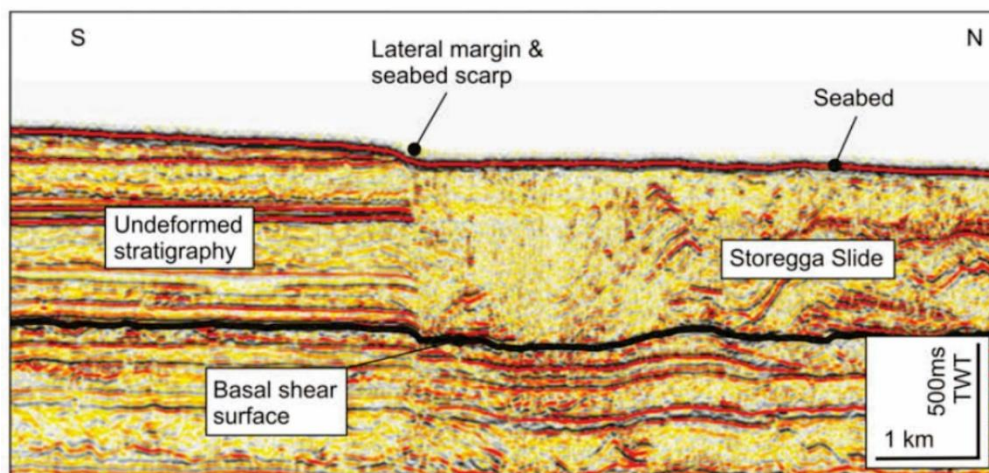


Figure III-7 The sharp divide between Storegga material and the adjacent, unreworked sediment

(Bull, Cartwright et al. 2009)

a) Sklinnadjupet slide

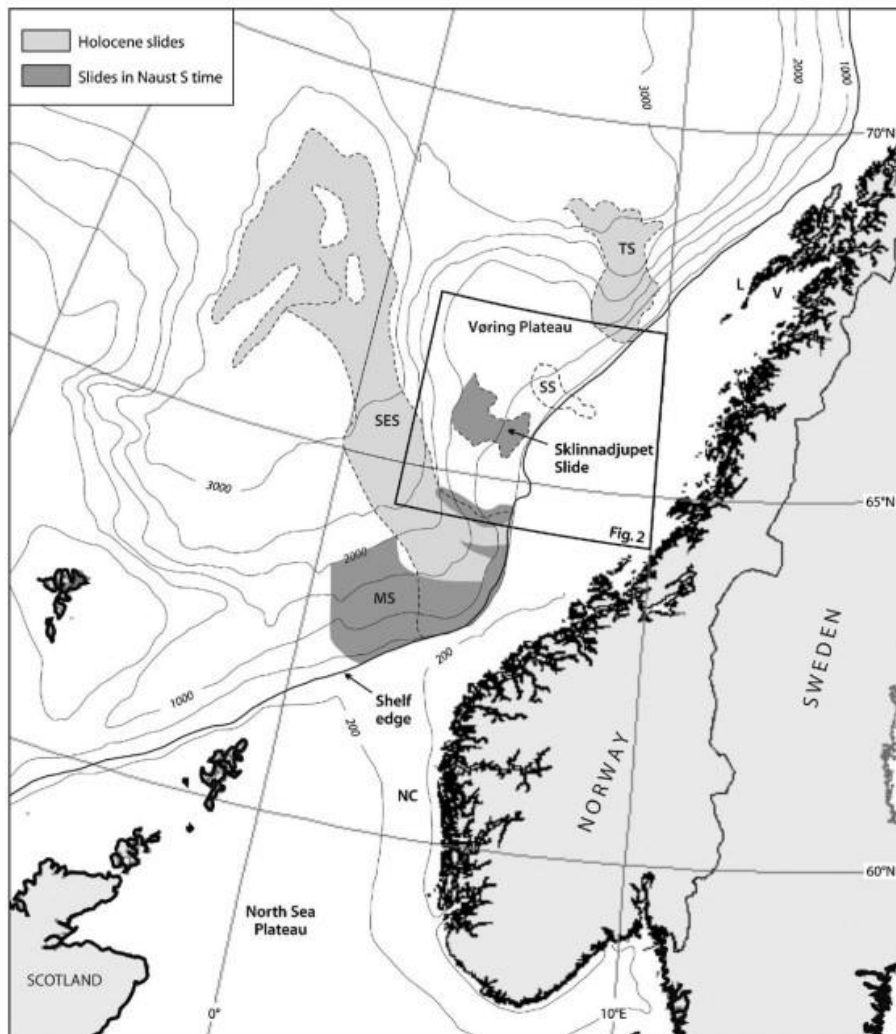


Figure III-8 Map of the Mid-Norwegian Margin with the location of catastrophic submarine slope failures indicated

As mentioned in the previous chapter, the Mid-Norwegian Margin is host to a number of submarine slope failures, large and small (some are shown above on Fig. III-7, but one of the major events has probably played a direct role in the evolution of the study area.

As shown previously on Figure III-1, over half of WIN19M02 lies inside the run-off area of the Sklinnadjupet slide.

The headwall is approximately 90 kilometres wide, and located west of the Trøndelag platform. (Rise, Ottesen et al. 2006)

Starting roughly 500.000 years ago, in „NAUST S”, time, a period of high sedimentation affected the region stemming from an uplift of Scandinavia, and the processes

of the Elsterian glaciation.

The slide material was originally settled in a horn-shaped depression between the Træna- and Halten terraces, called the Sklinnadjupet palaeo-trough. (Fjellaksel 2012)

From this basin the sediments moved westward through gravitational transport, and built a fan-shaped structure beyond the current shelf edge.

The angle of sedimentation was near-horizontal until the Helland-Hansen Arch but as deposition continued, the excess material „grew over” the anticline and subsequently settled on the western slope of the arch, at a much steeper angle.

Original slope angle in the palaeo-trough is estimated to have been 0.5°, which should have been stable, under ideal conditions – the eventual collapse of the slope can be attributed to a combination of factors.

First, the rapid accumulation of sediments (*depositional sediment loading*) caused a build-up of pore pressure in the palaeo-trough (vertical fluid flow is hypothesised to have also contributed to the increase).

Based on borehole-data gathered from nearby sites, the „NAUST S”-material is clayey, with some silt and sand mixed in intermittently, and a small amount of larger fractions.

Overall, this blend has low permeability, leading to a slow dissipation of excess pore pressure. Additionally, the structure of the Helland-Hansen Arch that bolstered much of the sediment mass, changed suddenly; the previously mentioned fluid-flow processes most likely led to the rapid evacuation of built-up gas, forming several craters and further destabilising the slope.

An earthquake (which were relatively common in the region) may have then caused the initial slide, which was followed by a series of smaller failures of the now unsupported material.

Figure III-9 on the following page is a simplified illustration of the main stages of the landslide.

There is a sediment mass referred to as the Vigrid slide, which may be either a part of the Sklinnadjupet slide, or the deposits of a separate, younger event. (Fjellaksel 2012)

Two of the nearest major mass wasting events were the Trænadjupet Slide at the northern boundary of the Vøring Plateau, and the Storegga Slide to the south – probably neither affecting the study area as their run-off areas are at lower depths.

Another smaller, nearby event was the Stratagem Slide from the Pleistocene, before the Sklinnadjupet Slide, and its run-off area is projected to terminate well before reaching WIN19M02.

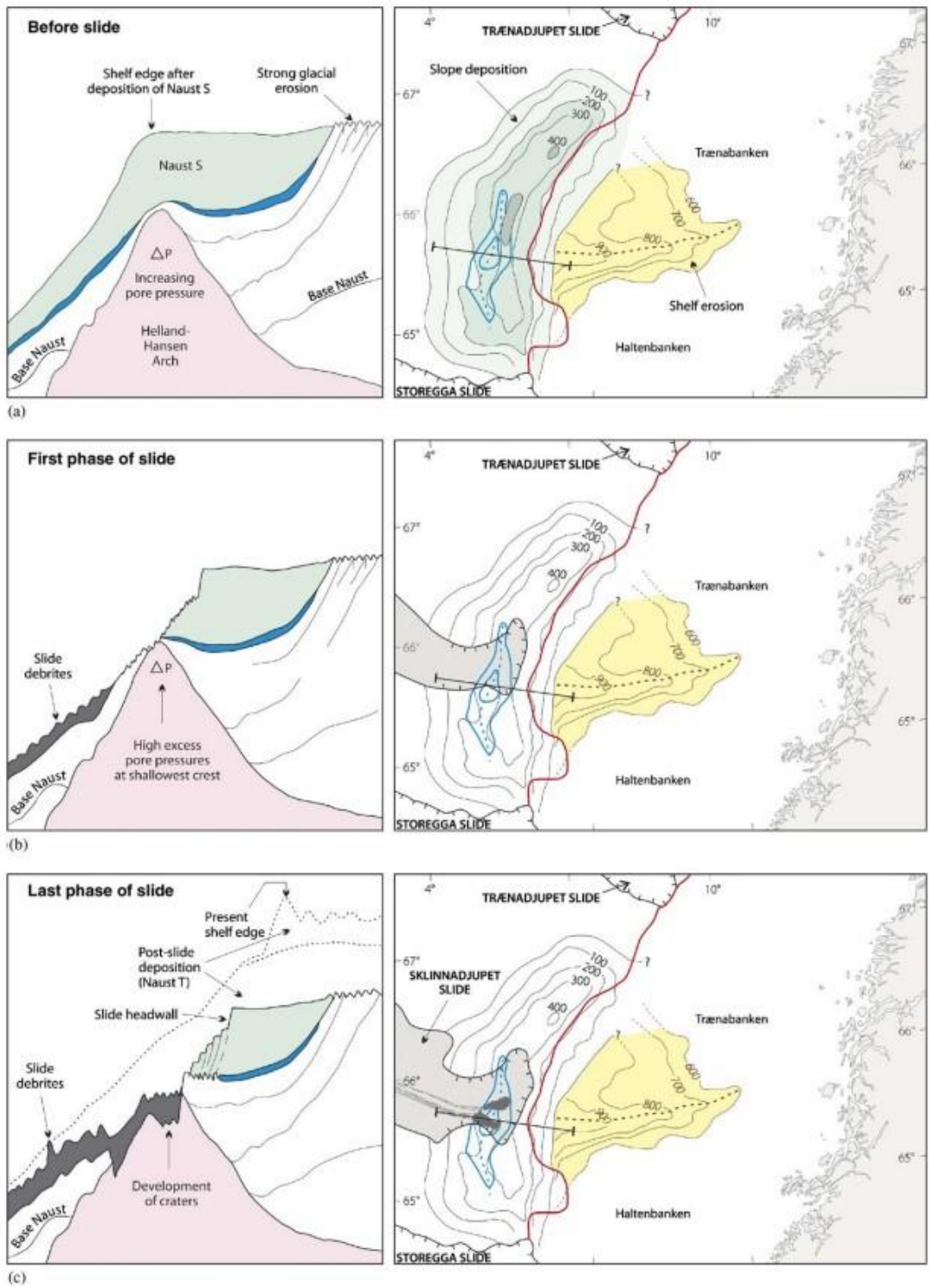


Figure III-9 Main stages of the Sklinnadjupet Slide

(Rise, Ottesen et al. 2006)

b) *Kinematic Indicators*

Studies of submarine mass-transport complexes (*abbr:MTCs*) have revealed that certain similar features often appear in the sediment.

These structures and patterns may be used to define a mass in motion with respect to the characteristics of both the movement and the material as well.

Collectively, the features that mark these attributes are called kinematic indicators.

Three-dimensional seismic surveys have found benefit in using them for mapping mass wasting events, and their history from mass-wasting event to eventual settling.

The final morphology (both internal and then-surface) of a MTC is influenced by topography, rheology of the displaced material and the method of initiation for mass wasting (see Chapter III. „Background”, subchapter 2/A).

A wide range of different deformation patterns belong under the umbrella of kinematic indicators.

Considering their diversity, Bull et al. (2009) categorised them based on their location in the mass-transport complex.

The diagram taken from the same article and shown below provides a good overview of the defining characteristics (*see Figure III-10*).

As this subchapter is only meant as a short introduction to the topic, only short definitions will be added to *Fig. III-10*.

For definitions of the domains, see Chapter III. Subchapter 2/A.

Headwall domain:

- *Headwall scarps* – typically arced, vertical to near-vertical detachment surfaces; may be singular, or a series of scarps in case of a sequential failure; may reveal the initial direction of the sliding
- *Extensional ridges and blocks* – generally, not all of the slide material is evacuated from the the headwall area; coherent, possible distorted objects initially aligned with the headwall scarp

Translational domain:

Lateral margins – the margins may or may not connect the headwall to the toe domain, but they often lose prominence with distance from the former; may show signs of transpression or transtension; if identified, they often show on seismic data as linear feature parallel to the direction of sliding

Basal shear surface:

- *Ramps and flats* – the base of the slide shifting vertically into a new stratigraphic level; usually, but not exclusively near-perpendicular to sliding direction
- *Grooves and striations* – long, linear incisions typically progressing downslope, caused by larger blocks of debris travelling in front, or inside the main body of the sliding material, damaging the shear surface
- *Other basal shear surface features* – all other types of deformations on the detachment surface

Internal translational domain (these features may or may not affect the „outside” appearance of the slide deposit):

- *Blocks (translated, outrunner and remnant)* – comparatively large objects transported within, or ahead of the sliding material OR, in the case of *remnant blocks*, masses inside the slide deposit that have resisted the wasting event
- *Slump folds* – folding in a failed mass seems to correspond with the magnitude of translation, and is affected by paeoslope angle and the direction of slide movement

Top slide surface (all kinematic indicators listed belonging to the translational domain may potentially express on the top surface of a slide):

- *Longitudinal shear zones* – downslope-trending, often paired continuous linear features formed by differential velocities inside the transported material; seismic data shows these zones as small scarps atop the slide deposit
- *Second order flow fabrics* – while the material of longitudinal shear zones have sufficient velocity/mass to form continuous structures, other sections of the top slide surface are incapable to remove or destroy „obstacles”, and their patterns of deposition are strongly affected by base topography, or other features such as the previously mentioned *remnant blocks*

Toe domain:

- *Pressure ridges* – Generally fan-shaped and aligned perpendicular to the direction of transport, created by the greatest downward pressure from the weight of the mass-transport complex; ideally, these structures form at the distal boundaries, but they can occur anywhere where the further downslope movement of the failed mass is blocked;
- *Thrust and fold system* – usually extensive structures present in the toe domain from lower to upper boundary of the slide deposit; they show up on seismic data as large, coherent blocks subjected to folding and thrust, situated in heavily disorganised material

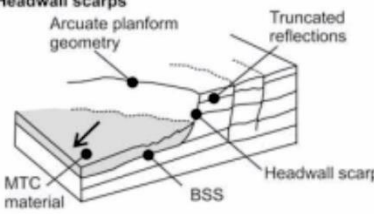
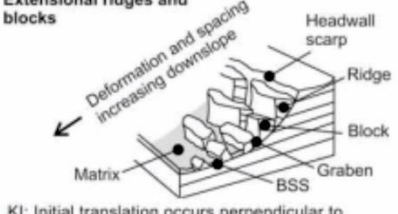
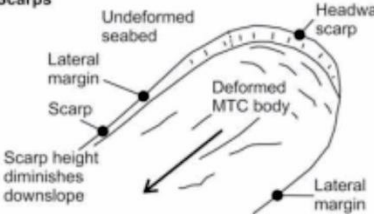
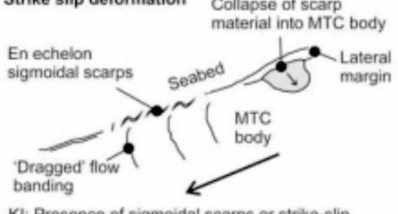
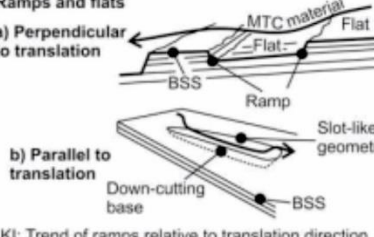
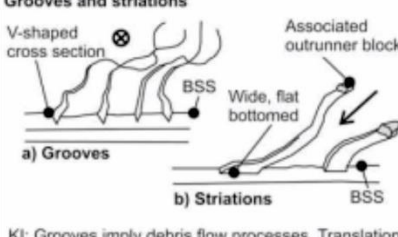
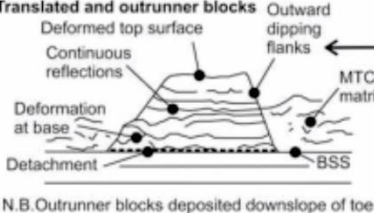
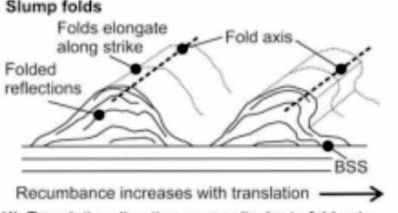
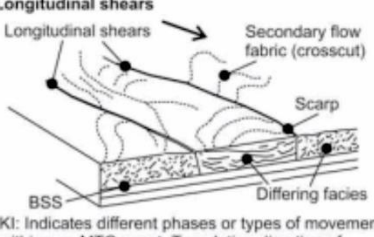
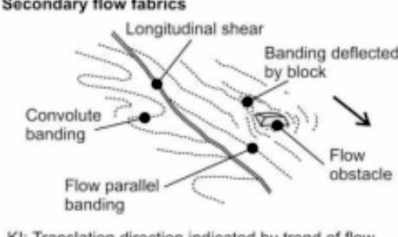
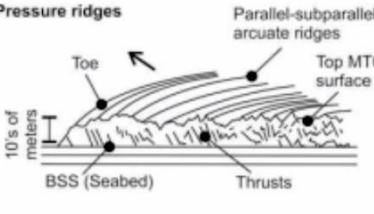
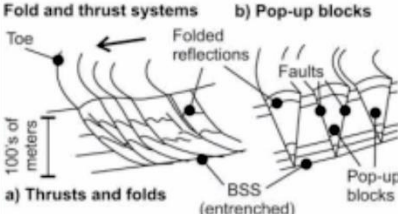
Headwall domain	<p>Headwall scarps</p>  <p>KI: Direction of initial movement roughly perpendicular to headwall propagation</p>	<p>Extensional ridges and blocks</p>  <p>KI: Initial translation occurs perpendicular to headwall scarp. Blocks may re-align to be parallel to transport direction.</p>
Lateral margins	<p>Scarps</p>  <p>KI: Delimits strike-parallel extent of MTC and constrains gross general transport direction.</p>	<p>Strike slip deformation</p>  <p>KI: Presence of sigmoidal scarps or strike-slip affected MTC material differentiates lateral margin from headwall scarp.</p>
Basal shear surface	<p>Ramps and flats</p>  <p>KI: Trend of ramps relative to translation direction must be confirmed by evaluation of other indicators</p>	<p>Grooves and striations</p>  <p>KI: Grooves imply debris flow processes. Translation direction is parallel to trend of grooves and striations</p>
Internal MTC body	<p>Translated and outrunner blocks</p>  <p>N.B. Outrunner blocks deposited downslope of toe KI: General translation direction provided by path of blocks. Blocks often align long-axis downslope.</p>	<p>Slump folds</p>  <p>Recumbance increases with translation KI: Translation direction perpendicular to fold axis. Indicates plastic deformation. Fold attitude can assist in constraint of translation.</p>
Top slide surface	<p>Longitudinal shears</p>  <p>KI: Indicates different phases or types of movement within one MTC event. Translation direction of material within shears constrained by their trend</p>	<p>Secondary flow fabrics</p>  <p>KI: Translation direction indicated by trend of flow parallel banding</p>
Toe domain	<p>Pressure ridges</p>  <p>KI: Translation perpendicular to alignment of ridges.</p>	<p>Fold and thrust systems b) Pop-up blocks</p>  <p>KI: Translation perpendicular to strike of thrust faults or faults defining pop-up blocks.</p>

Figure III-10 An introduction to kinematic indicators and their defining traits

B. Polygonal faulting

This type of brittle deformation is named after the polygonal pattern displayed by a network of layer-bound fractures that can develop in fine-grained (clay-grade) sediments. Polygonal faulting has only been definitively identified during the 1990s after methods for acquiring and analysing three-dimensional seismic data were developed. (Cartwright 2011)

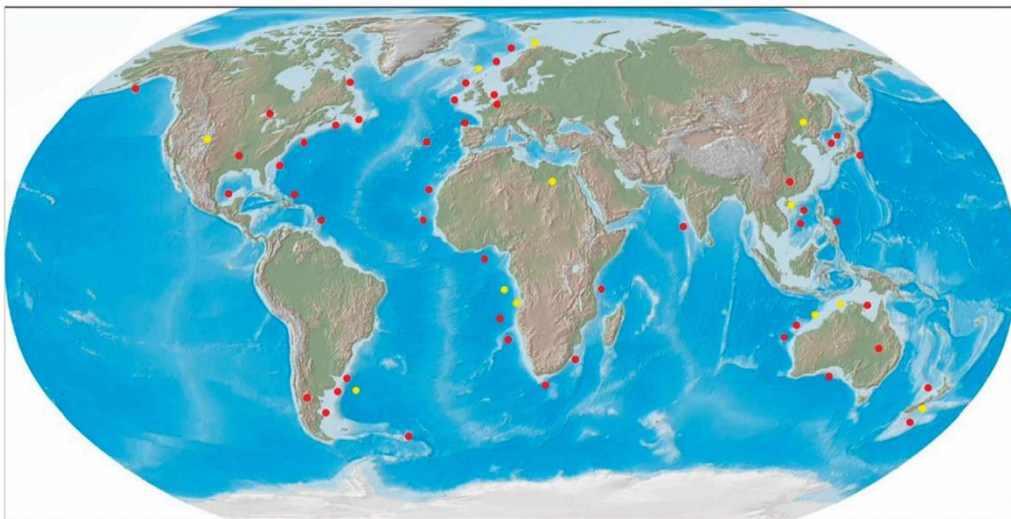
Component faults in a polygonal faulting zone (henceforth: PFZ) are defined by the following characteristics:

- Fault throw ranges between 10-50 metres
- Fault displacement typically under 100 metres
- Dip angles usually range between 40-70 degrees
- Lateral extent usually under 1500 metres
- **Strikes are multi-directional!**

(Xia, Yang et al. 2022)

As of 2022, instances of these features have been described at more than a 100 locations, mostly in sedimentary basins along continental margins, (Xia, Yang et al. 2022) but a number of them have been found in abyssal basins, and a few in foreland- and intracratonic basins as well, but these are rare. (Cartwright 2011)

The map of *Figure III-11* shows how the major known locations are distributed worldwide.



Global distribution of the polygonal faults discovered all over the world (modified after Cartwright, 2011). In this study PF occurrences discovered after 2010 (yellow dots) are added which is a supplement of previous compilation (red dots; Cartwright, 2011).

Figure III-11 Polygonal faulting zones as of 2022

Only normal faulting has been documented in these zones, and the individual fractures are typically layer-bound, forming in so-called „tiers” of varying thickness. Fault geometry appears to correspond to the thickness of tiers, and also to relative distance to current seafloor.

All PFZs described so far cover a significant portion of their hosting basins. (Cartwright 2011)

There hasn't been one specific explanation established as to how these features are formed yet, a list of different mechanisms have been linked to various identified PFZs as originators.

Genesis mechanisms	Description	Key study area	References
Density inversion	After drainage during compaction, the top and bottom of the mudstone becomes dense forming low permeable sealed layers. The water in the middle of the mudstone cannot be expelled, generating overpressure. When it is critically overpressured, hydraulic fractures may occur with faults and collapses forming at the top, leading to the formation of PFs.	North Sea Basin, Lake Hope region, Farafra Oasis of Western Desert of Egypt	Henriet et al. (1988,1991) Cartwright (1994a), Cartwright (1994b) Cartwright and Lonergan (1996) Watterson et al. (2000) Tewksbury et al. (2014)
Gravity sliding	Downslope gravitational collapse produces a strong alignment of fault strikes perpendicular to the direction of sliding towards the depoleft.	Outer Moray Firth of northern North Sea	Higgs and McClay (1993) Clausen et al. (1999)
Low coefficients of friction	Low coefficients of friction can increase the displacement on localized fault surfaces and the concentrated stress around the dislocation loop may bound the slip zone. It may enable the outward propagation of the polygonal fault after initial slip which eventually coalesces with others into a polygonal fault system.	Eormanga Basin, North Sea Basin	Gouly (2002) Gouly and Swarbrick (2005) Gouly (2008)
Syneresis	Syneresis occurs during the early stage of compaction and dewatering, and the three-dimensional contraction of smectite-rich gels favors the PF formation. This genesis mechanism is driven by the interparticle attractive forces between clay particles, and mainly occurs in layers composed of smectitic claystone and carbonate chalks.	Stable Subbasin, North Sea Basin, Qiongdongnan Basin	Cartwright (1996) Lonergan et al. (1998b) Hansen et al. (2004) Wu et al. (2009) Sun et al. (2010) Han et al. (2016)
Shear failure	The conversion of opal-A to opal-CT reduces the bulk rock volume and induces differential compaction and shear failure during regional diagenetic processes of siliceous sediments. It is accompanied by stress changes, and therefore can cause PFs initiation.	Voring Basin, More Basin, Sanzhao Sag of Songliao Basin, Great South Basin	Cartwright. (2011) Davies and Ireland (2011) Ding et al. (2013) Li et al. (2020)

Table 2 An overview of genesis mechanisms for polygonal faulting

On the representative list in **Table 2**, shear failure has been mentioned in relation to the Vøring Basin, one of the more common processes overall.

Shear failure happens when certain minerals dissolve during sediment diagenesis, which leads to a reduction of horizontal stress.

This apparently cannot occur in deposits that lack biogenic silicates. (Xia, Yang et al. 2022)

Polygonal faulting is a relatively common feature of the sediments belonging to the Late-Oligocene – Early Miocene epochs (Brygge- and Kai formations, see Chapter III. 1)D/a, Lithostratigraphy subchapter) along the Mid-Norwegian margin, and their presence has been repeatedly noted at the Vøring Basin in previous studies, such as (Berndt, Bünz et al. 2003). The same article mentions how PFZs have influenced the depositional pattern of the overlying sedimentary sequence, the Naust formation.

(Berndt, Bünz et al. 2003) further describes vertical fluid flow structures they call *pipes* that an earlier study determined to be built by episodic fluid expulsion.

These originate from supposed gas-bearing deposits, or the upper limits of the polygonal faults, but as they point out, never from inside or below the PFZ.

(shown below on *Figure III-12*)

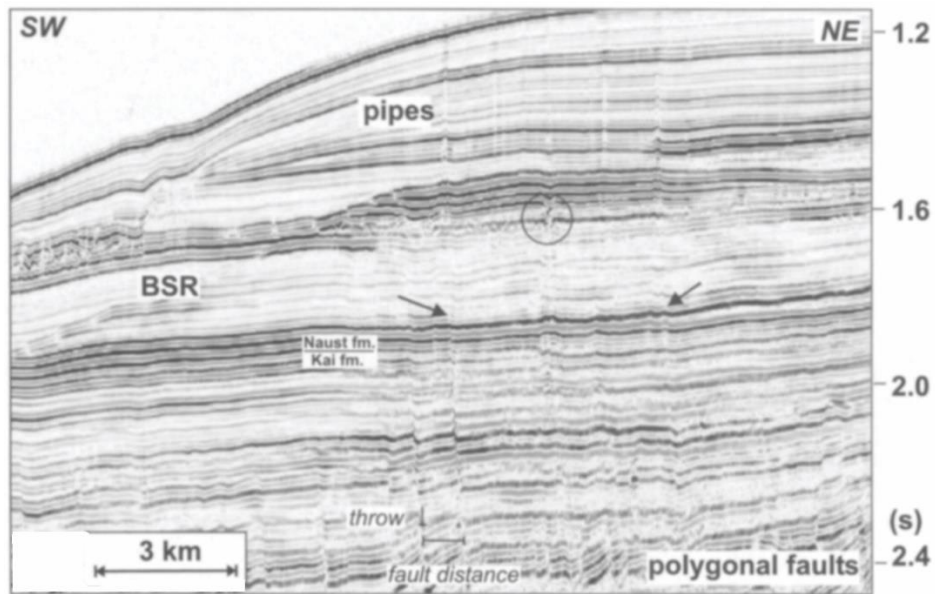


Figure III-12 Example of fluid flow structures rooted in a PFZ

Another thing they note is how the number of fractures increase with the depth in the PFZ and the associated fault blocks are generally smaller near the lower termination of the zone – this change in scale of deformation indicates that polygonal faulting is a protracted process, instead of a single, momentary event. (Berndt, Bünz et al. 2003)

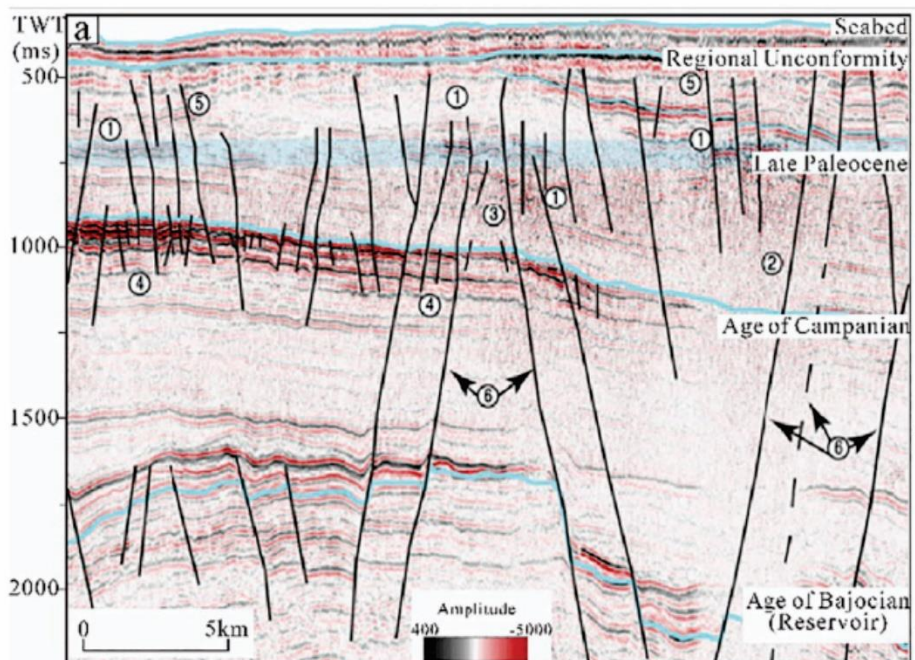


Figure III-13 An example of a seismic section showing the distribution of fractures in a PFZ

As in the previous subchapter, Figures III-12 and -13 have been included to illustrate the appearance of an established polygonal faulting zone on a seismic recording.

Fig. III-13 is a section of the Hammerfest Basin.

IV. Methodology

This chapter will introduce the process of gathering seismic recordings of a submerged area, preparing this data in order to make it „legible” (removing imperfections from the signal, performing corrections for non-related external impulses, etc.) and then finally the arduous process of examining the dataset for the necessary information.

The major focus in this section of the thesis is **IV.3) Seismic Interpretation**, where the practical steps performed with the Petrel Software Package during this work will receive some attention.

Since the first two stages have already been performed previously, these will be given a brief general introduction only, with some details about the specific methods related to WIN19M02 where they were available.

The data shown in Tables 3. and 4. have been provided by Prof. Stefan Bünz.

1) Acquisition of WIN19M02

The dataset WIN19M02 is a combination of three previously recorded seismic blocks: SH0402, SH0903, SH1001. The general term used for the method used during the three expeditions in question researching the sediments of the Vøring margin is called “reflection seismics”, and is based on measuring the time it takes for a signal to reach seismic reflectors and then “bounce back” to a receiver – this is called “two-way travel time”, or “TWT” for short. (Chowdhury 2014)

This initial signal may originate from natural sources, but for research, purpose-built devices are preferable for the sake of practicality and repeatability.

Used for both terrestrial- and marine environments, the ship-based version uses controlled shockwaves created by compressed air.

There are versions of this technique where the signal source and the recording device (hydrophone) travel attached to the same towed platform, and also where the two instruments are trailing after separate vessels.

Figure IV-1 on the following page provides a schematic for this process.

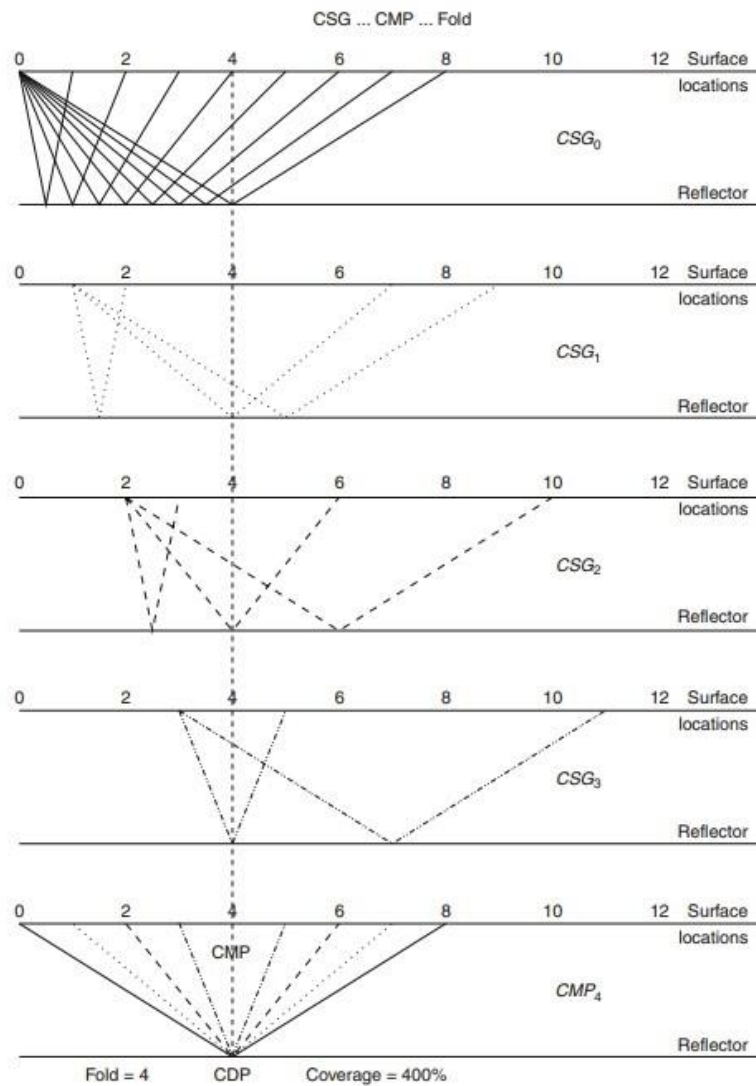


Figure IV-2 Simplified illustration showing the acquisition process

These days the receivers are usually dragged behind a research vessel as multiple chains of small pressure meters arranged side-by-side, all of which are constructed with their own GPS locators and are linked to the ship either with fibre-optic cables, or via wireless connection.

This means that every initiated shockwave (“shot”) gets recorded multiple times, slightly differently (since the hydrophones float at a known distance from each other). (Chowdhury 2014)

C01 CLIENT:WINTERSHALL, PROJECT: WIN19M02, LICENSE: PL944, PROCESSED BY:ION			
C02 AREA: NORWEGIAN SEA, GJALLAR RIDGE,			
BLOCKS	6603/09	6603/12	6604/05-12
C03 DATA FORMAT:SEG-Y, SURVEY:WIN19M02, DATE:07/2019,			
NPDID	4262	7102	7213
C04 DATA TYPE: RTM FINAL STACK (TIME)			
C05 ACQUISITION PARAMETERS	SH0402	SH0903	SH1001
C06 RECORDING CONTRACTOR: WESTERN/CGG/CGG			
DATE:	2004	2009	2010
C07 RECORDING SAMPLE RATE: 2MS			
REC LENGTH:	7168MS	7000MS	7000MS
C08 ENERGY SOURCE: DUAL ARRAY, SHOT INTERVAL:18.75M,			
DEPTH:	6M	8M	8M
C09 SOURCE SEP: 37.5/50/50M, GROUP INT: 12.5M,			
CABLE DEPTH:	7M	10M	10M
C10 CABLE SEP: 75/100/100M, CABLE LENGTH: 5/6/6KM,			
NUM CHANS:	10x398	10x480	10x480
C11 NOMINAL FOLD:	63	80	80
C12			

Table 3 Overview of data pertaining to the acquisition process of the three surveys

The dataset WIN19M02 is a combination of three previously recorded datasets: SH0402, SH0903, SH1001.

Table 2 shows some of the parameters of these surveys, with some of the brackets having thicker borders for ease of differentiating between groups of data.

The methods and equipment for SH0903 and SH1001 in 2009- and 2010, respectively, is identical, with 2004's recording apparently having been taken from a higher altitude with fewer receivers.

This suggests slightly lower resolution for SH0402.

2) Seismic processing

Seismic data acquisition is complicated by the presence of superfluous information – every part of the recorded data that is not the signal is collectively referred to as “seismic noise”.

It must be emphasised that signal in this context means the specific portion of the recording that is applicable to the purposes of the study.

Seismic noise can appear in the data as a result of ambient sources (sounds of fauna or anthropogenic sources for example), interference with the emitted shockwave (refraction errors of scattering), flaws in the setup or usage of instruments, or mistakes committed during processing itself.

The overall goal of this technique is to reduce the amount of excess data present in the recording against that of useful information (SNR – signal-to-noise ratio) to the highest reasonable degree.

An unfortunate reality of working with seismic data that it is quite impossible to completely separate noise from the signal.

(Chowdhury 2014)

C13 REPROCESSING SEQUENCE:			
C14 <i>INPUT NAV-MERGED SEGY</i>	APPLY T**2 GAIN	DEBIAS FILTER 1-2HZ	DEBUBBLE,
C15 DE-SWELL	TAUP DE-SWELL	RADFILT	WIBAND
POST-WIBAND	DENOISE		
C16 RES DEBUBBLE AND ZERO PHASE	TIDAL STATICS	WC STATICS	LOCAL FOOTPRINT
C17 REC MO CORR	SURVEY MATCH	2 PASS SRME (MMADSUB)	RADON (450MS CUT)
C18 GLOBAL FOOTPRINT	SURVEY MERGE	4D REG (12.5x12.5M)	OFFSET PLANE DENOISE
C19 REMOVE T**2 GAIN	PHASE ONLY INVERSE Q=135	ANGLE MUTE FOR RTM (0-40DEG)	
C20 PRES DM VMB (4xIT)	RTM MIG (3000M HALF AP, 45 MAX FREQ FLAT SPECTRUM		
C21 OUTPUT TO 6.25x6.25m GRID, 8000(5)M	SECTION BALANCE	3D COHERENCY FILT	
C22 DEPTH TO TIME	31PT LS MATCH TO KIRCHHOFF FINAL STACK	<i>SEG YOUT</i>	

Table 4 An outline of seismic processing performed on WIN19M02

Table 3. above is an abbreviated list of the various functions performed on this particular dataset.

As these first two subchapters are only meant to show how such a project might look from start to finish, the contents of the table above will not be comprehensively detailed.

Only a few, arbitrarily selected functions will illustrate the previously completed *cleaning* that served as precondition for this thesis.

Their definitions were taken from the online database of the Society of Exploration Geophysicists. (<https://wiki.seg.org/>)

Debubble: removes the interference of transitory gases from the water column

De-swell: corrects for shifts in hydrostatic pressure caused by changes on the water surface

Tidal Statics: refers to changes in elevation/water depth caused by tides

Global/Local Footprint: footprint means deviations of the signal pattern caused during processing

RTM MIG: correction for the Reverse-Time Migration, which is the duration of the signals return from a reflector

3) Seismic interpretation

This subchapter gives a step-by-step detailing of the various processes performed in Schlumberger's Petrel Subsurface Software package during the practical phase of this work. The provided dataset has already been processed and merged into a data block.

The actual first practical step performed for this thesis was the recreation of this 3D block through different „Volume attributes” which means highlighting certain properties of the dataset.

The three attributes chosen were:

- Variance: emphasises the range extremes of the signal amplitude, to help identify discontinuities
- RMS amplitude: calculates the RMS (root mean square) of individual traces in a pre-defined range
- Structural Smoothing: takes average values of the signal and eliminates momentary extremes (noise), thus allowing for easier interpretation

Next, distinctive layers were chosen and (assisted by the software – guided auto-tracking) tracked on vertical sections of the dataset.

This was an arduous process, and involved much backtracking and second-guessing. Initially, 13 such layers were interpreted (and a failed attempt at a 14th), but much of this effort pointed beyond the scope of this thesis and all but four of these horizons were abandoned (the seafloor and H-01-02-03, the three shallowest).

Horizon 04 was used as a reference but not interpreted, and a number of vertical discontinuities were tracked in the underlying strata but this, again, was subsequently deemed superfluous – indeed, the mapping of these faults might be the basis of an entirely separate Master's thesis.

After it was determined which layers were useful for this project (and then re-interpreted multiple times until satisfaction) polygons were drawn around most of the dataset. Most, because the software revealed hiatuses, repeated patterns and other suspicious features (often forming ridiculous protuberances) which were determined to be recording errors that could not be accounted for during processing – therefore, these parts of the dataset were „left outside” the newly drawn boundaries.

In the next phase, some „cosmetic work” followed.

To remove hiatuses from the newly interpreted layers, Petrel was made to extrapolate from existing data using the „Paintbrush autotracking” function.

The software would attempt to link known, but unconnected points in the data in a constrained area.

This was highly repetitive, but eventually yielded results.

Through tweaking the sensitivity of autotracking, the program would first continue traces only to a small degree, but lowering the correlation quality means Petrel would eventually extrapolate using its own extrapolations and these hiatuses would eventually close.

With careful progress, this process would provide results with reasonable confidence.

The newly coherent horizons then were merged into surfaces using the polygons, the faulty partitions excised from the useful data.

Two-way travel time maps are automatically created during this process, then the surfaces were recreated using to emphasise different attributes:

- Variance: (see „Volume attributes”)
- RMS amplitude: (same as above)
- Isochron thickness: distance between two interpreted layers

After this, the two-dimensional sections were examined again, and based on this and the different representations of the surface a high number of temporal offsets were created with Petrel, which means the software draws a different surface based on the interpreted layers, but at a set TWT value removed from it.

Many of these offset were created, much more then referenced in this thesis, and it is no exaggeration to say that these formed the backbone of the project.

The only remaining step was the actual examination of data – moving back-and-forth through the seismic sections along both the Inlines and Crosslines and the time slices (the Z-axis) when necessary.

Where the angles were not favourable, arbitrarily selected composite lines were drawn to inspect features.

V. Results

In the preliminary evaluation of the dataset (in addition to the seafloor) 14 prominent reflectors were selected in the Petrel Software package.

These stratigraphic boundaries have been designated Horizons 14-01, but not all can be displayed on the same seismic section - the most comprehensive overview is provided by a combination of two images (see *Figures V-1* and *V-2*).

Not all reflectors cover the entirety of WIN19M02, some are presumed to be irregularly shaped, extensive and coherent structures instead of stratigraphic boundaries.

The sections' location is also shown on the attached map of the area (*Fig. V-1*).

There is some repetition of marking colours, but since the affected horizons are only the deepest, unexamined ones, allowances were made.

Initially, three massive deposits were interpreted between the third and first reflectors that were deemed pertinent to the topic of this thesis.

Later, this was re-evaluated, and six distinct sedimentary units were established for further inspection

One other unit seems to be present at these depths, but eventually was not interpreted for reasons explained later in this chapter (Unit X).

Horizon 04 and the layers between it and H03 were not examined in detail, but they appear to have influenced some of the overlapping sediment.

The strata between Horizon 01 and the Seafloor seems to contain no features immediately relevant to this thesis.

All the reflectors interpreted here dip generally westward and slightly toward the northwest.

After the preliminary stage it was decided that sediments below -2300ms TWT would not be studied for this thesis.

The deeper horizons are not high-confidence interpretations, as *Figure V-2* illustrates, there are several discontinuities and some sudden shifts in elevation, which are could be attributed to scattering, brittle deformation or at times faint amplitude signatures.

Nevertheless, some features of the deeper strata are very interesting and might merit further study in separate projects.

For the included seismic images, with a few exceptions both an interpreted and an unaltered version will be presented in this chapter, in that order, for comparison purposes.

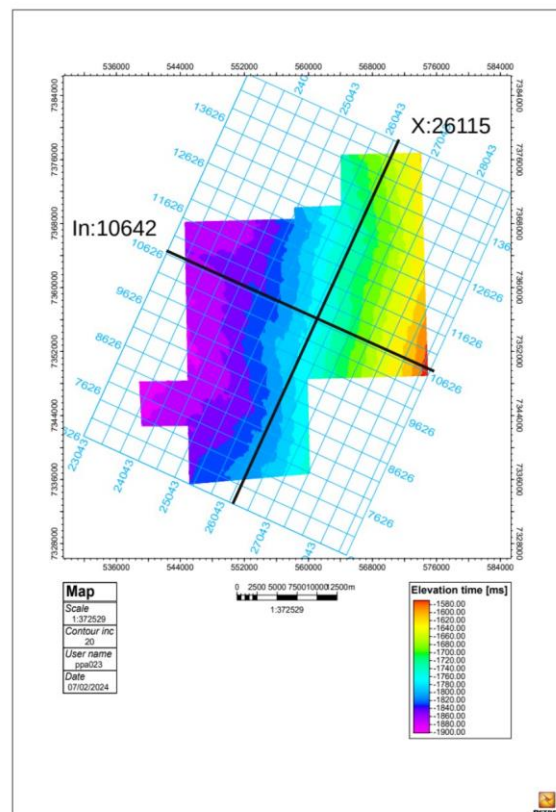


Figure V-1 Schematic map of the area showing the location of overview-sections

When it comes to the attribute maps, this was deemed excessive, considering that the same ones will have to be repeatedly shown.

The displayed ranges for the colour schemes used when generating the attribute maps included in (and also omitted from) this thesis were always chosen according to best visibility of features, and not uniformly adhering to an established set of values.

On the other hand, the chosen colours used for emphasis of structures and pertinent masses were kept consistent at least on a subchapter-scale with the exception of Anomaly 04.

A number of arbitrarily chosen composite lines were drawn for the work on this chapter – in the end, most of them were deemed superfluous for the descriptions.

To maintain proper organisation, the identified features are described starting from the south towards the northern boundary and grouped according to depth.

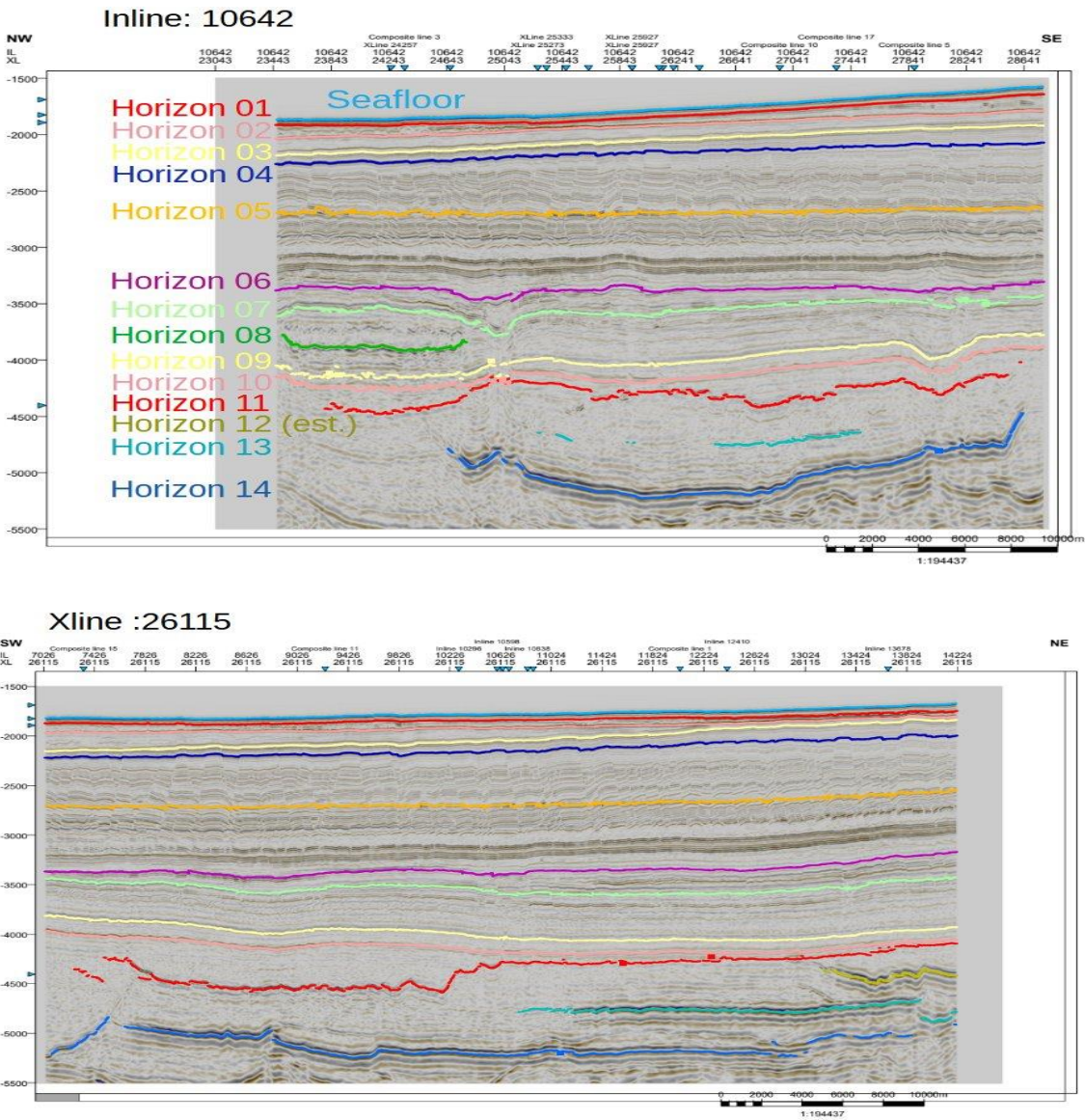


Figure V-2 The two overview-sections showing the marked reflectors of the preliminary evaluation

1) HORIZON 03

The main object of interest here is “Unit-1”, a sediment mass located on top of Horizon-03 (“H03”), and the various structures observed therein. It will become clear later that U-1 completely dominates the region in these strata, but it seems to terminate short of the northern boundary of the study area. However, it does extend beyond the eastern, southern and western borders of it, therefore the precise dimensions of this mass are unknown.

On the seismic images, approximately $\frac{3}{4}$ of the total area is covered by the generally disorganised sediment mass of Unit-1, while only simple lineation can be seen above the rest. To illustrate this, *Figure V-3*. shows an arbitrarily chosen Xline transecting the region from the northeast to the southwest without interruptions.

Unit 1 has been marked in pale green.

There is a relatively high amplitude layer running underneath Unit-1 paralleling H03 itself, but with the disappearance of the sediment mass it terminates against H02.

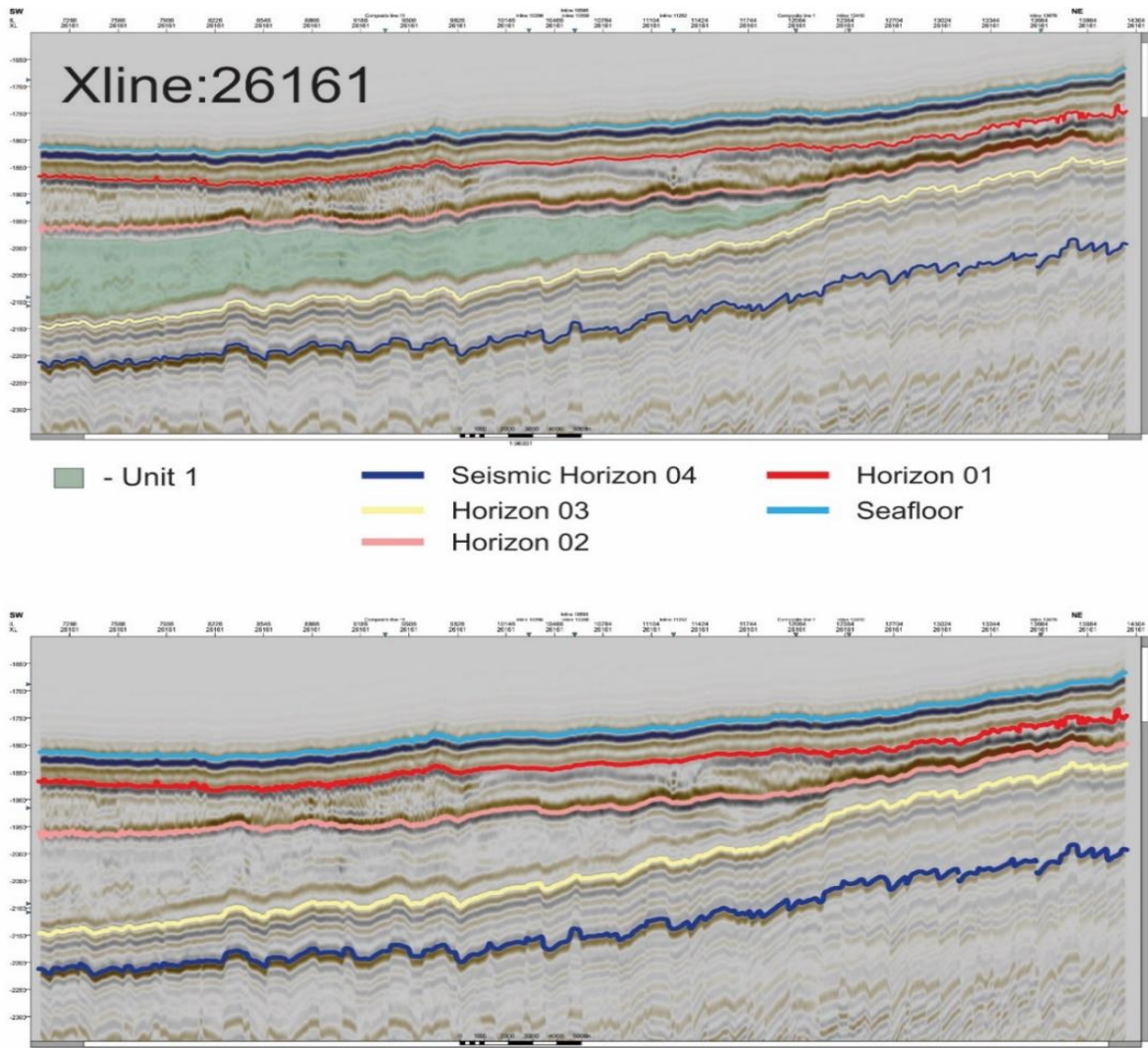


Figure V-3 Complete cross-section of the study area with all interpreted horizons. Location of this Xline is shown on Fig. V-2

Figure V-4 shows the location of this cross-section on a TWT map of the study area, and an isochron map which is perhaps best to showcase the magnitude of Unit 1. Both it, and the seismic images (Fig. V-3) show the orderly layers to the north with a rather uniform thickness and a gentle decline and the sudden increase in both slope angle and the amount of material as U-1 begins. The TWT map to the right suggests that although the horizon itself is characterised by a general westward decline, the overlying strata show a slight NE-SW shift. It also shows an overall pattern resembling fish scales. A different surface attribute was chosen to better observe this peculiarity.

The appearance of H03 on a variance map closely resembles a network of often kilometre-long mudcracks (see Figure V-5) – a multitude of vertical discontinuities cross the underlying strata, but as can be seen on all the seismic images shown in this subchapter the majority of them do not extend all the way to H03, and only the occasional one seems to

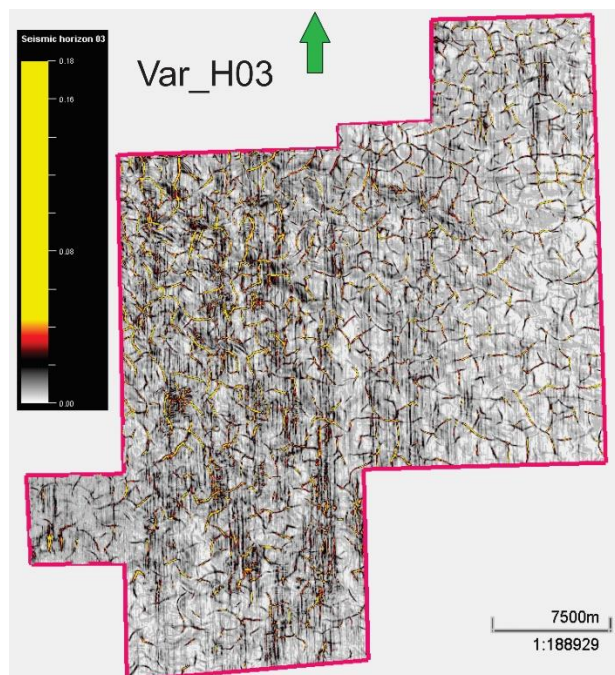
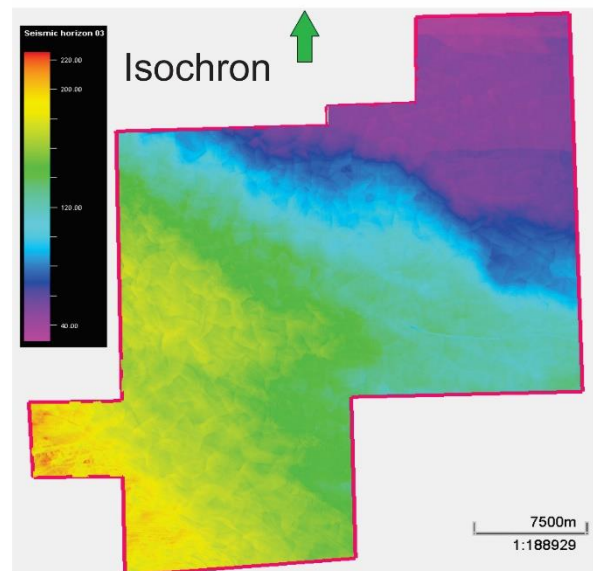
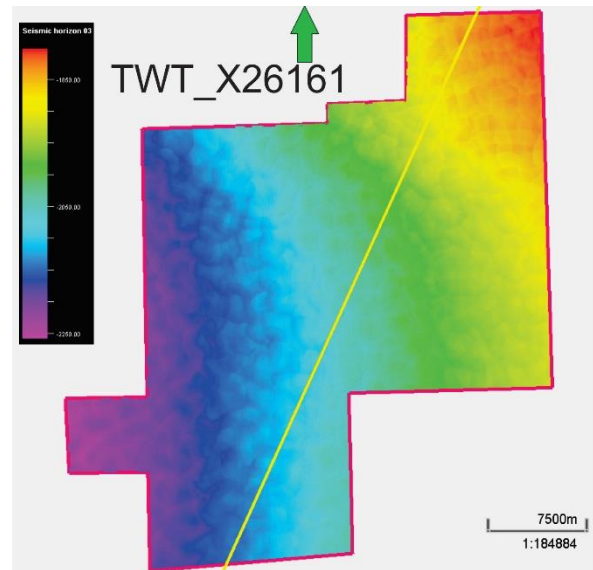


Figure V-5 Variance map of Horizon 3

actually breach it.

Figure V-4 Two-way travel time- and isochron maps of H03

More of the cracks appear on the western half of the study area, and with higher variance-values, but the difference is not too prominent.

It is possible that the mudcrack-like pattern exhibits more curves on the southwest. Apart from these, no other structures were identified at this depth, and with distance from H03, these cracks become largely obscured.

The thinner facies' on the northeast – both

between H03-H02 and H02-H01 – still show these expressions which are presumed to originate underneath H03.

Also included below is a composite picture of variance maps derived at different temporal offsets above H03 and the anomalous objects and structures found in relation to Unit-1. (see Figure V-5)

These features will be described in four different subgroups depending on the depth at which they seem most prominent.

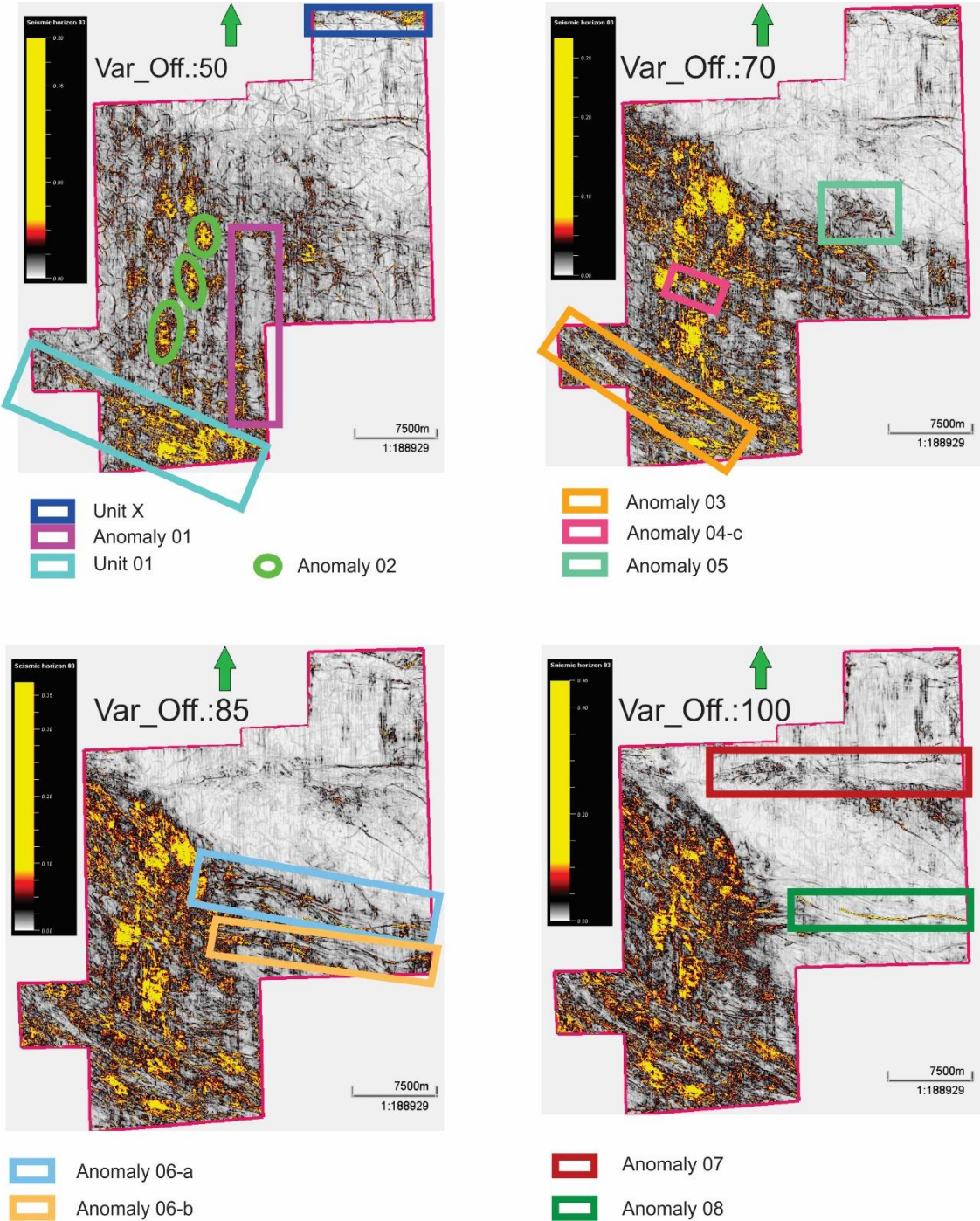


Figure V-6 Composite image of all used offsets based on H03 and a complete assortment of examined structures

A. Horizon 03 – Offset: 50

The variance maps show that beginning on the south, some of the sediment seems to be arranged in a linear configuration, and to follow an approximately unidirectional northwesterly path. The amount of material thus arranged seems to grow with increased distance from H03 up to a point, then recede on “Var_Off.:100”. (Figure V-6)

Figure V-3 shows that near the southern border of the study area, Unit 1 almost touches Horizon 03, but the average distance between the two is approximately 40 milliseconds. Accordingly, an offset of 50 milliseconds was deemed appropriate to examine the bottom of U-1. Since the linear arrangement can be seen on parts of “Var_Off.:50” where there is less material between U-1 and H03, by logic this pattern seems to reflect the internal arrangement of Unit 1 – this area is shown in teal on Figure V-7.

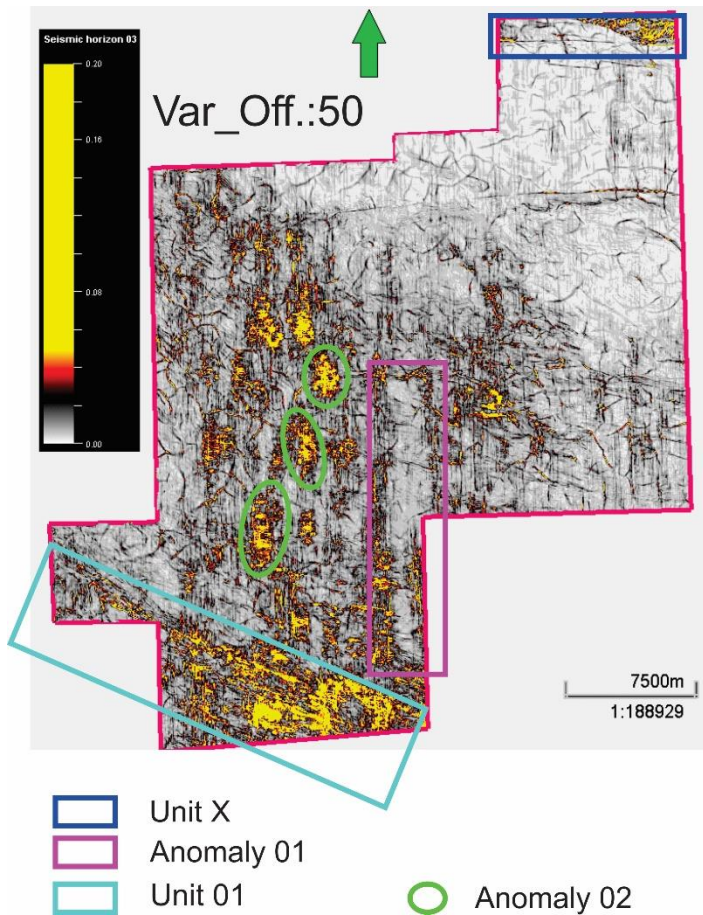


Figure V-7 Selected features near the bottom of Unit 1

a) Anomaly 01 – Roll

Right in the middle a relatively smooth, semi-regular rectangle can be seen. Neither the seismic data, nor the variance map shows many features in this particular area. In the southern parts, not even layering can be seen, but near the middle of the structure two prominent layers appear and remain for its full northward extent. (Inline: 9672 shows this – see Figure V-8)

These layers appear almost completely smooth, with no interruptions or discernible signs of stress, but outside of A01 the same strata become slightly disturbed to both the immediate southeast and northwest.

Around the middle of the structure, a slightly elevated block underneath H03 is visible on the Inline, that corresponds to the dimensions of the Roll, but it is not present everywhere.

Anomaly 01 is completely unnoticeable on RMS, and the isochron map also.

The latter wasn't even included here.

A portion of the Roll seems to extend further than the eastern boundary of the study area, but this can't be verified.

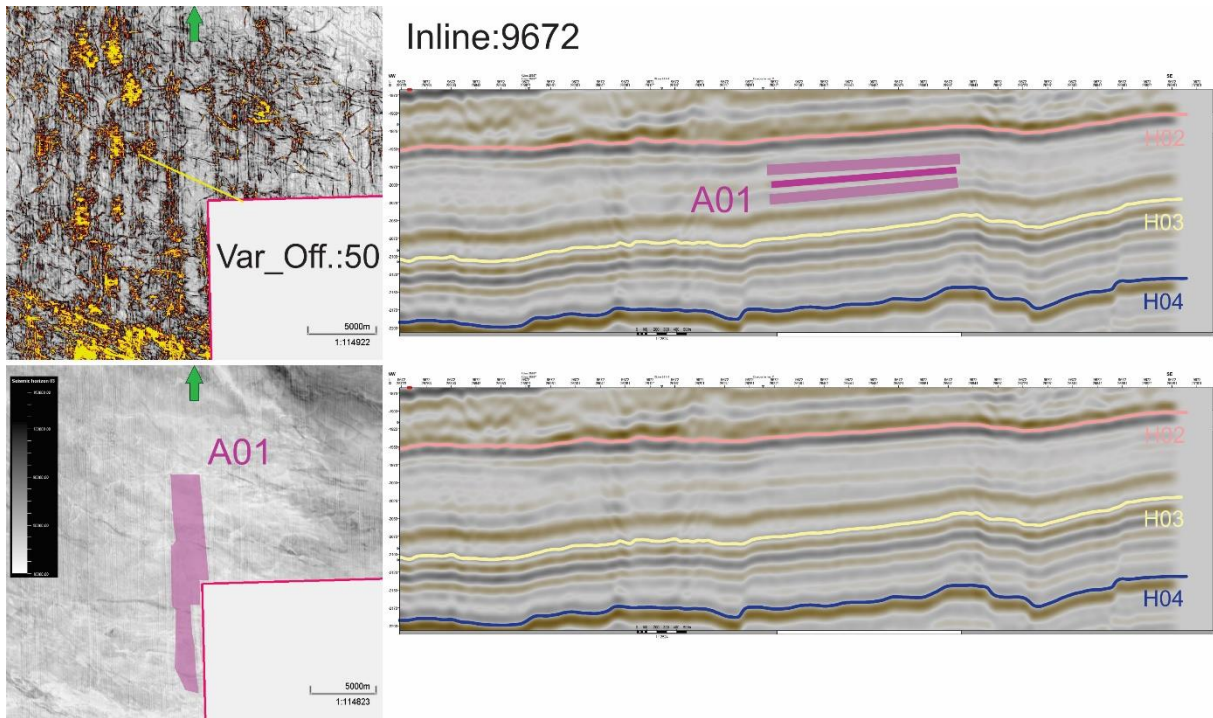


Figure V-8 Approximated location of Anomaly 01

b) Anomaly 02 – Clusters

To the East-Northeast, the mass is dominated by several irregularly distributed clusters of sediment (three representatives of these have been designated “Anomaly 02” – for the general location of these see *Figures V-6-7*, and a more precise illustration on *Fig. V-9*).

Although these features of high variance values are present in some form all throughout U-1, they are best observed at this depth as individual structures.

They draw no discernible pattern on the seismic images, and no underlying structures can be linked to the Clusters, but the facies above H02 seem to be more distorted than the ones between H03-H02 at these locations.

For this reason, only approximations can be shown to illustrate Anomaly 02, but using the Petrel Software the visible extent of three of these Clusters on the variance map were followed on the Xline to mark the otherwise invisible features.

The layering appears fragmented at all similar Clusters, with objects of varying size scattered above the marked areas, but these do not seem to correspond with the dimensions of A02 instances.

Once again, no significant amplitude shift can be associated with the feature, and none of the A02 features appear to influence the thickness of the strata.

Var_Off.:50
Xline: 25333

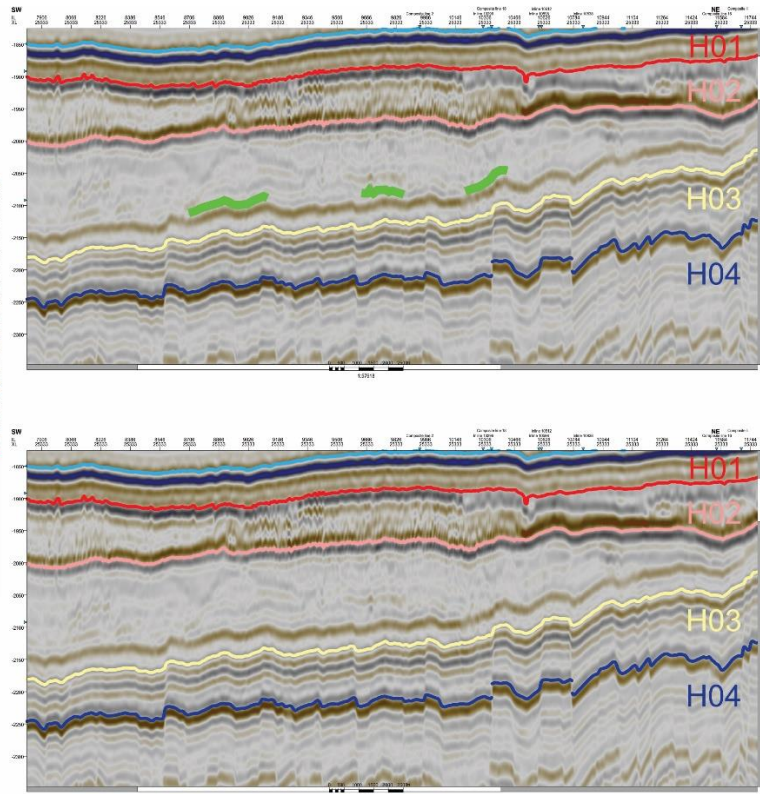
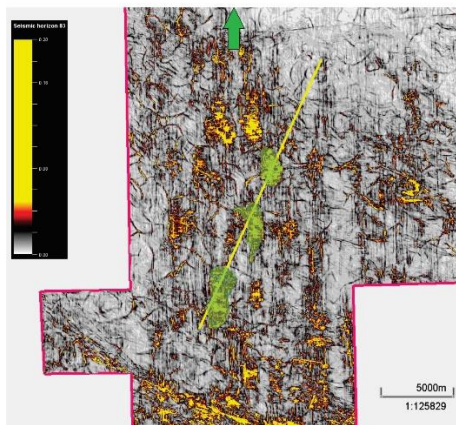


Figure V-9 The three instances of Anomaly 02

B. Horizon 03 – Offset.:70

A slightly increased temporal offset (20 milliseconds above) reinforces the earlier statement concerning the general alignment of Unit 1.

On “Var_Off.:70”, shown on Figure V-10, the majority of visible features appears to follow the NW-SE alignment seen at the southern boundary on the 50 millisecond offset.

Not only the overall pattern has “grown” to cover almost the entire area thought to be U-1, two of the three major anomalies marked at this depth seem to be elongated in this direction as well (Fig V-10).

Please note that the magenta rectangle has the designation “Anomaly 04-c” – that is the only member of a collection of structures visible on the variance attribute map.

Detailed descriptions are to follow.

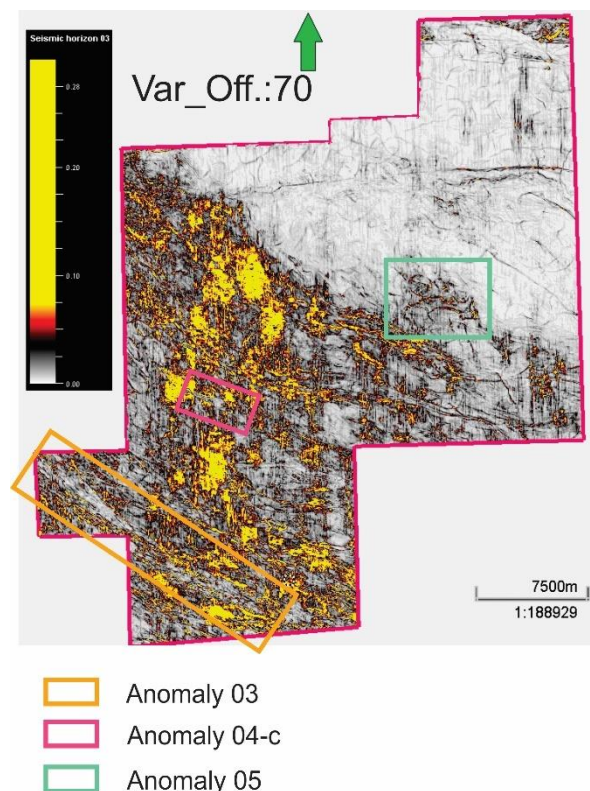


Figure V-10 Variance map of 70 milliseconds above Horizon 03

a) *Anomaly 03 - Raindrop*

To the southwest, there is a slightly curved, elongated area of low variance that displays stronger amplitudes and some lineation amongst disorganised deposits. The structure is not fully visible on any of the variance images, because of significant, gradual change in altitude.

Time-slices have also been checked, without satisfactory result – the structure couldn't be displayed in its entirety.

The portion seen on “Var_Off.:70” has an elongated raindrop-like shape, but the RMS map of the same offset displays very little variation in the width of the structure (see Figures V-11 and -12).

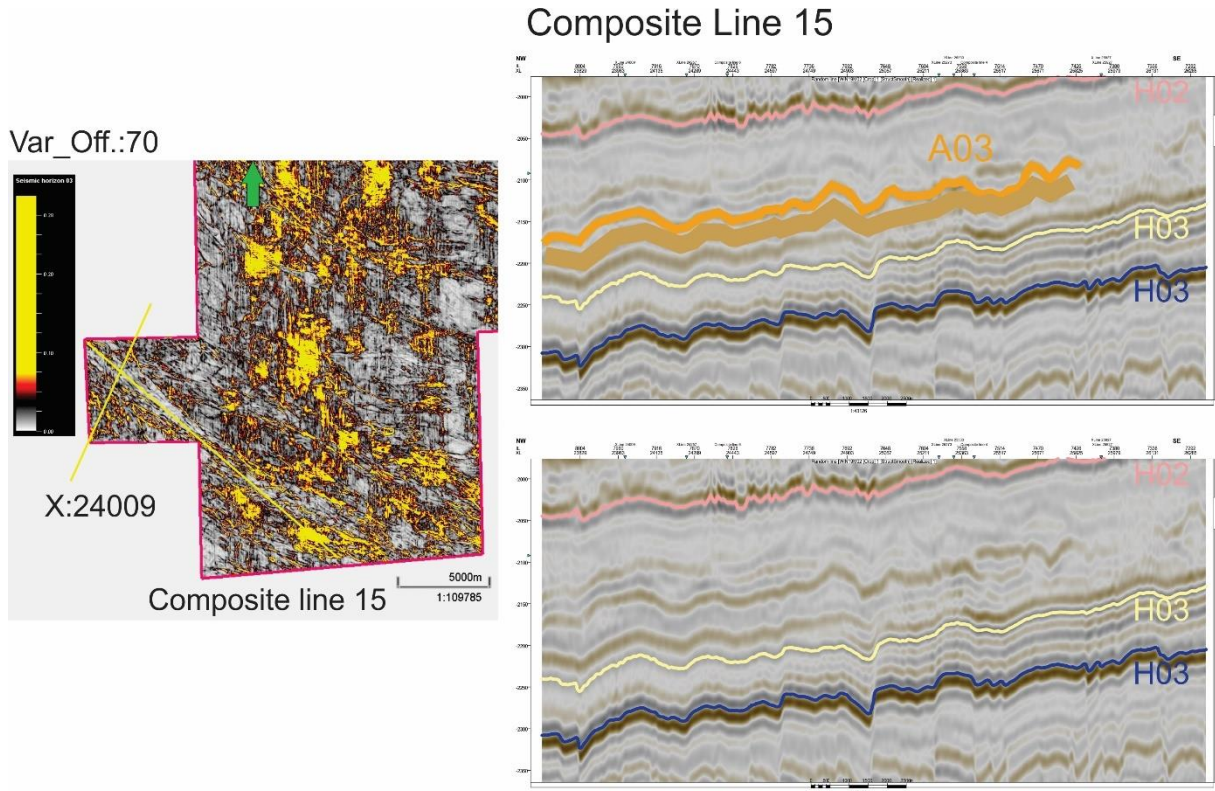


Figure V-11 Variance map with both pertinent seismic lines indicated

A composite line (15) has been drawn but doesn't show the entire extent due to a shift in direction, causing the abrupt termination seen on Fig. V-11.

The band of sediment composing the “Raindrop” does, in fact, continue beyond the southern and western boundaries of the study area.

Several vertical discontinuities can be found underneath, but their effect on the shape of A03 is not always discernible.

The Xlines show a pronounced anticline near the western boundary, and a wider amplitude range compared to surrounding strata.

Moving towards the southeast on the seismic image, the anticline loses its semi-regular shape, and some interruptions also appear.

On the other hand, the composite line shows no interruptions in the feature and seems to roughly correspond to the elevation changes of H03, but there are some notable deviations as

well. (Figure V-12)

The crosslines not included here show a structure with a similar amplitude signature to the S, but too little is visible of this to allow interpretation.

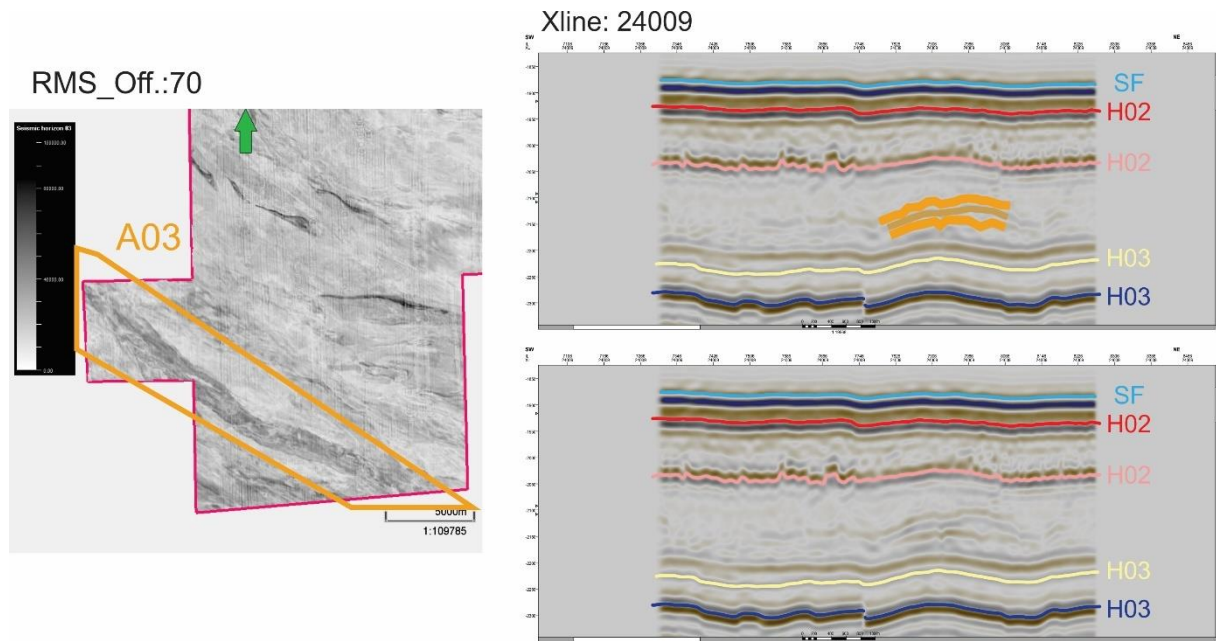


Figure V-12 RMS map with the whole area of A03 highlighted and the seismic cross-section of it

b) Anomaly 04 – Scars

There is an interesting feature near the western boundary – an object akin to those designated as Anomaly 02 - Clusters appears to have been “cut into”. (Figures V-13-14-15) On “Var_Off.:70” a narrow V-shaped slice is mostly featureless in an area characterized by a chaotical arrangement of high variance points, but the seismic data shows stronger amplitudes in this small section.

Due to the shape and alignment of the formation, interpretation is easier on the inlines (In: 9332) This feature appears as a sudden strengthening of one particular layers amplitude signature, and an equally abrupt weakening afterwards.

On the RMS image (same, 70 ms offset) this “slice” resembles a badly healed wound and it is surrounded by four other structures. These don’t show up on any of the variance maps but interpretation has revealed these to display the exact same characteristics as A04-c, besides general shape, and even in this there are similarities. Their appearance and distribution can be seen on Figure V-13.

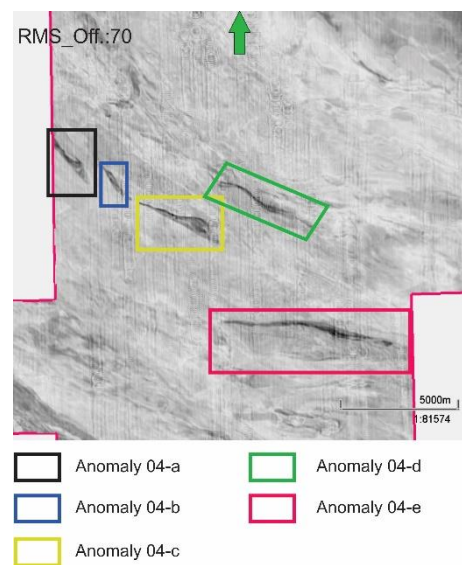


Figure V-13 All five of the identified "Scars"

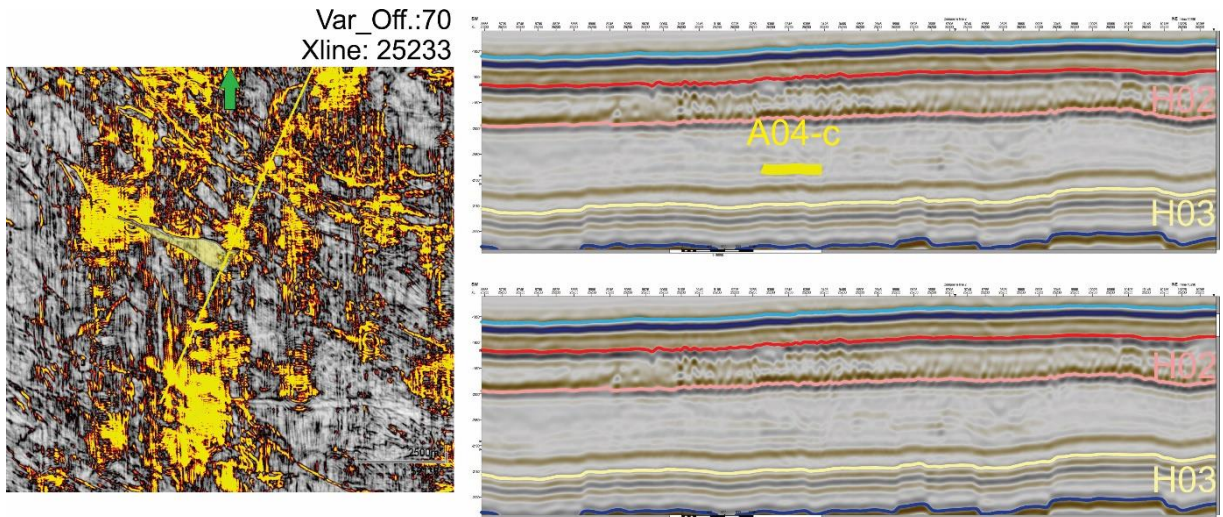


Figure V-14 The only instance of Anomaly 04 that is clearly visible on the variance map

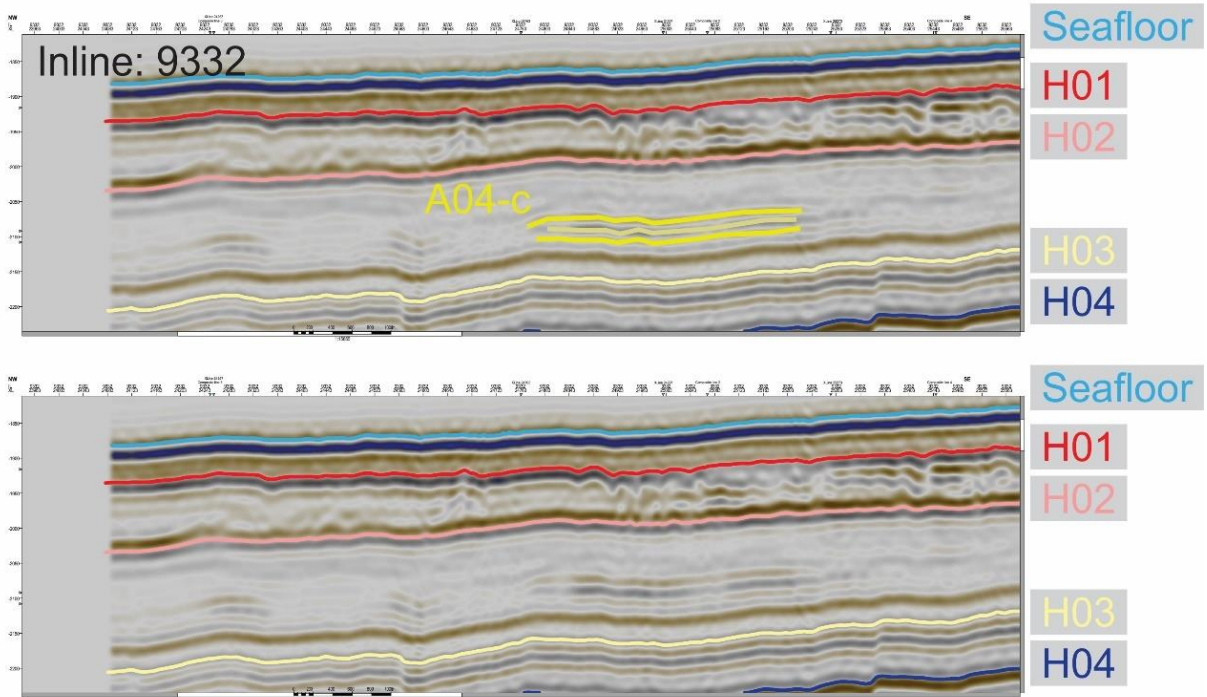


Figure V-15 The same structure from a different angle highlighted

c) *Anomaly 05 – Hairball*

On “Var_Off.:70” (Figure V-16, on the right), Anomaly 05 appears as a collection of chaotically arranged, somewhat higher variance sediment strips relatively close to the estimated northern termination of Unit 1.

Although prominent on the variance map, on the Xlines these curved lines show up as miniscule protuberances; the vertical discontinuities of the underlying strata do not match the number of, or always align with individual “hairs” in A05, moreover, at certain points the seismic data in this area appears almost featureless.

To illustrate the shift, two other variance maps of the same area were provided on Figure V-17, taken from different temporal offsets.

On closer scrutiny of “Var_Off.:50” elements of A05 are still recognisable, if slightly obscured, but the variance map of Horizon 03 shows a different pattern – the colour scale is also not consistent between Figs. V-16 and V-17.

The “W”-shaped object accented with a green, broken circle is the one identified exception to this, otherwise the Xlines seem to support this perceived lack of connection.

The pale green markings on Figure V-18 are slightly exaggerated, and the rectangle drawn with a broken line denotes the approximated extent of the “Hairball”

The pale green markings on Figure V-18 are slightly exaggerated, and the rectangle drawn with a broken line denotes the approximated extent of the “Hairball”

Var_Off.:70

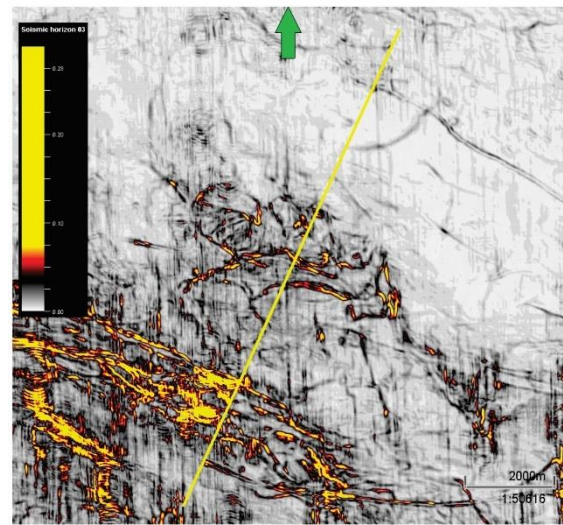
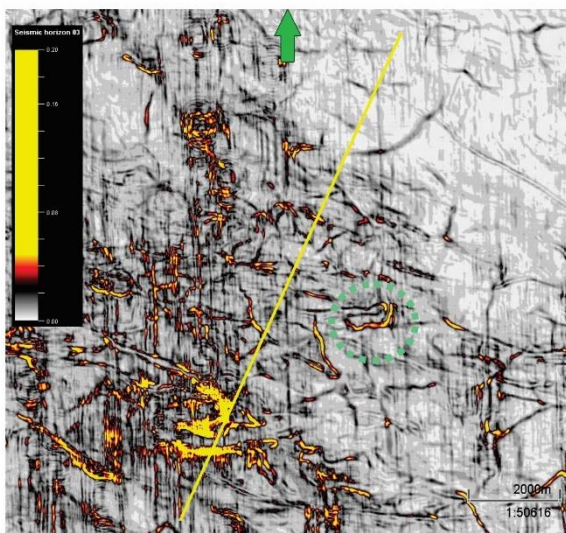


Figure V-16 The pattern drawn by Anomaly 05 is clearest on this offset

Var_Off.:50



Var_Off.:0

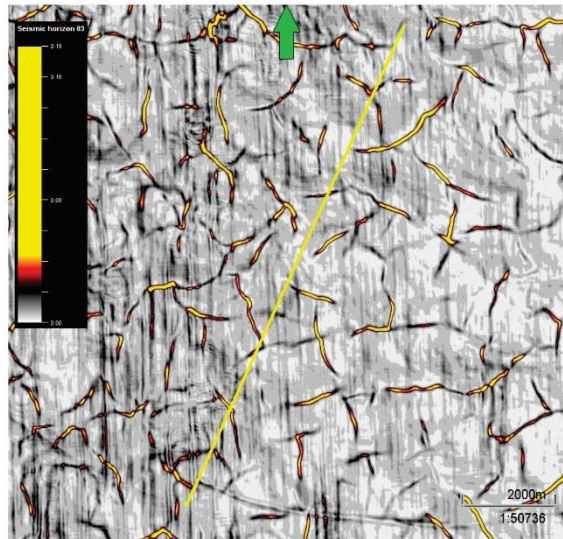


Figure V-17 The variance maps for comparison

RMS images were not included, since they do not show the feature clearly – the amplitude signature of the layer directly under U-1 in this area shows a gradual strengthening (see the unmarked image on Fig. V-18) which might obscure any small changes associated with A05, if they exist.

For this reason, the specific dimensions of the feature are difficult to determine. Markings aside, the image below itself might seem oversized, but this level of magnification was deemed necessary to counter for the small size and faintness of what has been determined to be the feature.

Furthermore, X:26851 was found to provide one of the clearest seismic representations of A05.

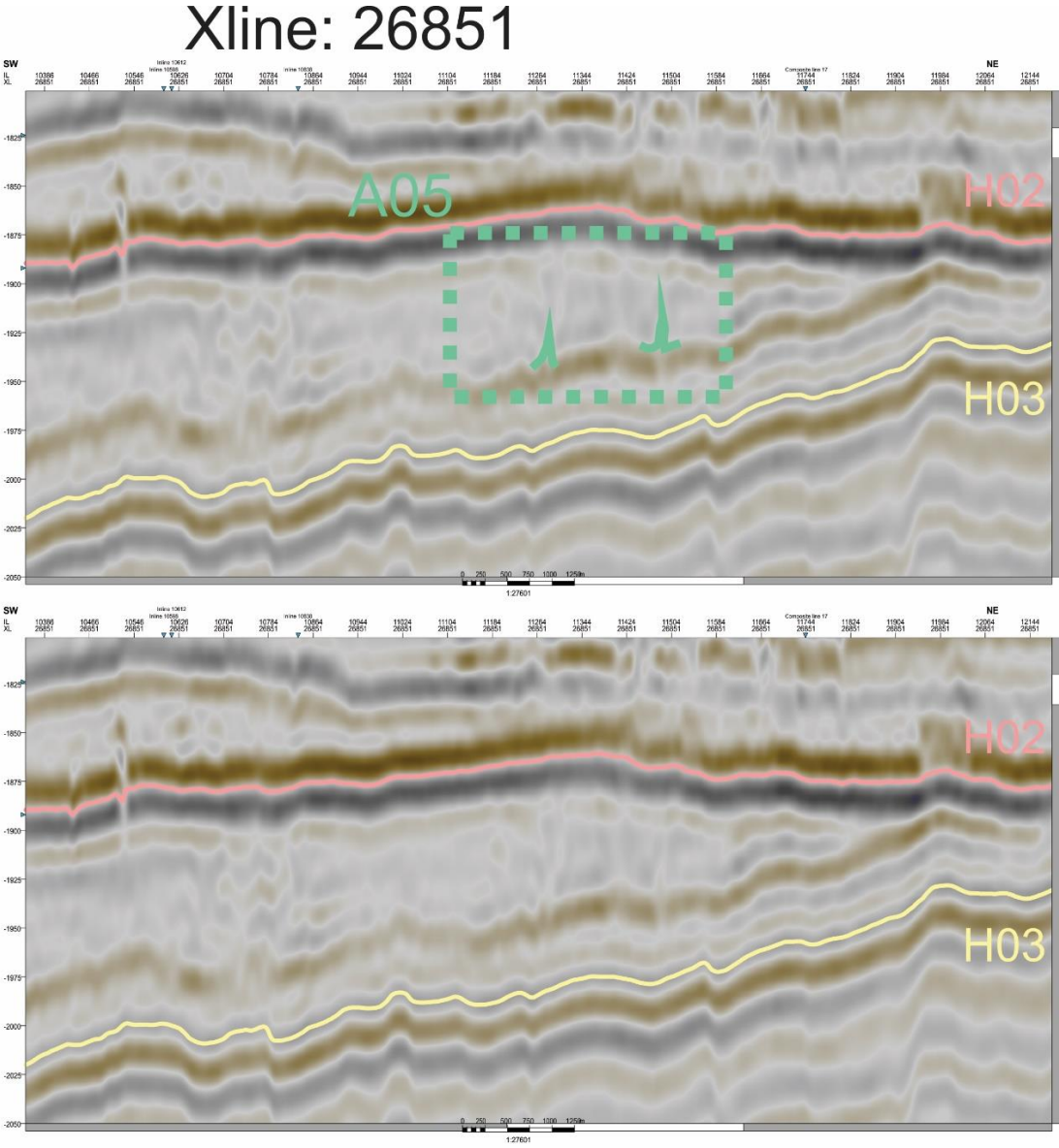


Figure V-18 The seismic line bisecting the Hairball

C. Horizon 03 – Offset: 85

Although the difference in two-way travel time is even lesser than before, the overall pattern drawn by Unit 1 is markedly different here.

The SE-NW alignment is still clear for the most part, A01, the Roll is visible, if not prominent, and A03 – Raindrop might be clearer at this depth.

On the other hand, the A02 Clusters are no longer a group of rounded spots, but an almost coherent, amorphous region of high variance values.

Likewise, the RMS image shows the Scars (Anomaly 04) but maybe less distinctly.

What makes this temporal offset noteworthy on its own, are the two instances of Anomaly 06.

At other depths, they are either missing, or are obscured by other features.

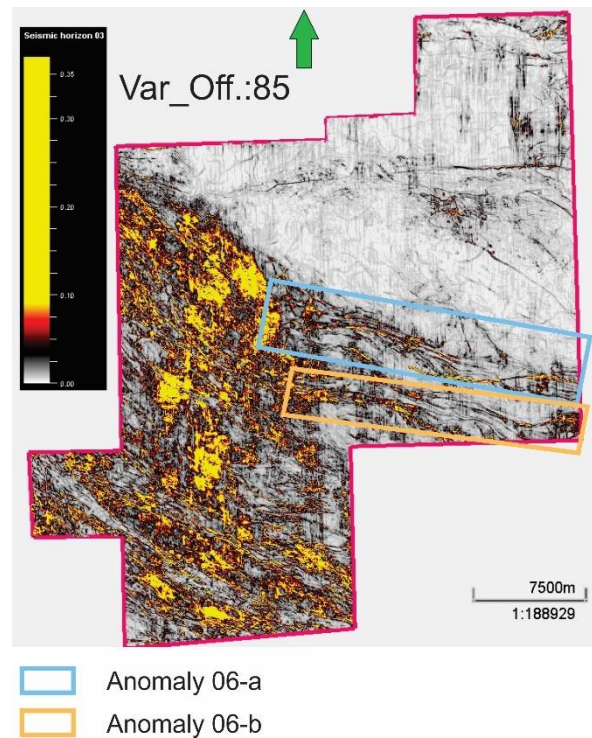


Figure V-19 Overall variance map of the study area at 85 milliseconds

d) Anomaly 06 – Riverbeds

These elongated structures are a duo of low variance strips of approximately 15 kilometers in length, in fact, it is mostly the surrounding high-variance material that give them contours (*general area marked on Figure V-19*).

They do not follow a straight line but meander instead, hence the name.

Nor are they uniform in width.

To emphasise their very similar characteristics, they have been grouped together and designated “Anomaly 06-a” (on the north) and “-b” (south), respectively.

They both extend beyond the eastern border of the study area, and their termination is uncertain – they both progress into a heavily distorted zone – the one that is dominated by the probable upward extensions of A02, mentioned in Chapter V, 1) A/b.

There is no one continuous layer running underneath either, but there is a slightly higher amplitude block beneath both – each of these objects showing signs of stress to a varying degree and sometimes connect to the bottom layer of U-1.

On the Xlines, neither “Riverbed” can be definitively separated from the surrounding material.

Both instances of A06 are similar, but they do have unique characteristics.

There is very little to differentiate A06-a from the amplitude signatures of the surrounding strata, so RMS images barely show the feature (neither 70 ms- or 80 ms offset).

The overlying layer (the top of Unit 1) is sometimes fragmented, and thickness changes as well.

The crosslines show it as an oblong mass with no internal features, but near the middle of the study area, where the structure widens significantly, some fragments might be present inside the “Riverbed”.

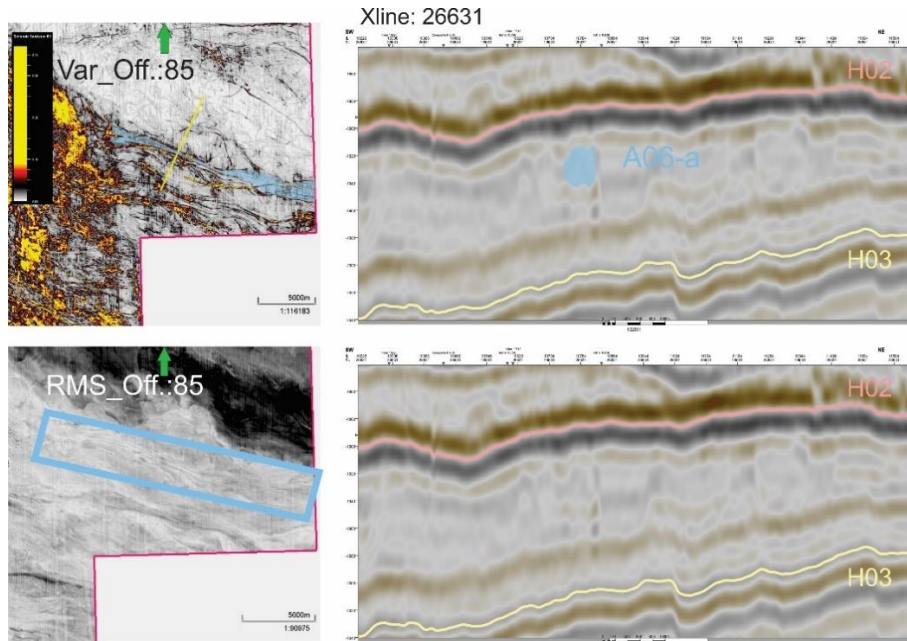


Figure V-20 The maps displaying the location of A06-a and a seismic line of its vicinity

Anomaly 06-b is generally wider, and mostly thicker than its northern counterpart, but there are momentary variations.

The notable differences are that the structure has a more pronounced amplitude signature and is arranged in a more regular tube-like shape on the seismic images.

The layer above does not break apart until near the southeastern boundary of the study area, and sometimes fragments of a different material definitely can be seen on the Xlines.

Also, it shows up more clearly on the RMS (80 millisecond offset) map, but not everywhere and so it would still be difficult to accurately interpret the feature based solely on this.

(see Figures V-20-21)

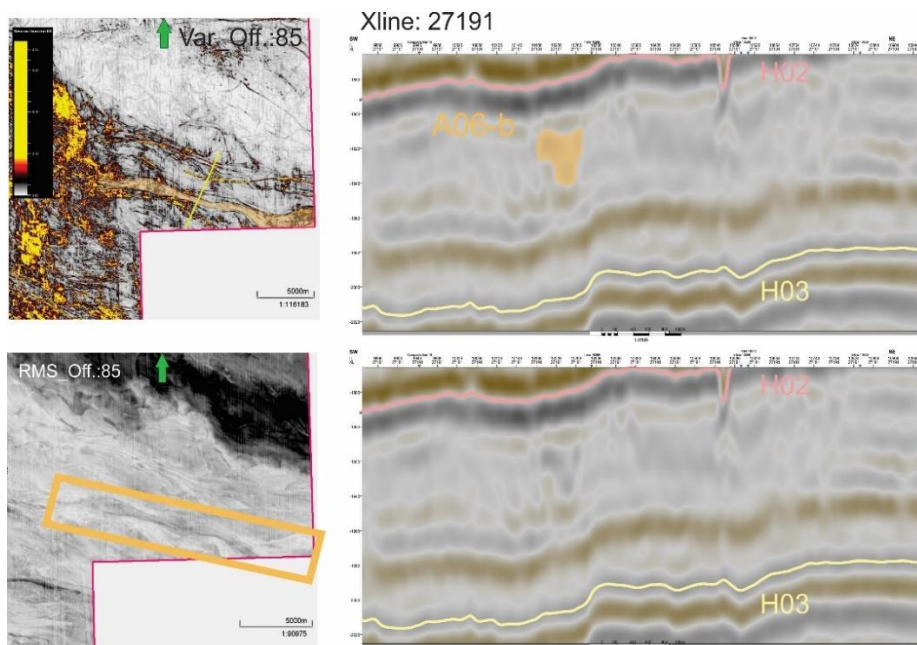


Figure V-21 The southern instance of Anomaly 06

D. Horizon 03 – Offset: 100

The last offset used to interpret the sediments between H03 and H02 has been drawn 100 milliseconds removed from the former and is already very close to the latter – in fact, both features described here belong to the higher horizon and only Anomaly 08 shows to have a discernible effect on the material of Unit-1. (Figure V-22)

A more detailed presentation will follow in the next subchapter (with the applicable attribute maps and seismic images of course), where both structures become pertinent.

At certain points towards the west, Anomaly 07 corresponds with the boundary of the northernmost extent of Unit-1, but the divergence steadily increases eastwards. In this area an offset of 100 milliseconds is already well above H02, and the structure is only mentioned here to avoid an impression of negligence.

Underneath A08, the crossline shows only a single layer of sediment between H03 and H02, no interruptions, and very little distortion.

Multiple vertical discontinuities can be found in the strata below H03, but the influence of these on Anomaly 07 is not discernible, also, none of them are a constant presence.

Anomaly 08 seems to extend down into Unit-1 from H02.

It starts beyond the boundary off the study area and progresses in a curved, unbroken line. The narrow, trough-like structure is already visible on an offset of 85 milliseconds but it clearly stands out from its surroundings on a variance map of an offset of 100 milliseconds. On the other hand, it is barely visible on the RMS image.

Approximately 5 kilometres from the eastern boundary of the study area the structure loses some of its prominence, but afterwards it becomes clearer again.

No clear indication can be found on the crossline as to why the imprint would become fainter momentarily.

As in the case of Anomaly 07, several discontinuities can be seen in the facies underneath H03, but none of these extend all the way to A08, and no other signs of stress can be identified on the immediate vicinity of the structure either.

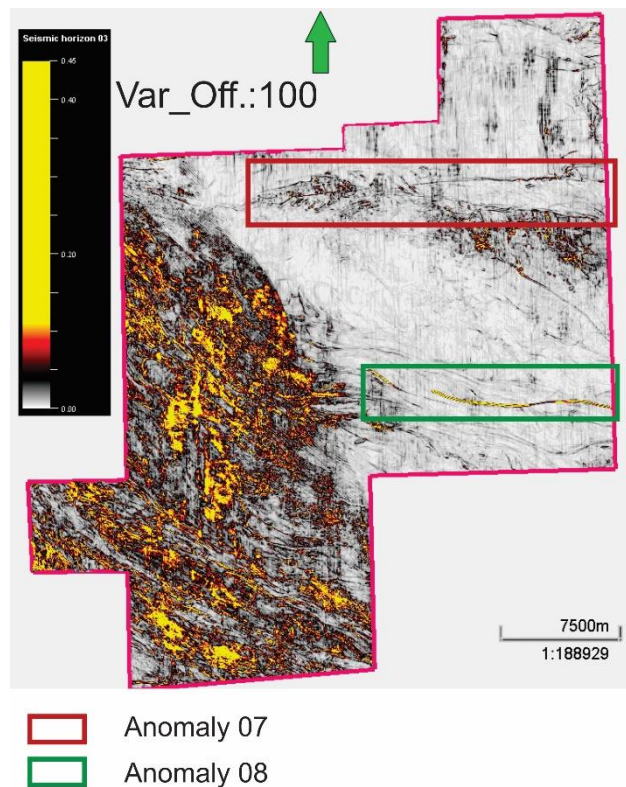


Figure V-22 Variance map showing the two anomalies "reaching down" from Horizon 02

E. Unit X

At the northern boundary a high variance area has been designated “Unit X”, which remains a constant presence between Horizon 03 and slightly above Horizon 01. (*Figure V-23, dark blue*)

On the Xlines, it seems to exert the strongest influence between H02 and H01.

Since it seems to be only a small part of a larger structure extending far beyond this study area, it has not been a subject of further scrutiny, but it will be mentioned at times.

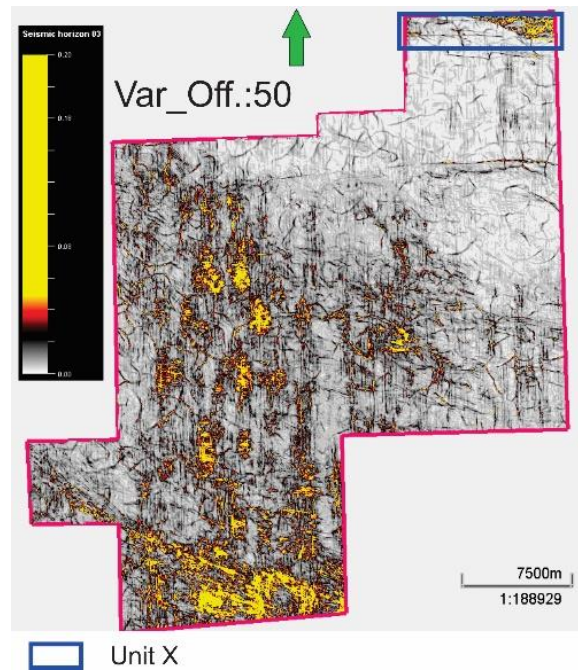


Figure V-23 Location of the visible portion of Unit X

2) HORIZON 02

The facies between the second and first horizons is generally thinner than the one between H03 and H02.

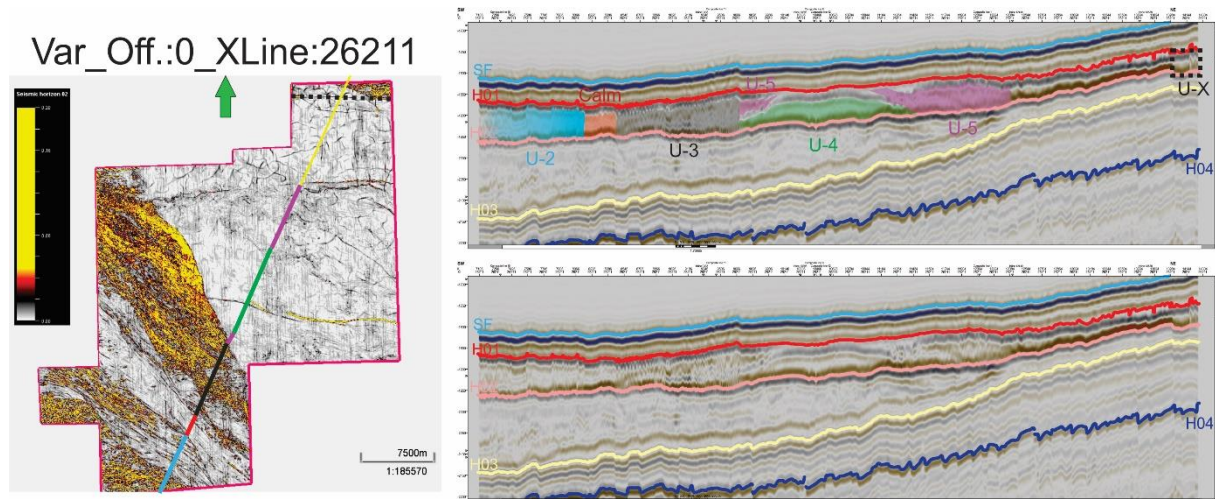


Figure V-24 The most comprehensive seismic image of the strata between H02 and H01

As in the previous subchapter, a complete cross-section of the study area was included here, based on which four main sedimentary units with markedly different properties were identified (*Figure V-24 above*).

Starting from the southwest, they have been designated as Units 2 through -5.

All but one of them extend beyond the range of the study area so precise dimensions cannot be established but based on the portions present, U2-5 all seem smaller than Unit 1 discussed in the previous subchapter.

The variance ranges of representation had to be increased on each offset with distance from the horizon; owing to this, a cursory comparison of the different variance maps might be misleading!

Furthermore, the component materials of Units 2, -3 and -5 are heavily disturbed and can be hard to comprehend.

Some notable structures and subunits were described, and for clarity's sake this subchapter is more strongly divided than the previous one.

Figure V-25. shows an incomplete selection of the various images generated with the Petrel Software Package to further illustrate the many aspects of these layers.

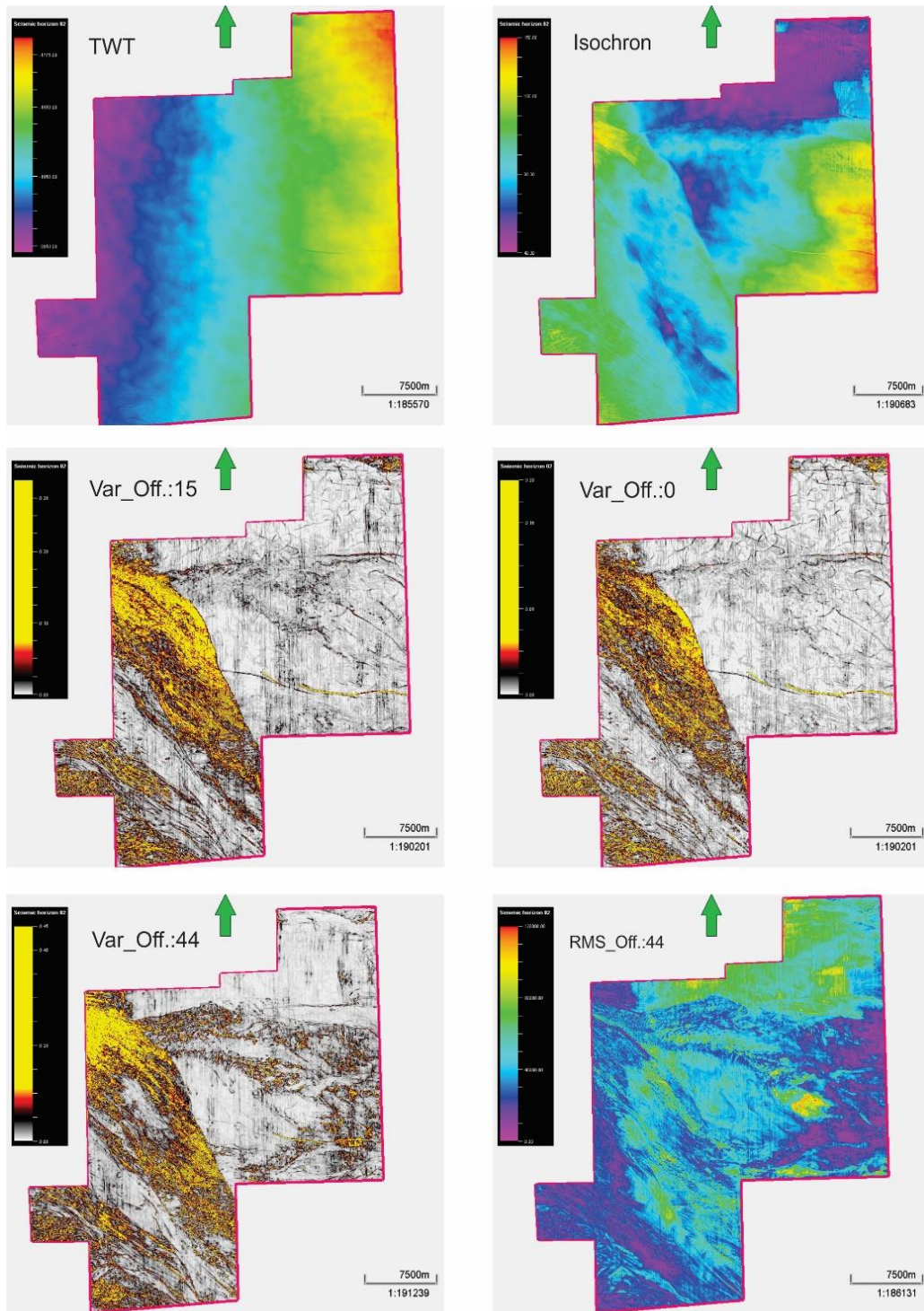


Figure V-25 The most significant visual representations of the study area

The order in which some of the described structures are presented is not sequential, as Anomalies 07 and -08 have been mentioned in the previous subchapter “Horizon 03”. To maintain a semblance of order, they are detailed alongside the two sediment masses (Units 4 and -5) where they are located.

A. UNIT-2

Unit-2 is located on the southern limits of the study area but extends further out of it.

The current elevation tendencies of U-2 suggest the composing sediment progressed along a SE-NW tangent .

The general appearance of the unit corresponds to the southern section of Unit-1 but H02 is clearly distinguishable, separating the two.

Based on the variance maps and Xlines, three subunits were identified as forming U-2. Subtle differences are also visible on RMS maps.

Neither the TWT- nor the isochron map shows very prominent differences, except in the case of some parts of U-2a, the southernmost one (Designation is “a-c”, once again in an ascending order starting from the south).

Some of the used images are included here on *Figure V-26*, on the right.

U-2a has a somewhat chaotic arrangement, as if the sediment unit has followed the general SE-NW tendency, but suddenly the entire subunit has rotated towards the south.

This is visible on the RMS map as well (*see Figure V-26.*), and U-2a shows a wider amplitude range when compared to U-2b and U-2c.

The overlying sediment appears smoother above U-2a when compared to the subsequent two subunits.

The ”rotated” sediments show increased thickness compared to the rest of Unit-2, but the difference is not extreme.

The middle subunit, U-2b, is a relatively narrow strip of low-variance deposit, but its width notably fluctuates. (*the variance map on the bottom of Figure V-27, associated with Xline: 25241 shows this well*)

One the Xlines, there is a very faint vertical

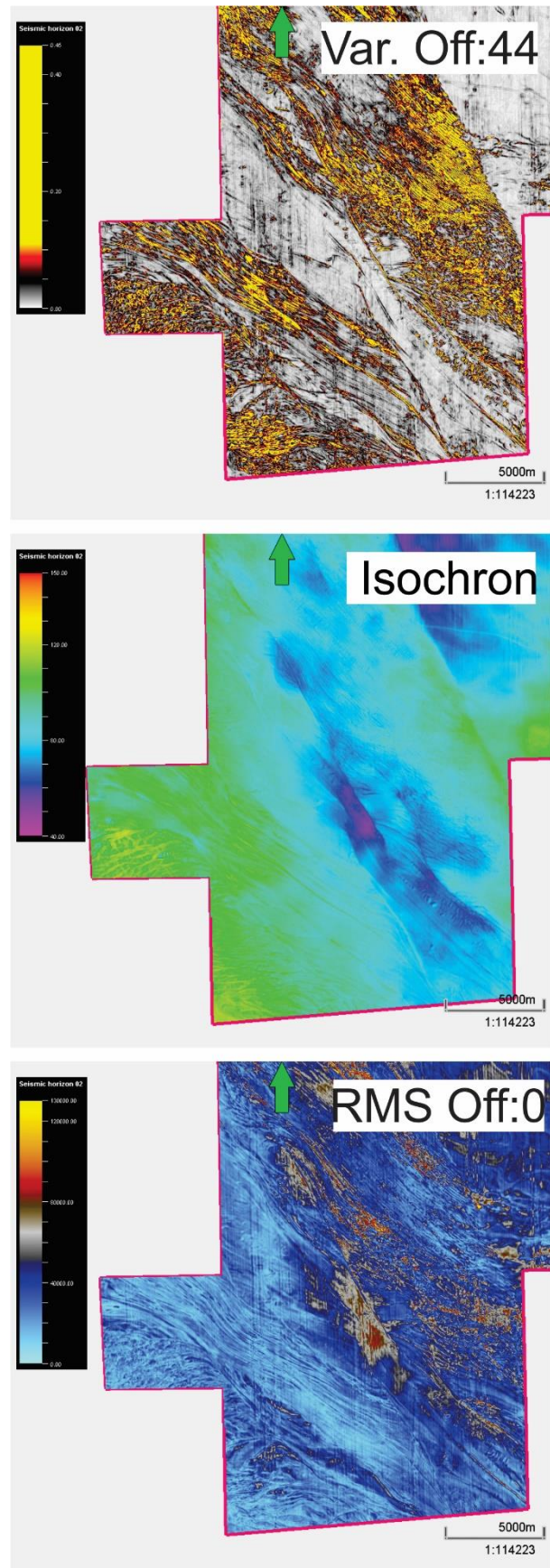


Figure V-26 Various representations of the southwestern portion of the study area.

displacement and a weakening of amplitude that demarcates U-2a from U-2b. The lower amplitude is characteristic everywhere under U-2b, but the degree to which the elevation shifts shows changes throughout. The nature of this division also varies; sometimes it seems like an organic shift, but at other places it is as distinct on the seismic data as a badly healed fracture would be. The boundary between U-2b and U-2c is a lot less prominent to the extent where its exact dimensions are hard to determine, as very little separates it from the next subunit on the seismic data. The amplitude shift is less noticeable but present, however there is no characteristic change in thickness here, and the composing sediments appear to be the same chaotically arranged mass with smaller, fragmented blocks within.

U-2c shows clear lineation in a SE-NW direction, and both H02 and H01 appear here as jagged lines. Internally, U-2c is disorganised and fragmented and a cursory observation might not make note of the subtle differences between U-2b and U-2c. Some of the blocks composing the subunit correspond to the uneven appearance of H01 here, but not enough to create a tendency – these are some momentary influences on the covering layer, but there are a large number of objects that didn't seem to have altered H01.

Figure V-27. shows how the three subunits described above have been separated. It is worth mentioning that near the southern edge of the study area the divisions become a lot less clear.

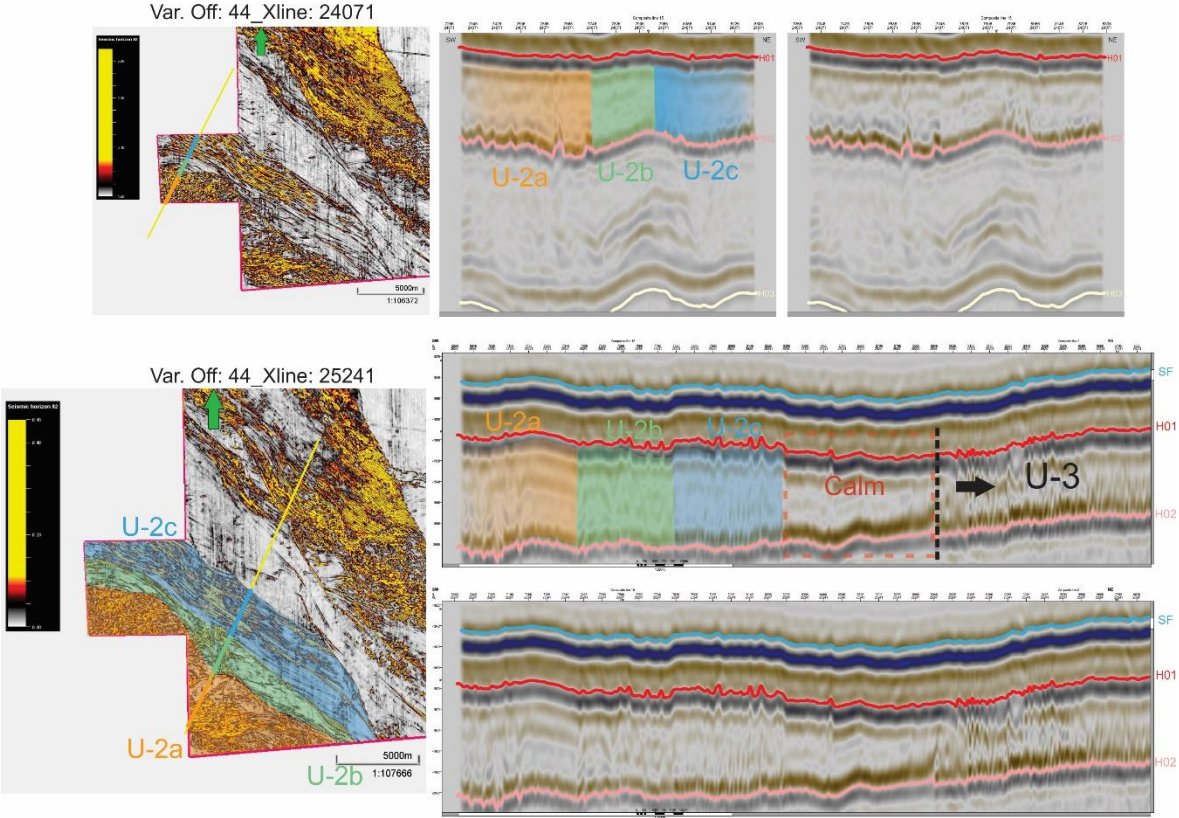


Figure V-27 Internal structure of U-2 and its subunits.

a) *Anomaly 09 - Spike*

There is, however, a noteworthy structure close to the mid-point of the subunit, whose appearance matches that of an upturned *Anomaly 08* - only less distinct since it is in a high-variance area to begin with. (*Figure V-28.*)

While normally the lineations form a pattern the way individual strands of hair make up an animal's fur, here is a single disproportionately long, coherent structure found in the subunit. As if an inverted, narrow channel had developed on H02 and imprinted itself on the subsequent deposits, all the way up to the seafloor.

There are plenty of similar anticlines both in- and outside of U-2, but this Anomaly 09 seems peculiar when the surrounding material is examined for signs of stress and there is also no indication of a tectonic trigger associated with the feature.

A comparison with the portion of U-3 shown on *Figure V-28.* should support this observation of A-09's singular nature.

At times, a clear discontinuity is present on the Xlines below H02 here (X:26121), but nothing was found on the variance maps belonging to offsets of H03.

No cause has been identifiable on H02 itself either.

This structure progresses beyond the study area to the south.

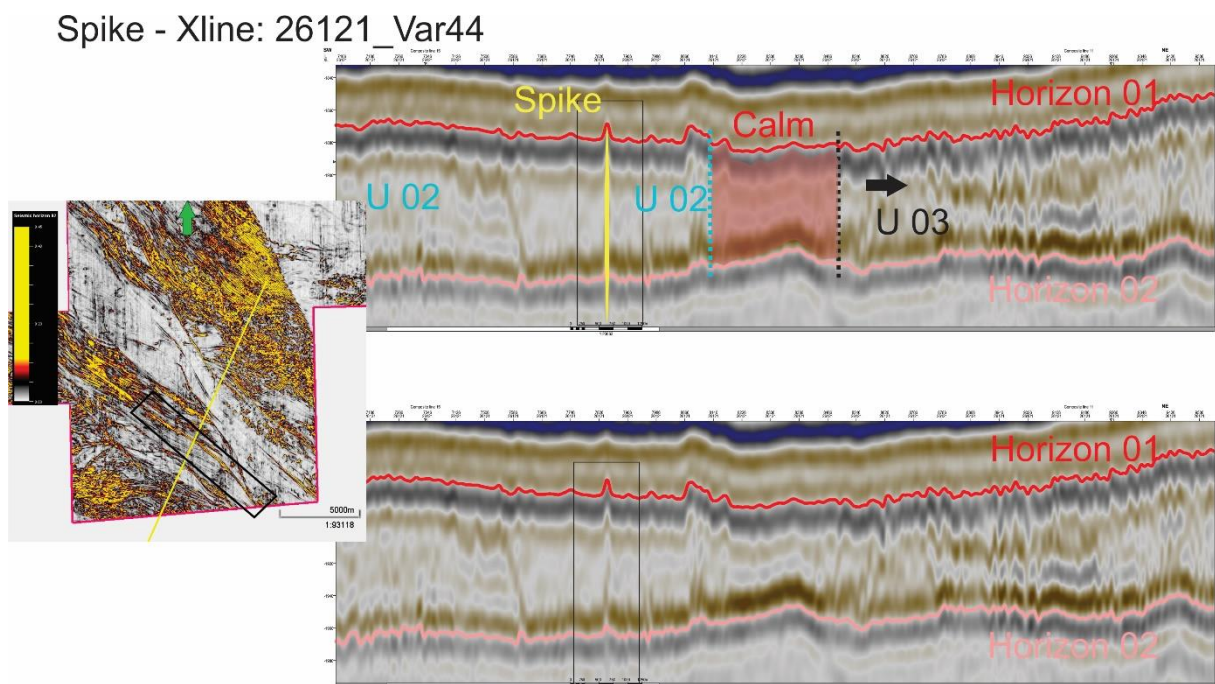


Figure V-28 The feature designated "Spike" and its environs.

b) "Calm"

Separating U-2 and U-3, an irregularly shaped area of low-variance can be seen. Like them, it extends beyond the study area both on the NW and SE. What clearly distinguishes it from these two units is a the comparatively few markers of stress. The "Calm" area's change in internal arrangement from U-2 is very sudden, and although this is less so with Unit 3, the change in depth and amplitude range are fairly distinct on *Figure V-29*. Faint shifts in amplitude can also be seen in the composing layers elsewhere. The RMS map shows obvious boundaries with both U-2 and U-3, but the general amplitude signature closely resembles that of the latter. On the isochron map, some notable changes can be seen, separating "Calm" form U-3, but these are not universal enough to form a tendency. When compared to Unit-2, while the localised depths of "Calm" are markedly different the changes in thickness of component sediments follow the same NE-SW thinning tendency of U-2. There is enough to differentiate "Calm" from either adjoining units, but some factors suggest it might be a part of either too. For this reason it was not assigned as one of the major sedimentary entities, but it still warranted detailed description to showcase to transition from U-2 to U-3.

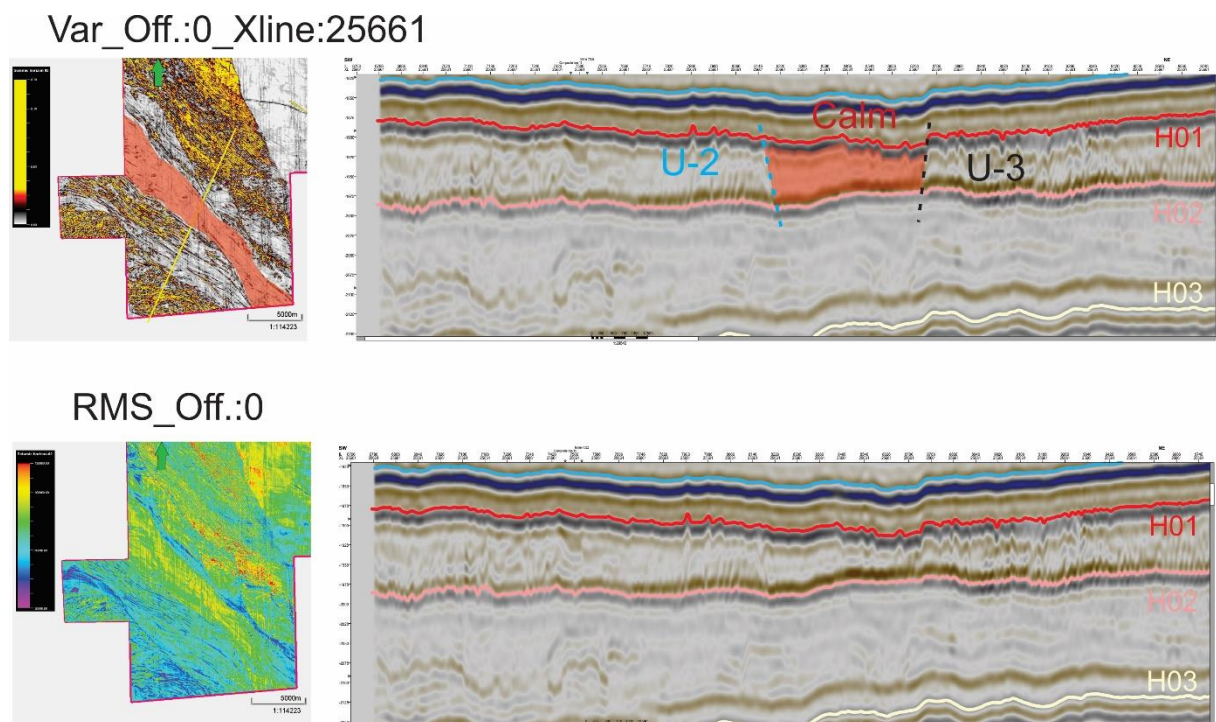


Figure V-29 The band separating Units -2 and -3

B. UNIT-3:

Unit-3 bisects the study area diagonally. Similarly to U-2 and the "smoother" area between the two, its full extent is unknown as it progresses beyond the study area on both the SE and the NW. Its general appearance shows a SE-NW lination; local variations occur, especially near the points where the unit exceeds the study area, but deviations are minor - there is no change in tendency.

Moving towards the NW boundary, U-3 widens laterally and is slightly rotated to a more westerly direction. As discussed above, the transition between U-3 and the calm zone to the SW is sometimes challenging to determine, but is characterised by a shift in signs of stress, and the amplitude signature of the layer underlying U-3 is slightly weaker - this aligns with stress markers, since less disturbed parts of U-3 to the NE seems to show the same amplitude as the "Calm" (X:26071 – see Figure V-31).

On the other hand, the northern/north-eastern boundary is very distinct. The RMS map in the bottom of Figure V-30. shows some variations that are significant in amplitude range, but not in lateral extent, which seem to follow the lateral deposition pattern of U-3 - The unit maintains its "striped" appearance on the RMS maps. The overlying layer (H-01) looks extremely jagged above the entirety of U-3, although local variations occur corresponding once again to the shifts in amplitude. This is shown on Figures V-31. and -32.

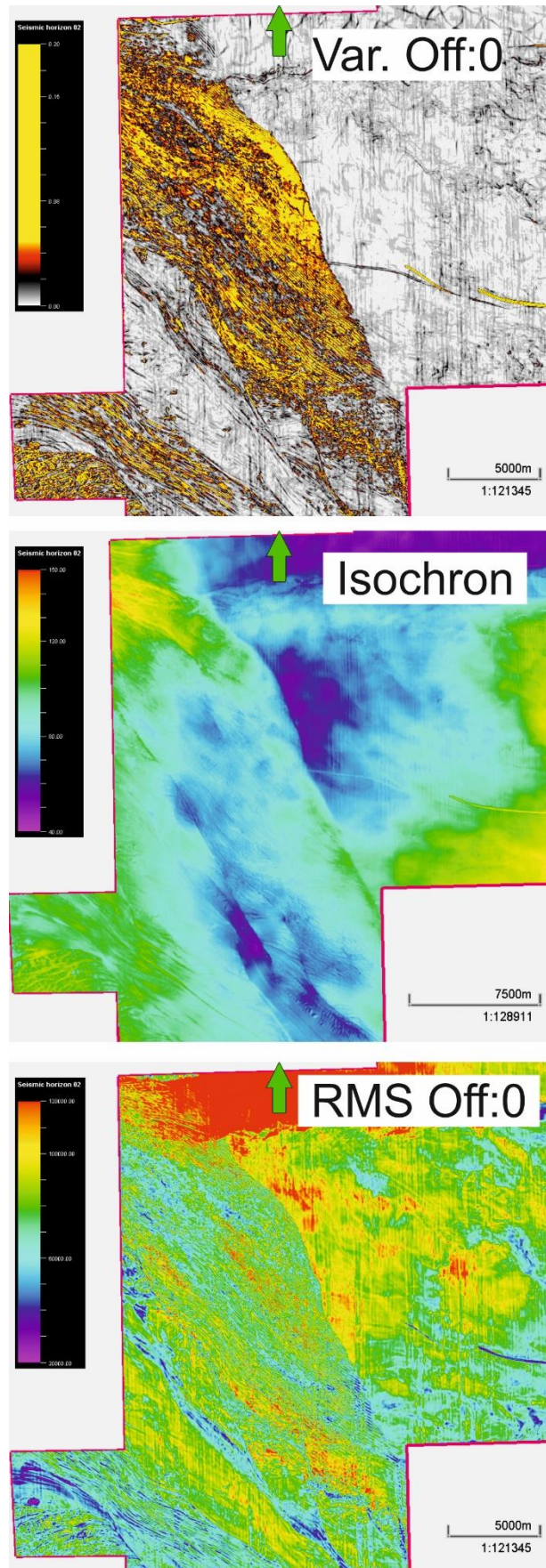


Figure V-30 Unit 3 in the middle of the study area

Var_Off.:0_Xline: 26071

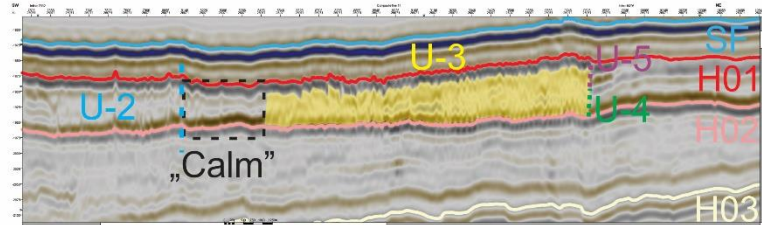
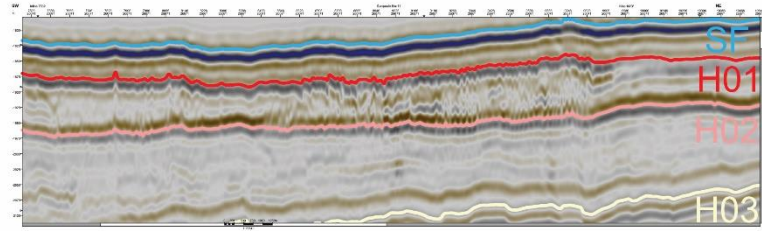
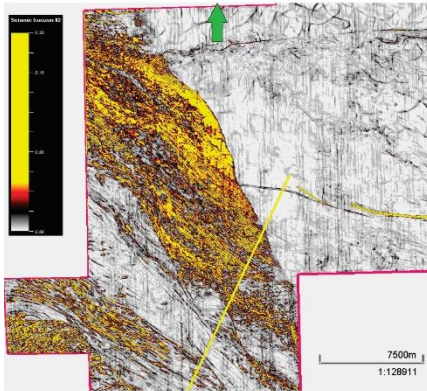


Figure V-31 The southeastern part of Unit 3

Var_Off.:0_Xline: 24051

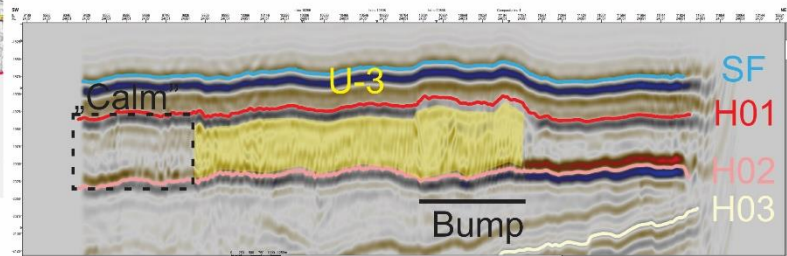
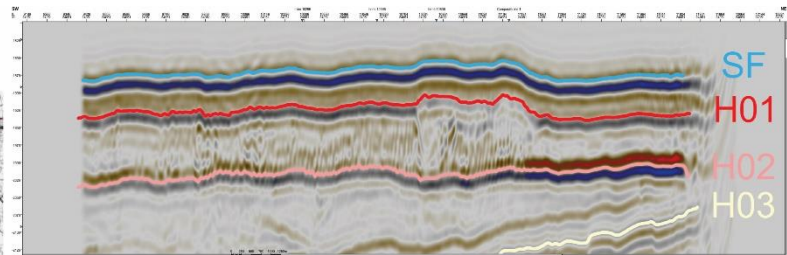
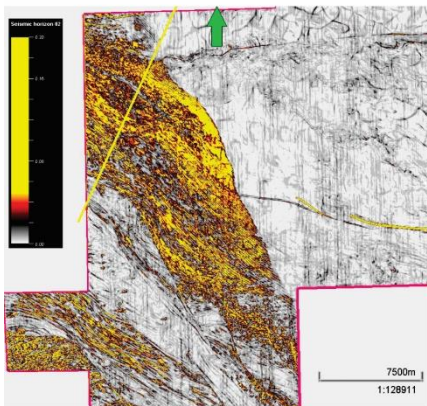


Figure V-32 The northwestern part of Unit 3 with the anomalous internal structure ("Bump")

a) Anomaly 10 - Bump

Generally, U-3 slightly thickens from SW-NE, and nearing the NW boundary of the study area, but only one anomalous shift occurs, in the form of the "Bump". Inside U-3 there is a (5-9 km long, but only some tens of metres wide) strip with a markedly lower variance signature that is not distinctive on the Xlines. This strip marks a divide between U-3 and a smaller subunit of the same that seems slightly elevated from the rest, but similarly distorted on Xline – saying it is "stretched out vertically" would not be a stretch. This subunit is 2.5-3 kms in width and maybe 13 kms long.

Difference in elevation is most prominent near the edge of the study area and becomes gradually indistinguishable with progress towards SE, but the amplitude signature of the

overlying layer remains distinctly lower. (same layer continues in both directions laterally). A variance map (Off.:0) only shows the "calm" borderline inside U-3 as distinct (*see Figures V-30-32*); based on the same image, the lineation inside Anomaly 10 is the same as in the rest of Unit-3 – aligned SE-NW.

The variance of higher offset maps (Off.:60) show the shift in elevation but it doesn't seem distinct enough to warrant further observation, however the Xlines do reveal something interesting here.

The portion of U-3 designated "Bump" actually appears to subside with southeasterly progress, leveling out around X:24520.

Figure V-33 illustrates the structure at multiple points (showing not the transition itself, but close to the two extremes of A-11).

Moving further towards the southeast, A-10 ends up significantly lower than the rest of U-3. The overall thickness of the mass between H01 and H02 shows very little variation, because the resultant bowl-like depression may have been filled with sediments, which have a distinctly lower amplitude signature.

Following this overlying mass reveals how it seems to be the same material as that covering U-4, and much of U-5 as well.

(Since the isochron map doesn't reflect this shift (*see Fig. V-33*) and the material of U-3 shows significant indications of stress this was initially missed – the amplitude change was discovered to be significant later, during interpretation of H01)

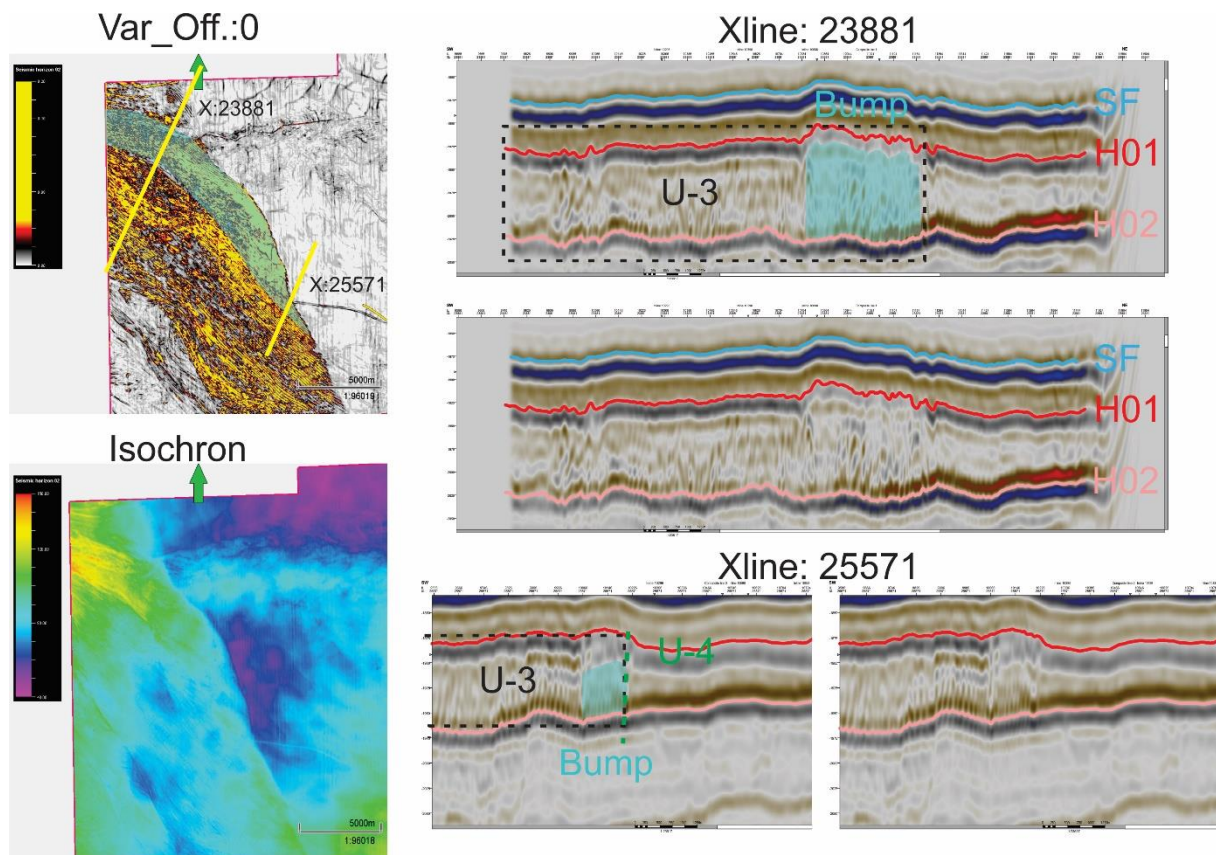


Figure V-33 A closer scrutiny of Anomaly 11

b) *Anomaly 11 - Spots*

Also noteworthy are some sizeable areas with comparatively lower variance inside Unit 3 that present as smooth fields surrounded by high variance deposits.

On the other hand, they are not particularly noticeable on most RMS images.

There is SOME difference, (RMS30) but if one were to examine the RMS image by itself, they might not be prominent enough to draw attention.

Best seen on the variance map with an offset of 44, the largest of them are ~7kms in length, and ~2kms in width, with local variations.

Internally, the seismic Inline (I: ~10112) shows this field as less fragmented compared to the adjoining deposits – so does the Xline, but the difference seems less distinct.

The overlying layer is relatively even, but this is not restricted to the extent of this smooth field (see *Xline:25881* on *Fig. V-34* for comparison).

The smaller smooth spot to the south is more distinct on the Xline and both the over- and underlying layer is less disturbed here than in adjoining areas.

Once again, the difference on the Inline stands out more.

Another low-variance area at the SE (*In:8852/X:25881*) shows on the seismic data as a less-disturbed, slightly elevated block of sediment (no marked elevation change compared to the rest of U-3, but a sharp drop compared to the area to the immediate south - minor changes on H02, no tendency).

Apart from the slight elevation shift (see *Figures V-30* for the *isochron map* and *Fig. V-34* for the *seismic images*), the field's appearance on variance maps, its amplitude signature and component layers' shape all make it more similar to "Calm", than to the rest of U-3.

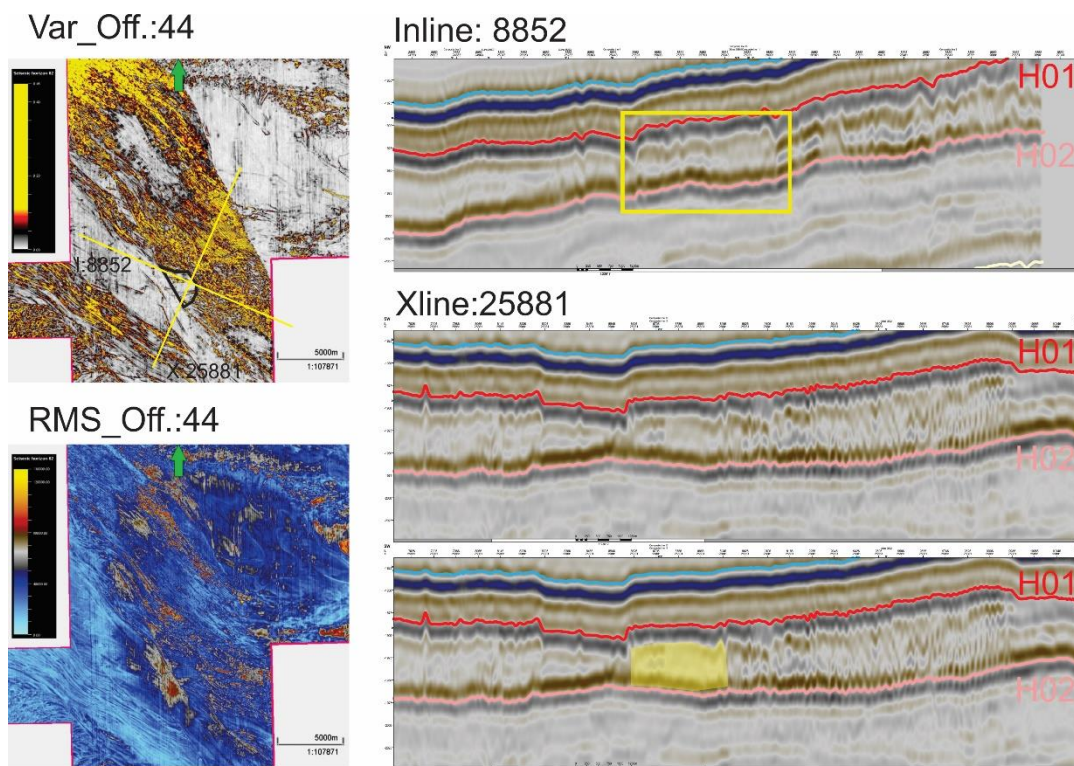


Figure V-34 A chosen representative of the areas designated A-11

C. UNIT 4

Unit 4 is vaguely triangular field in the center of the study area.

On the W-SW it meets U-3, forming a sharp divide on variance and isochron maps, and likewise the seismic data, but the differences displayed by amplitude signatures can be less pronounced, depending on the used offsets.

U-4 has relatively low variance throughout, the RMS maps display an increasing attitude towards the NW, especially near the U-3/4/5 triple boundary (this is best seen on the RMS map with an offset of 0), while the “RMS_Off.:44” map shows an irregular rippling pattern. *Figure V-35* was included for the sake of these comparisons.

From the north to south-east, U-5 surrounds U-4, with a smaller, possibly unaffected section of U-4 extending beyond the study area to the S-SE, although the seismic data shows there is another layer above U-4 there reaching out from U-3, but this layer is far less distorted than U-3, which complicates interpretation (*see Figure V-36*).

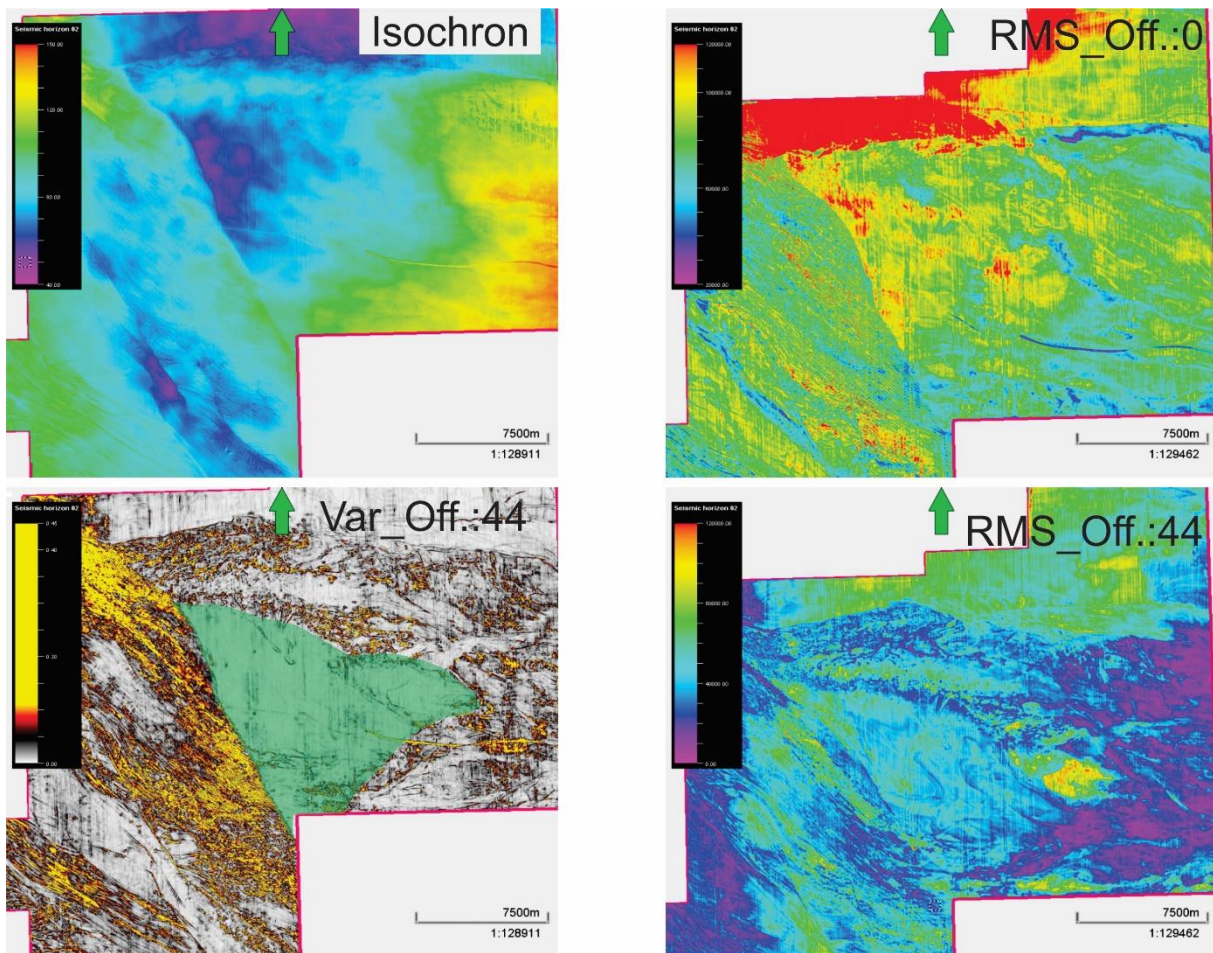


Figure V-35 Some of the generated maps of Unit-4.

At the eastern tip of the triangle, there is a partition of approximately 7km in length and 3km in width, with notably different properties.

On the variance map (*Off44*) it has a distinct border, and “RMS_Off.:44” shows markedly higher amplitudes in this area than anywhere else in U-4 at this depth (*see Fig. V-35*).

It is, however, completely unnoticeable on the isochron map.

The seismic data shows that there is another layer of sediment on top of U-4 at this point again that is heavily fragmented at places.

The Xlines depict the unit as a slight anticline, a relatively smooth, unbroken line from one end to the other, no stress markers and very few internal features.

On the Inlines, the overall shape of the unit is less pronounced, usually just a straight line following the general slope angle of the study area, although some momentary differences are visible.

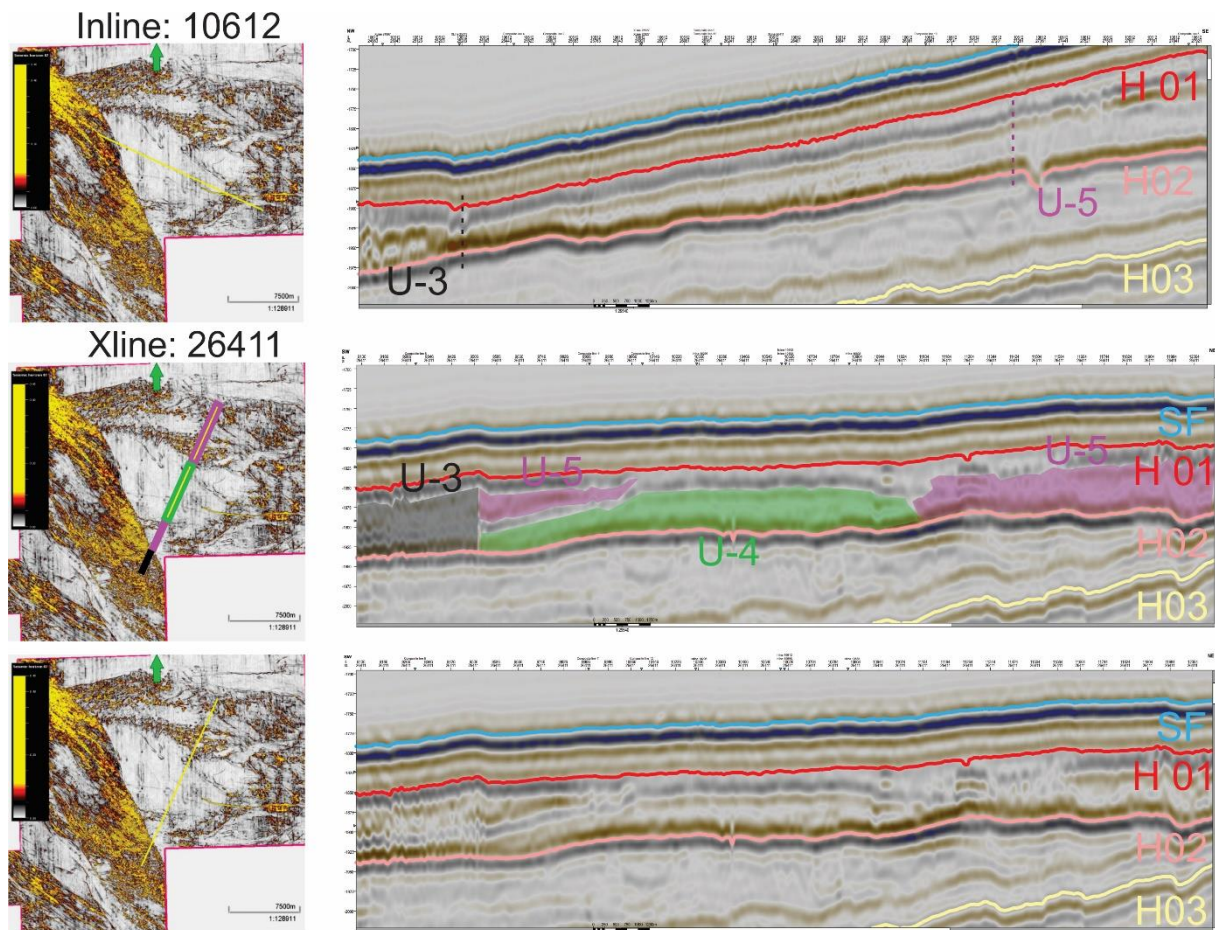


Figure V-36 Cross-sections of Unit 4

a) *Anomaly 08 - Channels*

In the previous subchapter “Horizon-3” a pair of linear structures have been mentioned.

Although the examined offsets of H03 have shown them, and they indeed seem to have created an impression extending into the sediment below H02, the structures themselves are located firmly atop H02.

In addition to the previously described two, a third such feature can also be found further to the west.

Starting with the most prominent of the three, extending out of the study area to the east, they have been designated A08-a, -b and -c (*Figure V-38, for a composite image showing each*).

The totality of the Channels adds up to a length of approximately 20-22 kilometres, over half

of the width of the study area at this point. While a good portion of A08-a is located underneath U-5 it extends well into U-4, and both A08-b and -c is located entirely on the bottom of the latter, although A08-c might continue on below U-3.

Owing to the disorganised internal arrangement of Unit 3 this can not be verified. (see Fig. V-38, X:25661)

Each of the three channels seems to gain some depth with westward progress, with momentary fluctuations, but not to the same degree. (shown on the isochron map of Fig. V-37.)

Furthermore, none of them appear to progress in a completely straight line, but rather following a light serpentine.

A08-a: The vertical extent of the structure is largely constant, with slight but gradual shallowing W-E until X.:27790, where A08-a almost disappears.

It starts to deepen again around X.:28000 and remains largely constant until this first channel leaves the study area on the east.

At X:26861, RMS maps with higher offsets (44-60) possibly show a rounded object at the termination of A08-a – also seen on the Xlines.

A08-b: It terminates at ~X:26200. Gradually loses its prominence with E-SE progress, and disappears around X.:26721. Might reappear around X.:26870 but this could be a coincidental alignment with a separate structure. The meandering shape is perhaps the least pronounced in the case of A08-b.

A08-c: This third channel is very faint, even less than A08-b; merges into U-3 at around X:25581.

A08-c shows very little change in vertical extent (between -1900-1950 ms)

This smaller channel seemingly separates from A08-b at ~X:26501, and has an even less pronounced vertical effect than that of A08-b.

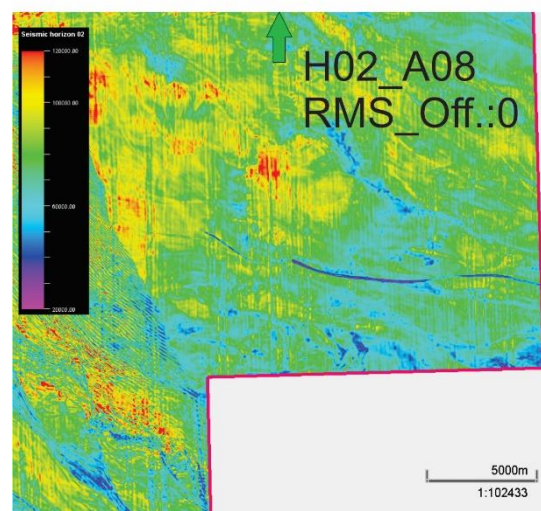
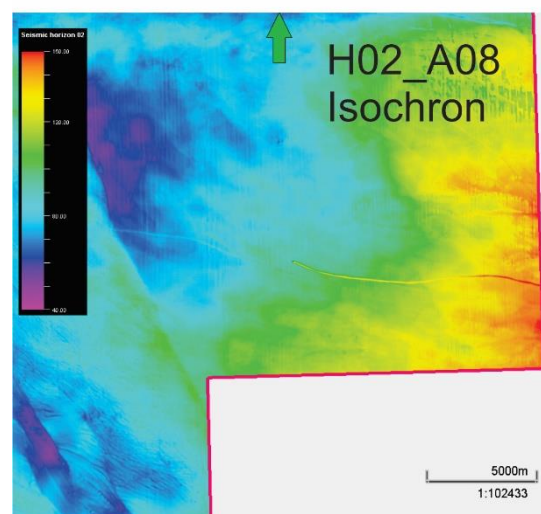
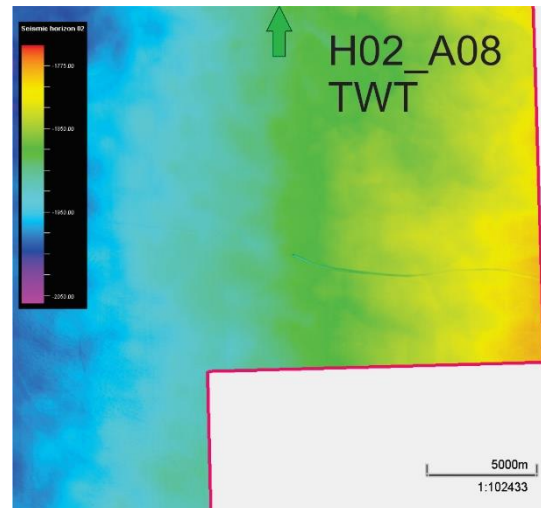
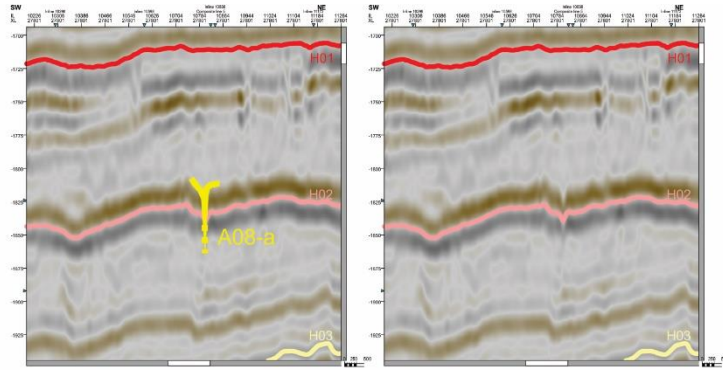
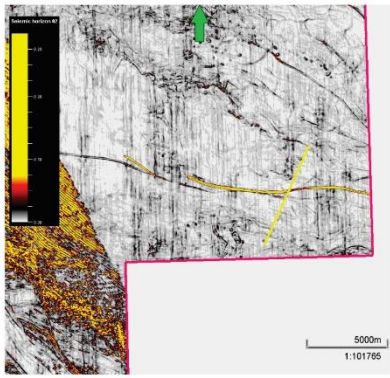
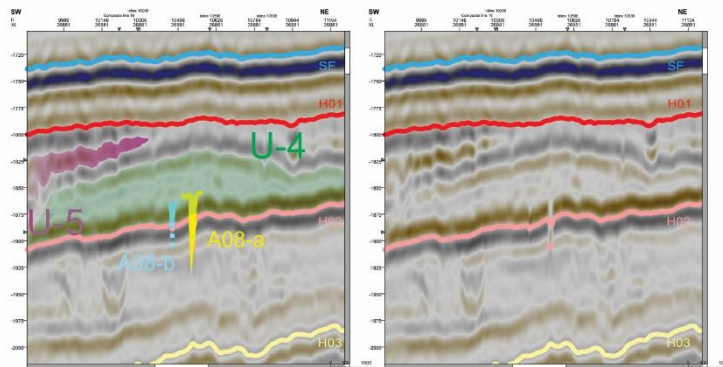
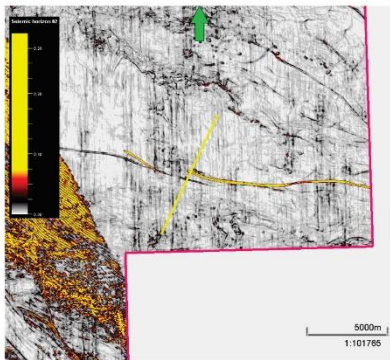


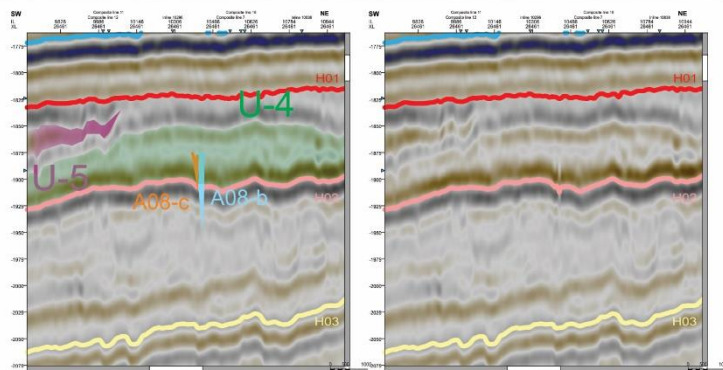
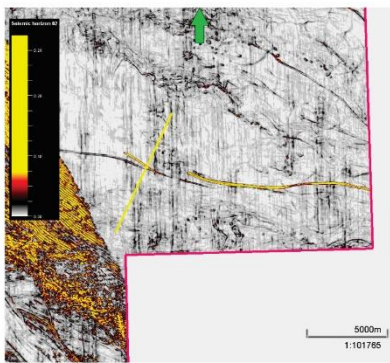
Figure V-37 Representations of A08's surroundings



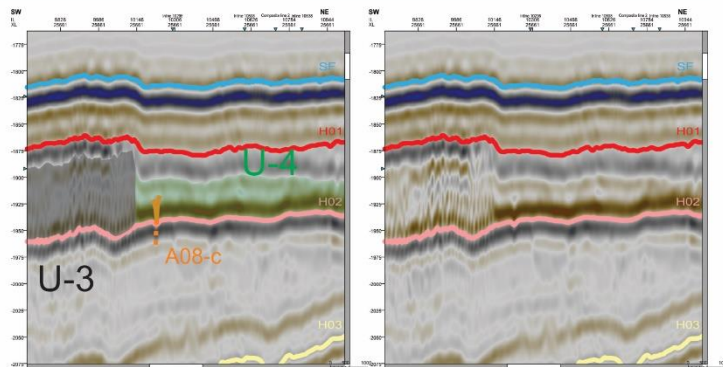
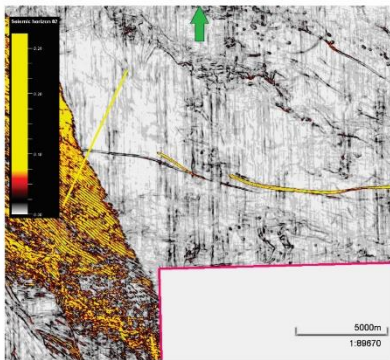
1. Xline: 27801



2. Xline: 26881



3. Xline: 26461



4. Xline: 25661

Figure V-38 Cross-sections of A08 from east to west

On the northern boundary of U-4 there are a number of vaguely linear features. Two of them have been chosen as representatives, but these are only notable for their shapes and because they are found in areas with lower variance where they are largely unconcealed.

b)

Anomaly 12 - Pipe:

A structure that looks somewhat similar to “A08 – Channels” on the seismic images, but is located at a slightly lower depth can be seen just shy of the northern boundary separating Units 4 and -5, with the majority of it inside U-4.

It has a distinctive smoking pipe-like shape.

Multiple spherical objects can be seen on the seismic images, the largest of these were found on X:25981 – they seem to be decreasing in size from SE to NW, but the change is rather gradual.

The two specific Xlines shown on *Figure V-39* were chosen to show both the more prominent end of the “Pipe”, where its originator would have reasonably been expected to be located, and the two “prongs” of the structure clearly separated (and not for the somewhat comical, facelike appearance of X:25851).

The small oblong’s path (*displayed on the variance maps of Fig. V-39*) appears slightly more erratic than the one of A-08, as if it was carved out by an object that has bounced around mid-movement.

The underlying sediment layer has small, but clearly defined indentations below the structure which helps to differentiate between it and other globular objects in the surrounding material.

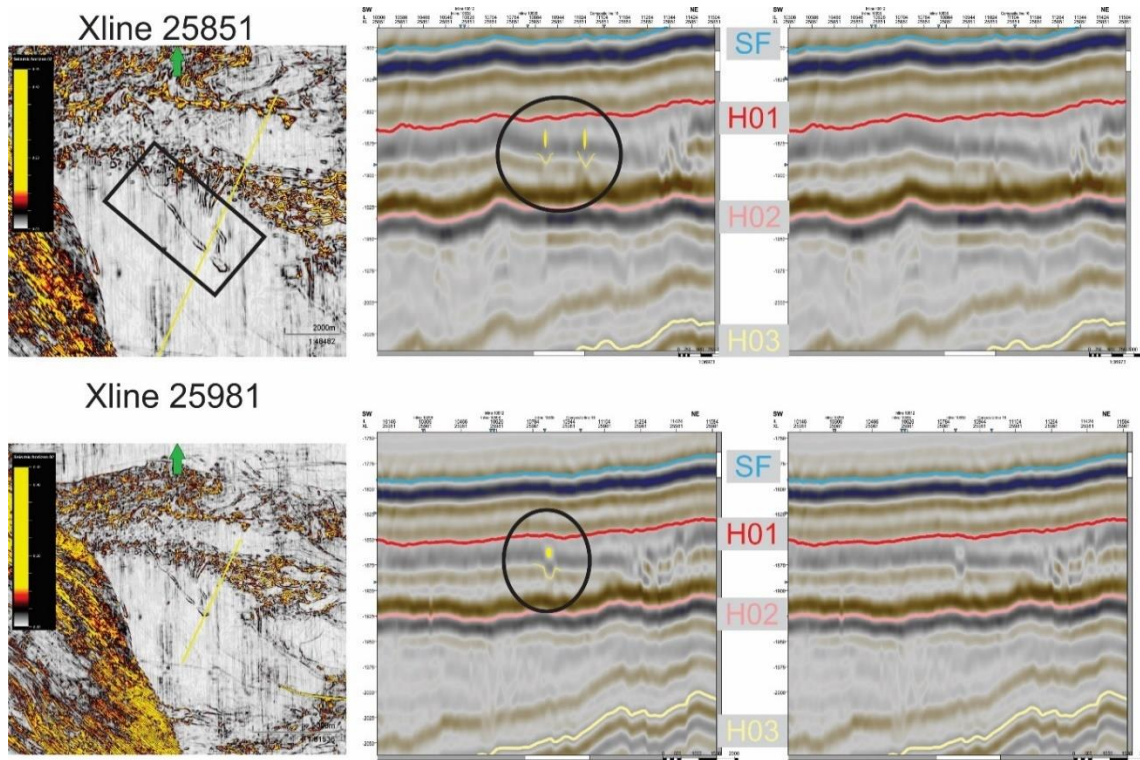


Figure V-39 Xlines from near the southeastern termination of Anomaly 12

A12’s depth increases towards the NW.

The Pipe causes no alterations in the overall volume of U-4 and is completely invisible on the

isochron map, but there is a faint amplitude anomaly associated with it, although not enough to be really prominent on the RMS image - it is merely a part of the general pattern of U-4 (see relevant images of Figure V-35).

c) Anomaly 13 - Hoofpick

Yet another feature has been dubbed “Hoofpick” and is located to the north of the “Pipe”, most of it directly alongside the southern edge of U-5.

Because of its arrangement, it was examined at first on the Inline (starts ~IN:11172) and seen as one in a chain of many irregularly shaped smaller rounded objects (see Figure V-40). Each has an imprint on H02 and a strengthening of the amplitude anomaly in the layer between them and H02.

The structure “rotates away” around I:11292 (not included here, not distinctive). After that point, the feature must be followed on the Xline (X:25901 and further, seen on the lower half of Fig. V-40) but little else has changed about it - irregularly shaped object, small depression underneath and slight amplitude anomaly; however there is no more "chain", the neighbouring areas show only a handful of similar "pebbles" to the SW and a continuous feature to the NE, none of which seem to connect.

It is faintly visible on the variance map of H02, and is indistinguishable from similar features on the 44 milliseconds temporal offset.

Also invisible on Isochron map.

The image “RMS_Off.:22” shows the “Hoofpick” possibly continues or meets another feature just like it (even though the objects are very small, the seismic data shows how A13’s shape changes suddenly, which makes it seem like they are merging, but uncertain).

The SE-NW-aligned part of the structure is approximately 1.2 kilometres long and NW-SE-aligned part is over 2km, if the possible continuation seen on the RMS map is disregarded. (Because of the objects’ small sizes, the previously used methods of highlighting were deemed counterproductive.)

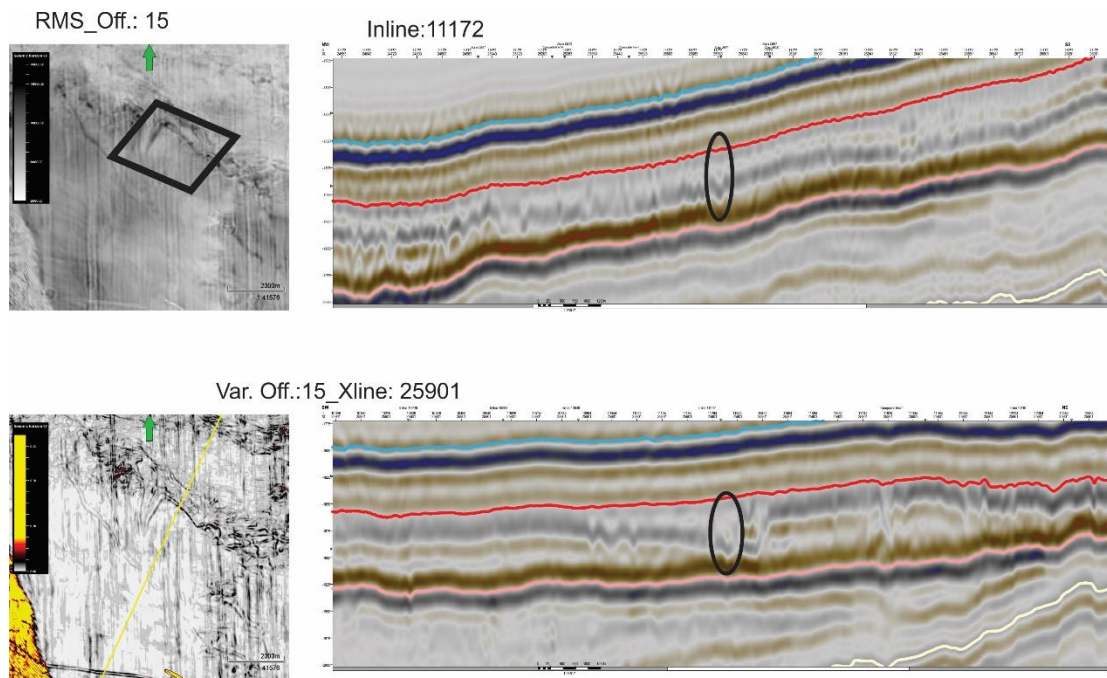


Figure V-40 In many ways, Anomaly 13 closely resembles A-12

D. UNIT 5

Unit 5 is an opened beak or chela-shaped mass located on the eastern half of the study area. It extends beyond its eastern and south-eastern boundaries and based on shape and apparent tangent of deposition, it would be reasonable to assume that the part visible here is only a small portion of an enormous sediment mass (see Figure V-41).

Of the examined offsets of Horizon 2, an offset of 44 milliseconds seems to be the best option for interpreting U-5. On this variance map, the overall pattern exhibited by the component sediments is quite chaotic, the

individual elements often curve, change direction, and are of varying, but limited size; the amplitude shifts are momentary as well, so establishing a general direction of progress for the unit is difficult.

The isochron map shows a E-W decrease (Fig V-42, in the middle).

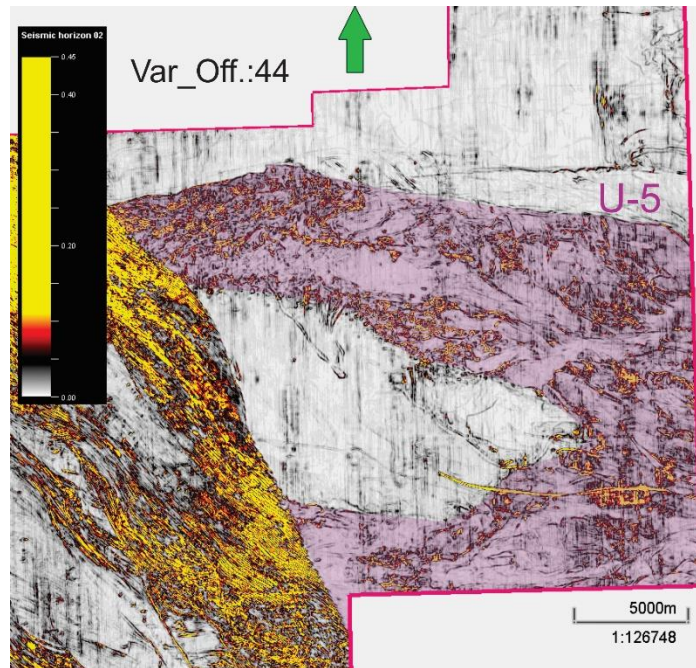


Figure V-41 The overall shape of U-5 highlighted

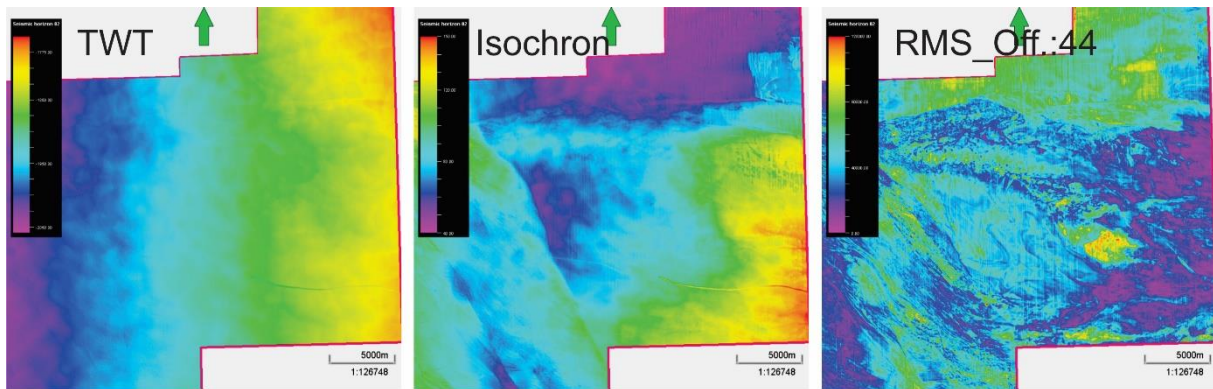


Figure V-42 Various representations of Unit 5

The bigger, northern part of the unit terminates against U-3, and while the variance map suggests a merging of the two and the differences in amplitude do not significantly differentiate between the units, both the isochron map and the seismic data shows an extremely sharp boundary.

The amplitude signature of the overlying layer is roughly the same as in the "Bump" section of U-3.

The RMS map on Figure V-42 shows that for the most part there is very little difference in amplitude ranges when compared to either U-3 or U-4, but the eastern portion of Unit 5 shows a markedly lower value.

While the component layers seem the same, and are equally fragmented, the sediment that makes up U-5 is much less distorted than those inside U-3, and there is also an immediate drop-off of around 10 milliseconds between the two. (X:24701, see *Figure V-44*) This is consistent all along the ~5km length where the two units "meet".

U-5 almost completely encompasses U-4, but their respective amplitude ranges are not markedly different, and eastward decrease in thickness is not distinctive enough to clearly separate the two units.

An arbitrarily chosen composite line (17) running through both the northern and southern part of U-5 as well as the atypical partition of U-4 shows how both the seismic data and the variance map displays the same characteristics in the two segments.

To illustrate, *Figure V-43* was included.

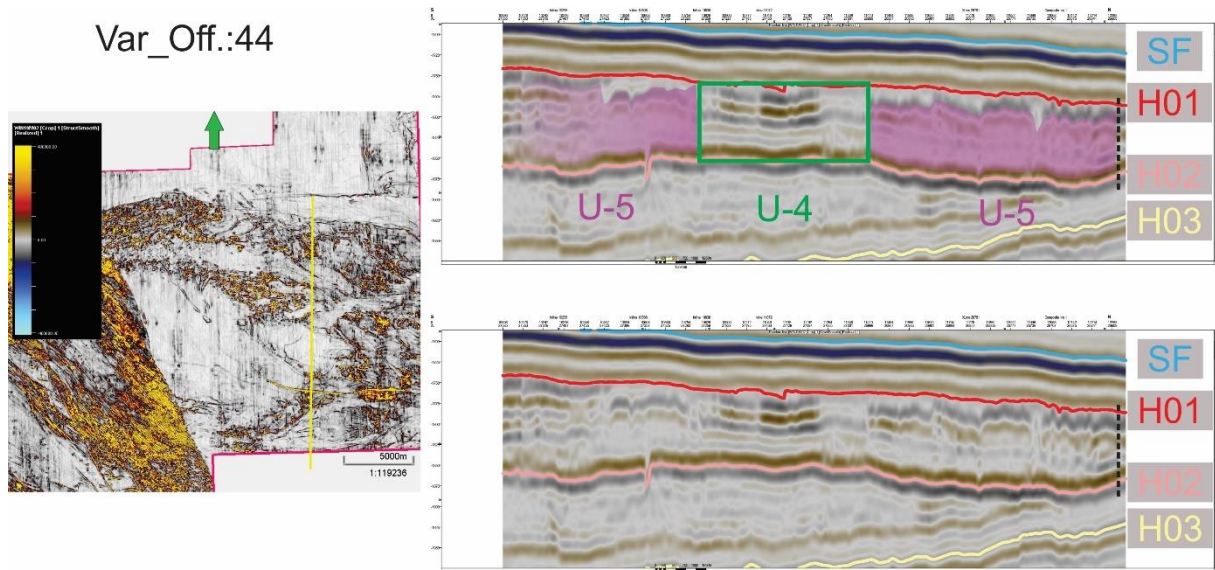


Figure V-43 Unit 5 bisected by Composite line 17

The internal structure follows the same pattern.

As mentioned above, neither the RMS map nor the isochron map offers reliable help for establishing clear boundaries between U-5 and U-4, and likewise there is also no notable difference between the northern and southern halves of the "beak".

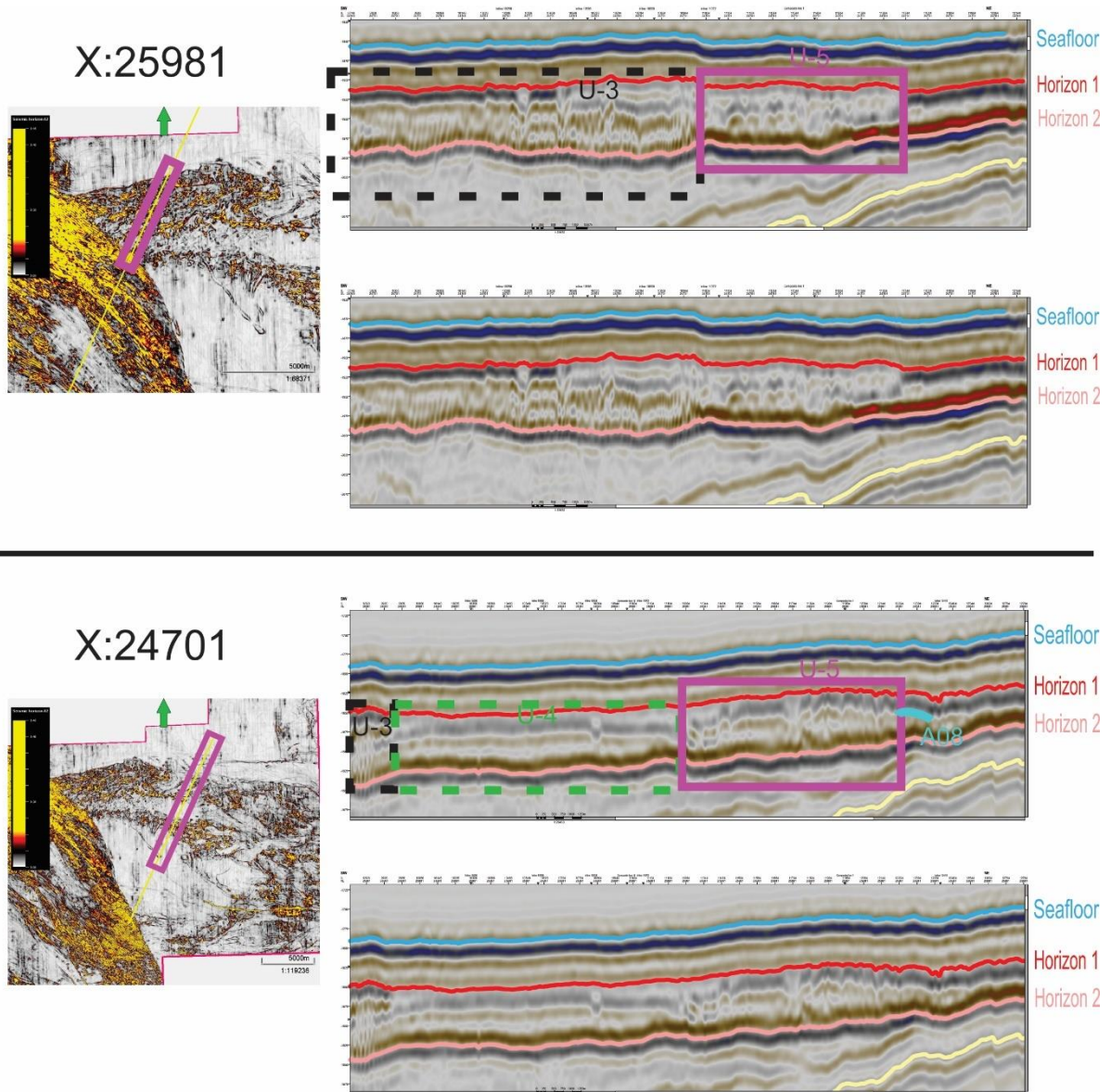


Figure V-44 Internal arrangement of the northern part of U-5

There are also some extensive low-variance areas contained within U-5, similar to "Calm" located between U-2 and U-3, or the "Smooth Spots" found inside U-3.

These areas are not visible on the isochron map, and the amplitude ranges associated with them slightly differ from their surroundings but not characteristic enough to form a pattern. Also, no features can be found in the seismic data (see X:25981 on Figure V-44 above) to suggest a particular reason for these smoother fields to exist.

a) *Anomaly 07 – Cut*

Mention was made in the previous subchapter (“Horizon 3”) about a set of linear features separating the majority of the study area from Unit-X and the relatively empty field to the north. During the examination of H02 and subsequent strata, it became apparent that Anomaly 07 marks the northern limit of Unit 5, at least in part. More on this later.

Viewed “from above” the feature starts outside the eastern boundary of the study area and presents as a pair of jagged lines, converging (but never quite meeting) until approximately 12 kilometres in (X:25833), where they become indiscernible. Accordingly, the isochron map (Fig. V-46) looks as if a fair amount of sediment were “missing” from the area where the Anomaly 07 loses its prominence.

A07 is clear on all of the generated surfaces (Variance- RMS- and isochron maps), although there is a complication.

Although the A07 is located in, or next to chaotically arranged material, and is therefore difficult to follow in the Xlines, the variance map of H02 itself suggests a continuous, only slightly curved line all the way from the eastern boundary to Unit 3. The southern “Cut” is not yet visible here.

Moving on to 30-, 44-, and 60 milliseconds on the variance images, the second part of A07 comes into view and the appearance of the sediment between the two lines is markedly different from those deposited either to the north or the south of A07. Although the twisting pattern exhibited by U-5 is missing, the material between the two “Cuts” does show signs of lateral movement, while there are no indications to this on the north. All these differences can be observed on Figure V-45.

All these differences can be observed on Figure V-45.

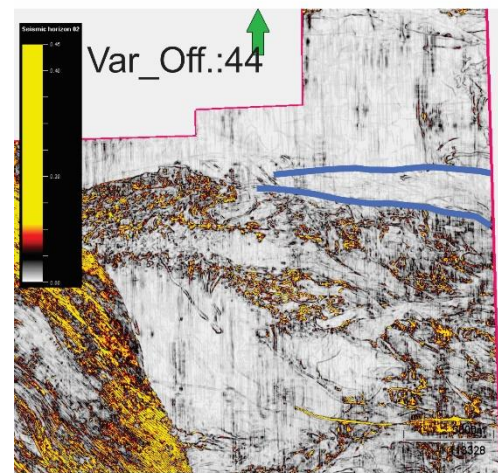
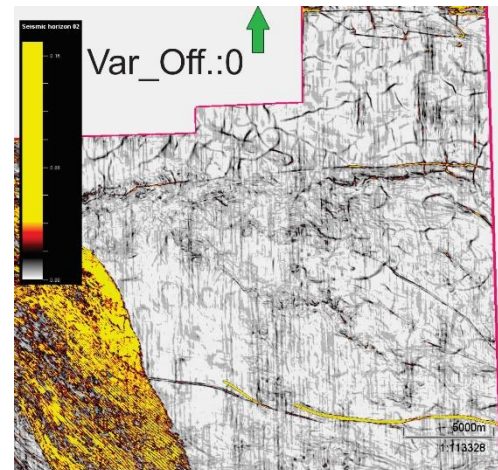


Figure V-45 Variance maps with the extent of A08 that has been identified with confidence

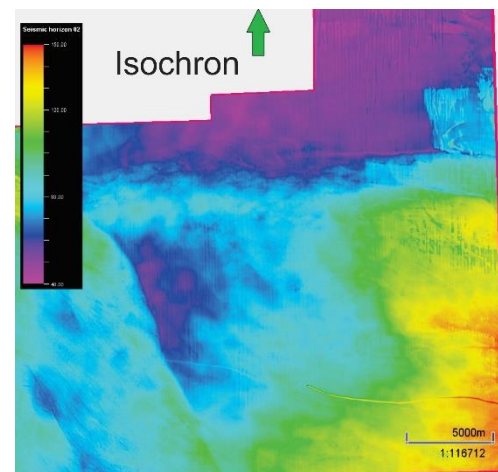


Figure V-46 Isochron map of the northern ranges

The RMS maps show the same tendency as the variance images, which *Figure V-47* illustrates. Both the 0- and 15 millisecond offsets show a sudden shift in amplitude on the northern boundary, but on the higher offsets, this margin moves further into the study area, to the southern “Cut” – moving towards Horizon 1, the amplitude ranges seem to notably rise in the area between the linear features composing A07.

As mentioned before, the seismic data shows several discontinuities on the underlying strata, and some of these align with the “Cut”, but not everywhere.

Although the variance images do not show such a marked difference, the northern line is always more prominent on the Xlines, and H02 even shows a slight vertical displacement here. The southern instance of A07 is not as noticeable on the seismic data (*Figure V-48*).

Once again, the “Cut” becomes extremely faint at a certain point, but on *RMS_Off.:30*, it seems as if the northern line continued and eventually terminated against the southern one, which then becomes the structure designated as Anomaly 07-b. This is very hard to see and only that single one of the generated surfaces suggests it.

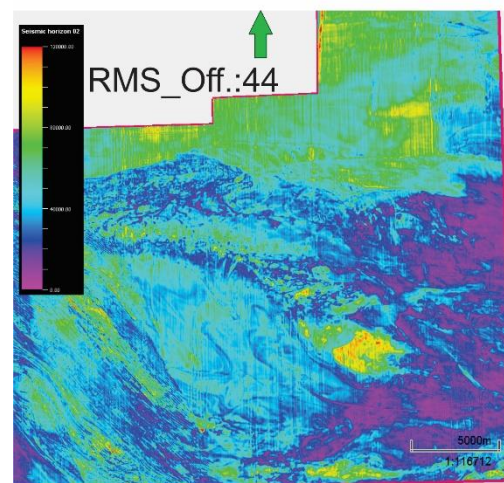
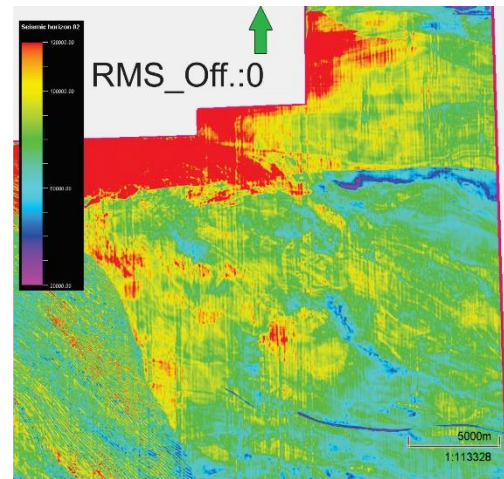


Figure V-47 RMS maps with different offsets for comparison

Xline: 26863

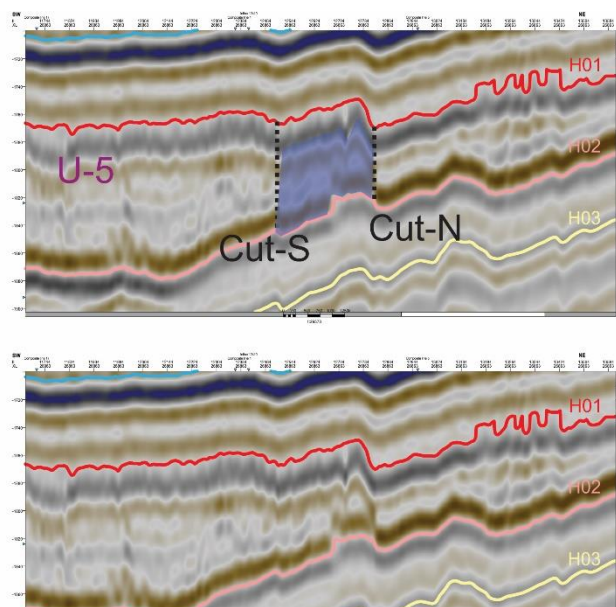
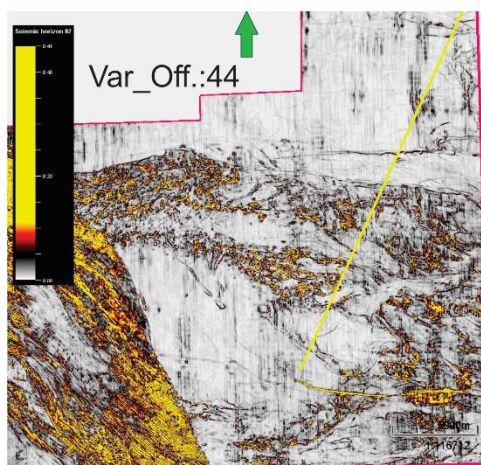


Figure V-48 A representative cross-section of A07 - "Cut"

b) *Anomaly 07-b - Ridge*

Accompanying A07, or perhaps a westward continuation of it, there is an elevated feature most distinctive on “*RMS_Off.:15*”.

It always follows the line of A07 and is located directly to the north of it, approximately 7 kilometres long.

While A07 is clearest on a variance map of Horizon 2 with 0 Offset, the “Ridge” is only slightly noticeable on a variance map with an offset of 15 and was found to be invisible on other examined offsets.

On *Var15*, a disorganised collection of globular objects can be seen, but they cannot be separated from the area south of A07, or the one east of the “Ridge”.

The Xlines (see *Figures V-49 and V-50, with X:24461 displayed*) show that the layer underneath has the stronger amplitude signature of the area between Unit-X and A07, as opposed to that of Unit-5, however the overlying layer shares its weaker amplitude with U-5.

The feature is discontinuous and the possible blocks seen on *Var15* are also seen on the Xlines.

No clear termination can be established, the “Ridge” shrinks, and eventually disappears as it joins Unit-3.

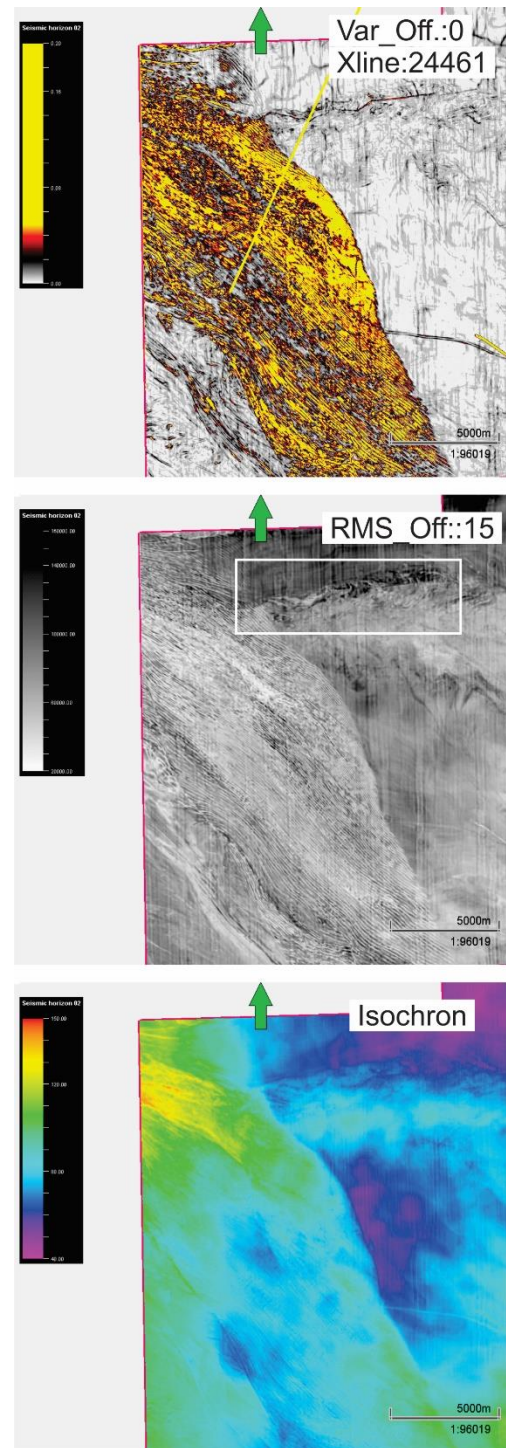


Figure V-49 Anomaly 07-b and its surroundings

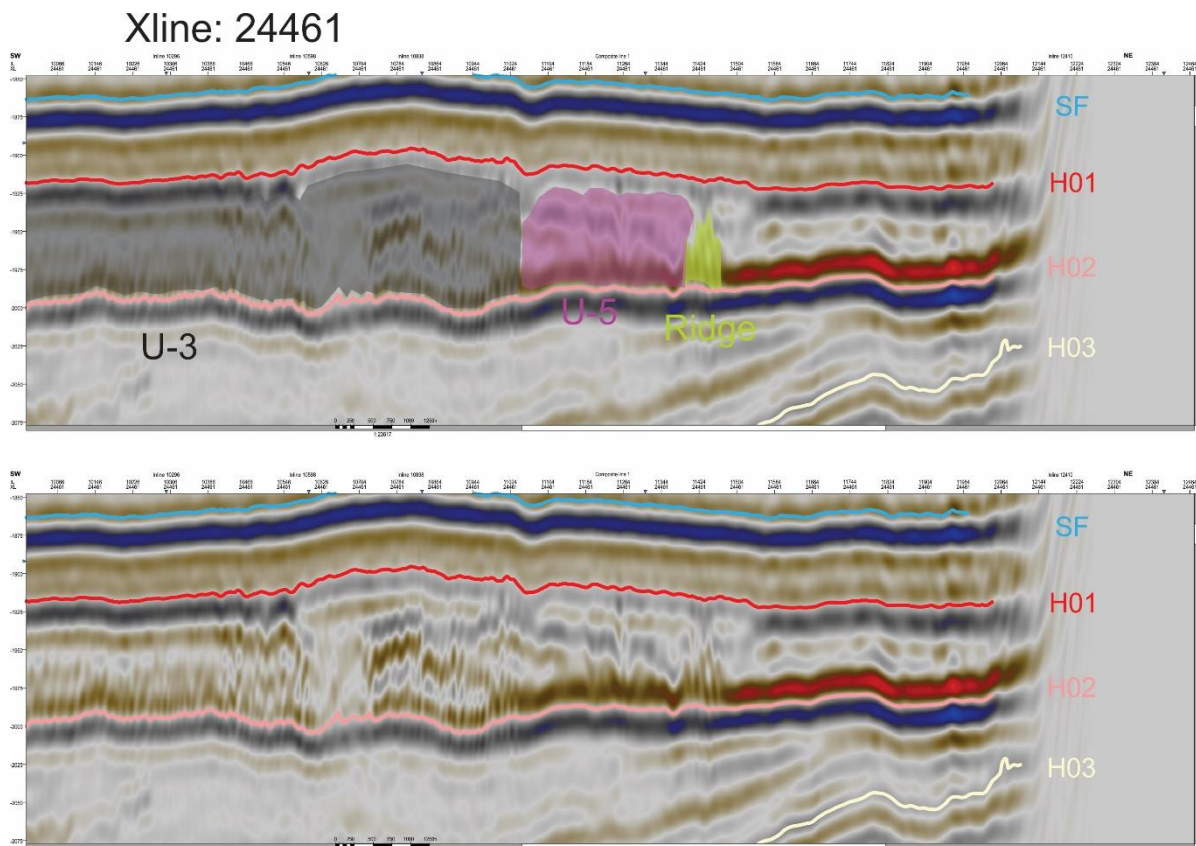


Figure V-50 Seismic line taken from near the western termination of Unit 5

E. UNIT X

As between Horizons 3 and -2, a vestige of a different unit is visible in the northernmost points of the study area – the one previously named Unit-X. Once again, it is too small for meaningful interpretation, but its presence must be noted.

There is a relatively large area with a low variance signature located between this Unit-X and the previously mentioned Anomaly-07 (“Cut”). It seems to show an irregular mud crack-like pattern seen in the underlying strata, and the many vertical fracture lines are seen on the Xlines as well, but only some of them reach H02. For the most part this region consists of two or three layers only, but approaching the point where it meets Unit-3 the sediment on top of it appears to be gradually thickening (see Figure V-50, the unmarked portion NE of the “Ridge”). Aside from this as seen on both the seismic data and the isochron maps (Figure V-46, for example), this region is almost uniformly thin, and it follows the overall dip of H02.

3) HORIZON 01 & SEAFLOOR

The first thing that becomes apparent when observing the seismic data taken of the sediment between H01 and the seafloor is that it is rather evenly distributed. The chaotic internal structure is completely absent, although there are some extremely faint signs of stress at certain points. These areas were marked with white circles on *Figure V-51*.

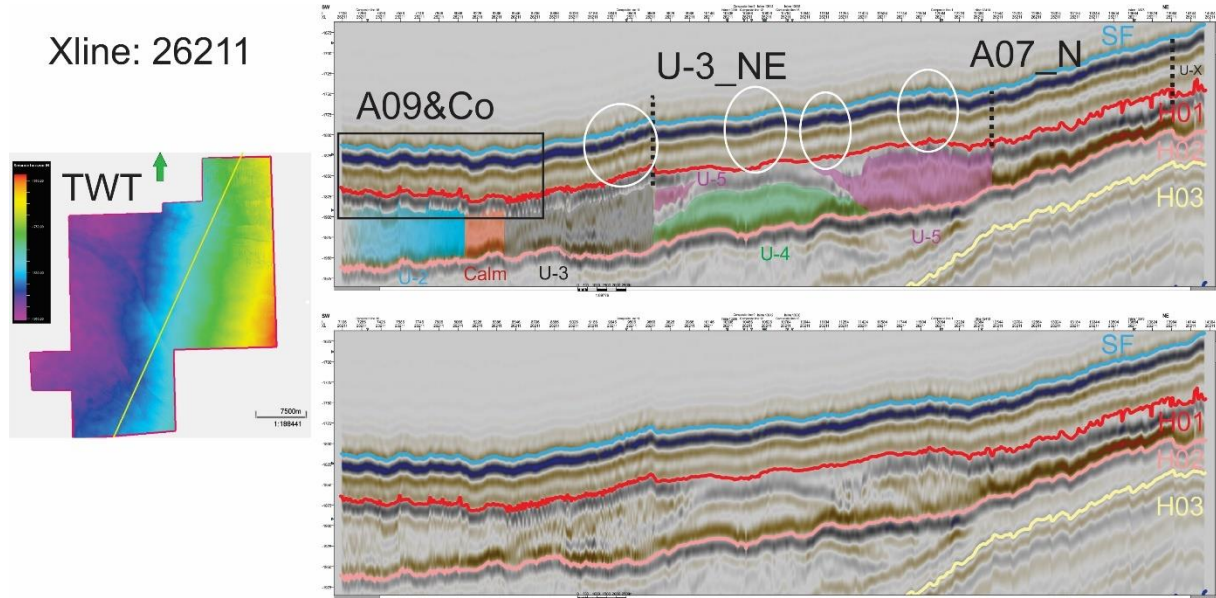


Figure V-51 Another cross-section of the study area with the shallower strata emphasised

The two surfaces closely mirror each other, and the average thickness of the strata is approximately 60 milliseconds, although there is a slight eastward thickening overall. Some momentary shifts are also visible, but there is some uncertainty in this. Horizon 01 certainly shows some small irregularities on the Xlines but a number of these, especially those on the northeastern ranges (*Figures V-51 and -52*), can be attributed to tracking errors, rather than real variance in subsurface topography. The transition between the strata is somewhat blurred, and precisely following H01 at these points was deemed both difficult and unproductive (*see Fig. V-51, between A07_N and Unit X*).

On the other hand, near the southern and western boundaries of the study area, above Units 2, -3 and the “Calm” several linear features are visible. Anomaly 09, the “Spike” has been identified, and other such anticlines seem to accompany it

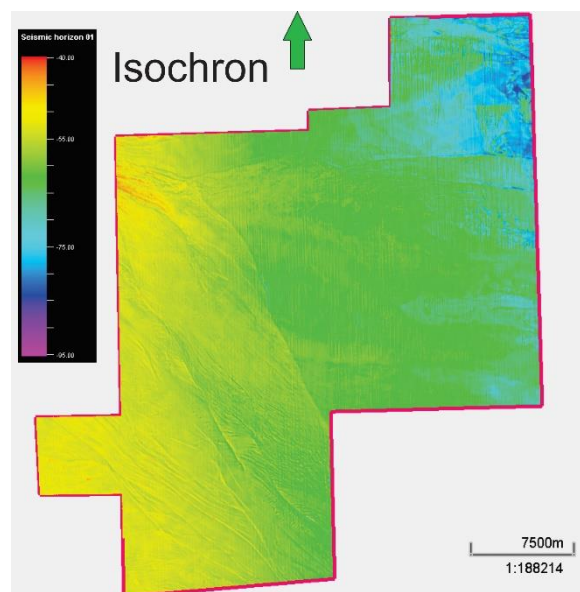


Figure V-52 Isochron map of the strata between H01 and the seafloor

- these are presumed to have been obscured on various maps examined for the previous subchapter, but since the material overlying H01 lacks the disorganised internal arrangement of Unit 2, they became observable.

The majority of these structures correspond to slight irregularities on the seafloor, but only the most prominent ones, those that have already been described in association with H02 can be identified on the SF variance map (the aforementioned “Spike”, the SW-NE borders of Unit 3, and Anomaly 07 – “Cut”).

The two variance maps provided on *Figure V-53* illustrate how the smaller features only interfered with deposition at close proximity of H01 itself – a difference of 30 milliseconds renders the strata largely featureless, even though the colour scheme for “*Var_Off.:30*” uses a range less than half of “*Var_Off.:0*” (larger emphasis).

A. UNIT 6

The strongly defined NE margin of U-3 interferes slightly, but the most remarkable feature of H01 is revealed on the RMS map with no offset.

It has been mentioned before how there is a mass of markedly lower amplitude lying on top of Unit 4, the majority of Unit 5 and the portion of U-3 designated as the “Bump”, or Anomaly 10. For the sake of clarity, all this material is designated Unit 6.

Although it would have been more precise to include U-6 in the previous subchapter as H01 covers it and not the other way around, accurate interpretation was deemed less challenging if done in relation to the overlying horizon.

On the western boundary, it starts with a relatively narrow passage, spreading out eastward not unlike a delta lobe, and continues on through the eastern and southeastern border of the study area, above U-5.

The Xlines reveal a slight altitude loss towards the NE (most prominent at the narrow part, on the west), but it is not really prominent, the change barely shows up on the isochron map. Otherwise, U-6 follows the general dip of Horizon 01 apart from a clear inconsistency shown at the southwestern margin of the mass, overlying Unit 3, as can be seen on the TWT map of *Fig. V-51*.

It is worth mentioning that an RMS map with an offset of -20 (that is, 20 milliseconds below Horizon 1 – this much is still U-6) displays the same rippling pattern previously seen on Horizon 2’s “*RMS_Off.:44*”, from inside Unit 04 (see *Figure V-42* in the previous

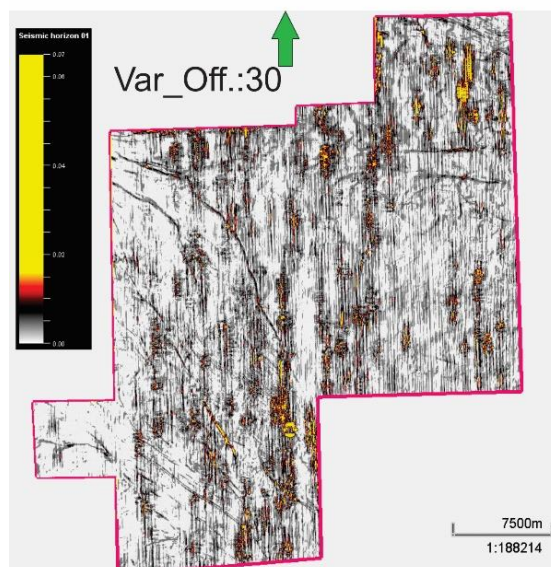
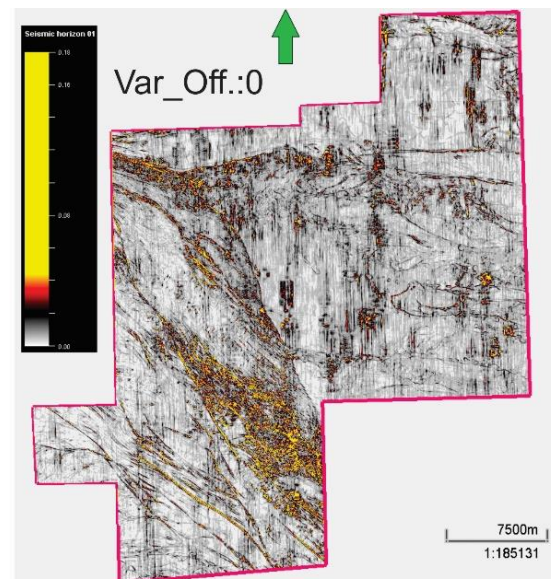


Figure V-53 Comparison of Horizon 1's variance maps

subchapter).

This pattern disappears with increased proximity to H01.

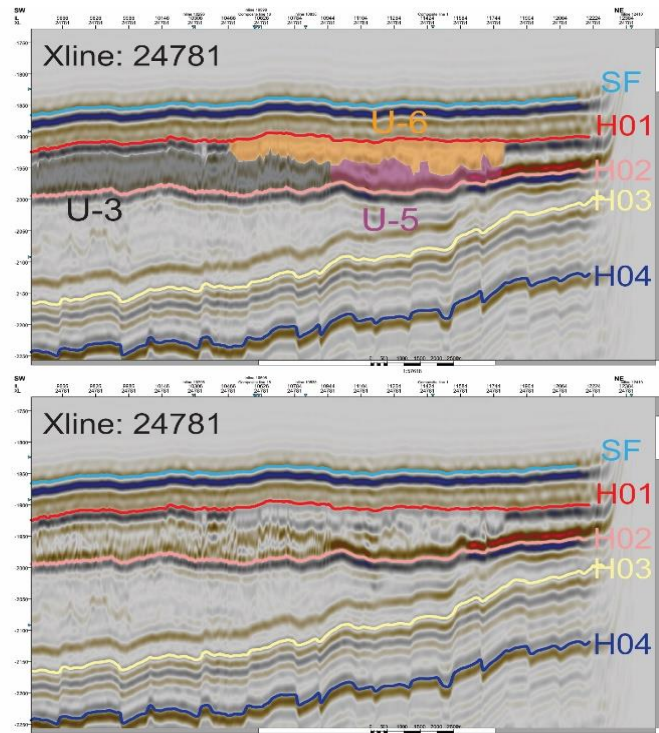
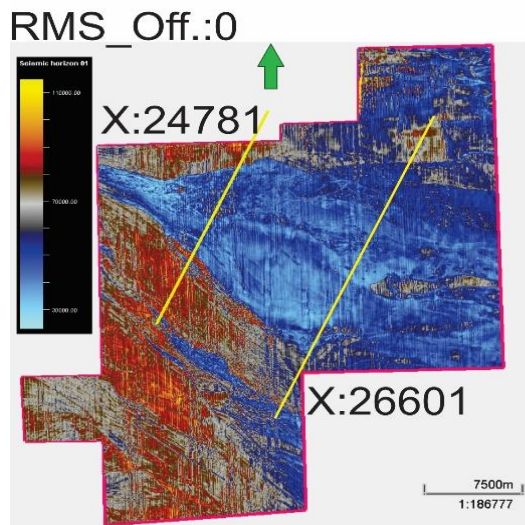


Figure V-54 The relevant RMS map with the two cross-sections indicated

While the extent of this unit can be established with relative ease on the west (see Figure V-54. for the marked RMS map and X:24781), looking eastward where U-6 is laterally expanded, the picture becomes somewhat more complicated once again. Although “RMS_Off.:0” (Fig. V-54) doesn’t reveal any interruptions here, the material covering U-5 shows a gradually increasing amplitude on the X:26601, and the Xlines show a possible vertical displacement here. The transition to different amplitudes is gradual and a northward termination of U-6 is hard to define. The issue on the south is similar. The material of U-6 seems to continue towards the SW both above and below the vestigial part of U-5. (see Fig. V-55)

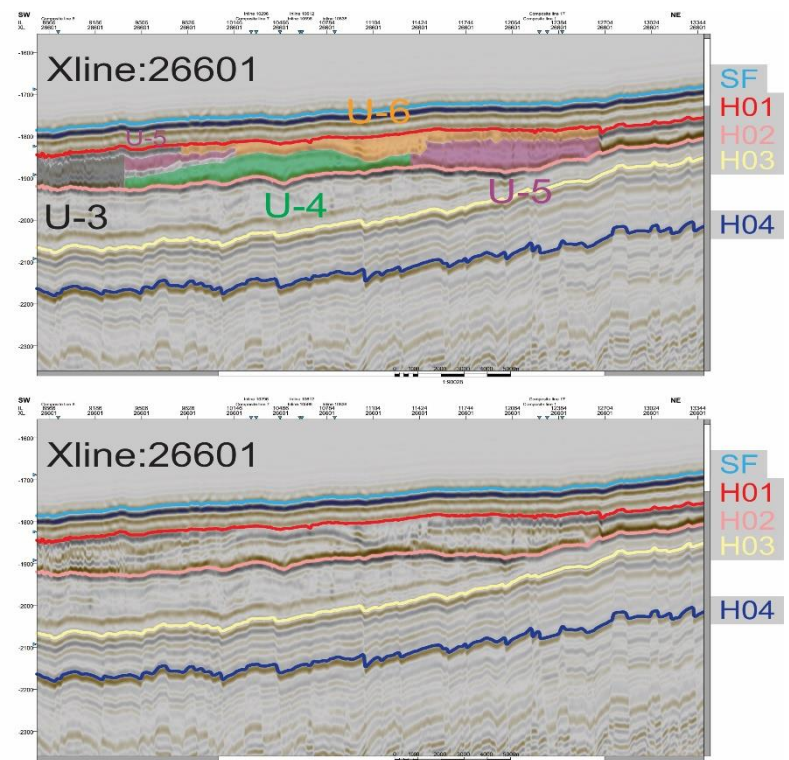


Figure V-55 The accompanying image to Fig. 52

B. SEAFLOOR

As for the seafloor, there are no significant features that can be identified apart from those already present in the layers above H01 - the same expressions from deeper-lying structures that have been described in this subchapter once already.

The relief of SF is almost exactly the same as H01's "Var_Off.:30", except the irregularities are less pronounced.

As mentioned, the seafloor more-or-less mirrors Horizon 1 and accordingly, the general dip follows the same west-northwesterly direction. The difference in altitude translates to approximately 160 milliseconds from the northern boundary of the study area to the southern border.

The RMS map doesn't reveal any particular pattern either.

On extreme magnification, a multitude of circular patterns are present on the surface, but these were later deemed to be acquisition errors.

All the relevant images are shown on *Figure V-56*.

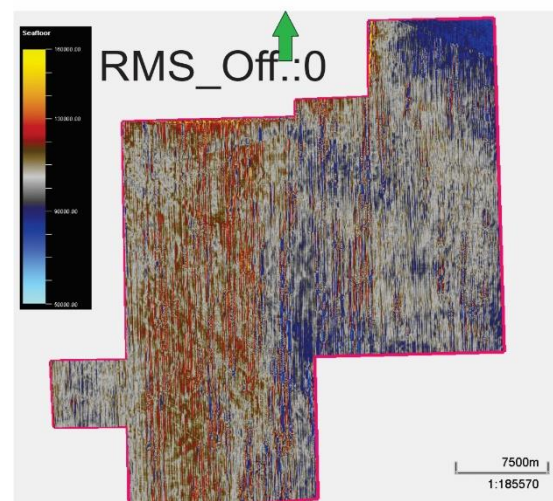
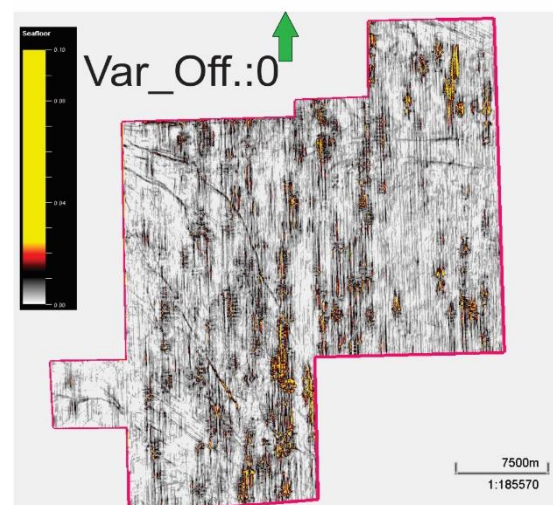
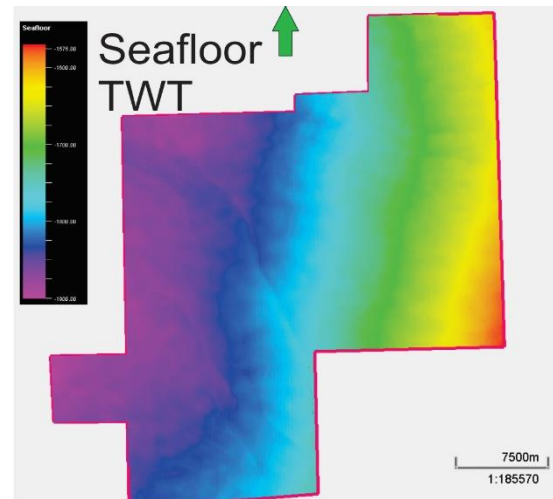


Figure V-56 The maps generated of the seafloor

VI. Discussion

In this chapter, the observations of the previous chapter will be put into perspective and a scenario will be prepared for the Late Cenozoic evolution of the study area focusing on the presumed mass wasting events based on the seismic characteristics, and internal and external morphology of the interpreted sedimentary units.

To conclusively determine the nature of the discussed strata, they will be evaluated against the criteria detailed in *Chapter III*.

The structures selected as representatives and designated „Anomaly No. ...” located in, or in proximity of the Units will also be examined and possible explanations will be given for their formation.

1) Lithostratigraphical boundaries in the study area

As a first phase of the Discussion chapter, the notes on lithostratigraphy detailed in Chapter III. 1) D/a, and the collected data of Chapter III. 2) is applied to observations about the studied strata and their environs to establish them on a geological timescale.

The underlying polygonal fault zone is also matched to criteria and identified conclusively.

Polygonal fault zone:

On Figure V-5, showing the variance attribute map generated of the reflector designated Horizon 03, an extensive network of fractures can be seen.

The variance map clearly displays how the fault lines do not follow any particular direction. As stated, these underlying strata were not subjected to interpretation, therefore precise values will not be provided, but seismic sections show that the fractures are generally near-vertical, and there is a notable discrepancy in the number of fractures when comparing the bottom of the zone to the top. (Xia, Yang et al. 2022)

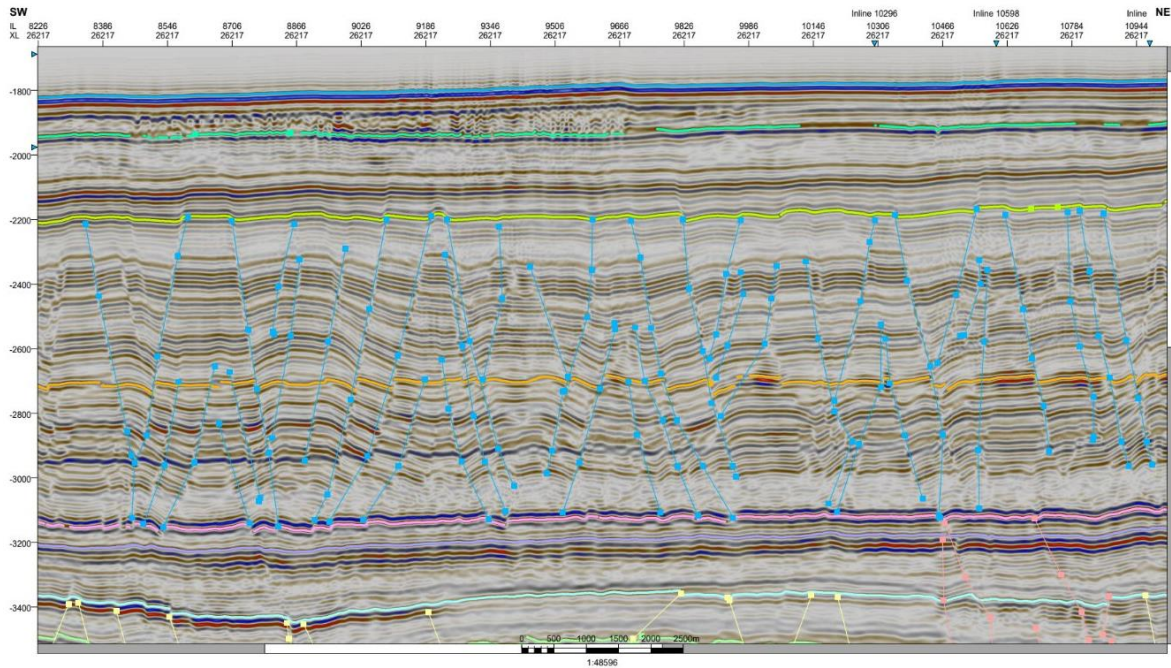


Figure VI-1 The polygonal faulting zone underlying the targeted deposits with some fracture lines marked

In Chapter III. 1) D/a, Lithostratigraphy, both the Brygge- and Kai formations are described as potential hosts to polygonal faulting. The Brygge material ranges from sands to oozes and the Kai sediments are oozes with a small amount of shales. (Berndt, Bünz et al. 2003) Taking therefore an average value of estimated ideal propagation velocities in a mass composed of a combination of wet sands, oozes and saturated shales to be ~1800ms, using the depth conversion formula results in an approximated thickness of 700 metres for the affected strata. (propagation values taken from the GeoSci database) Two-way travel time range for this zone was taken from Fig. ... above, which was made during the preliminary evaluation – the horizons do not reflect the final state of interpretation and should be ignored.

$$\text{TWT}/2 \text{ (s)} * \text{Velocity (m/s)} = \text{Depth (m)}$$

Based on this admittedly imprecise calculation, fault throw would be generally ~20 metres and displacement is no more than 20-30 metres. Locally, displacement may be higher near the deeper strata of the PFZ, but not excessively so.

This means the heavily faulted sediments beneath Horizon 03 fulfill four of the five criteria listed in Chapter III. 2)B and will be referred to as a polygonal faulting zone.

While the faults' lateral extent is difficult to measure due to their proximity to each other, some seem to exceed the 1500 metres established as an upper limit in the reference article "A Review of the Global Polygonal Faults: Are They Playing a Big Role in Fluid Migration?". Since the article doesn't state this as an iron-clad rule, (suggested the words „commonly“, „generally“ etc.) and the fact that the fractures often intersect (which, depending on their respective angles may cause multiple to appear as a single continuous feature) this should not be considered sufficient reason to exclude. (Xia, Yang et al. 2022).

It must be mentioned also that the numerical results shown here do not align with the wellbore data of the Norwegian Offshore directorate but they are applicable as proportional values. (Faktasider - Sokkeldirektoratet (sodir.no))

Preliminary observation of deeper strata revealed another facies defined by what has now been established to be polygonal faulting.

It is less fractured than the zone above, and some of the faults may in fact connect the two, but these are not common, and generally speaking a stratified and relatively undisturbed sedimentary unit separates the two.

Accepting the presence of not one, but two polygonal faulting zones in the dataset, these can be used to define the Brygge- and Kai formations. (Chand, Rise et al. 2011)

NAUST Formation

NAUST N – No massive deposit has been identified in the strata overlying the Kai formation in the study area. Thin bands of disorganised material may be seen but they are bounded by stratified sediments.

The sediments overlying the Kai formation further lack the wedge-shape noted to define the Naust N sequence – for these reasons it is assumed to be missing.

Since one possible explanation for the formation of the Brygge- and Kai polygonal faulting zones is overburden caused by the deposition of first the Naust N unit (and subsequently -A, -U, and -S), it might be reasonable to expect the entirety of Naust N unit to have been removed from WIN19M02 at one point prior to Naust A-time.

(Chand, Rise et al. 2011) (Rise, Chand et al. 2010)

NAUST A – Although described as dominated by massive glacial deposits similarly to Naust N, stratification has also been noted in the westward-prograding Naust A sequence. Accepting the strata atop the Kai formation as the Naust A, the bands described earlier could be the result of debris flow events. (Rise, Chand et al. 2010)

NAUST U – It must be mentioned that the boundary between Naust A and -U is uncertain. There is very little to differentiate the stratified layers directly above and below Horizon 03 and therefore it is more than possible that it does not signify the transition between Naust units -A and -U (Horizon 04 could be a candidate).

Nevertheless, the sequence is characterised by the presence of glacial debris, and a history of large-scale reworking by mass wasting.

A possible candidate for a mass transport complex has been noted in the local geohistory. (Rise, Chand et al. 2010)

This may or may not correspond to Unit – 1.

NAUST S – Massive Elsterian glacial sediments defined by generally transparent seismic profiles dominated the mid-Norwegian margin during Naust S time.

The Sklinnadjuvet slide removed much, but not all of this material. (Rise, Ottesen et al. 2006) mention the presence of glacial debris-flow lenses north of the slide.

NAUST T The layers between Horizon 01 and the seafloor are rather evenly distributed and display simple stratification. The isochron map only shows a small, gradual westward thickening.

There are no signs of massive glacial deposits, but considering that these are the uppermost strata, and they seem to contain the fine-grained stratified material described in (Rise, Chand

et al. 2010) it seems reasonable to assume these layers should correspond to the Naust T sequence.

A. Supplementary

Fluid flow: Preliminary observation revealed the presence of suspected fluid flow structures of considerable size in the dataset deep underneath the deposits this thesis focuses on. All of these terminate well beneath the Kai PFZ – for this reason, they were deemed not directly relevant to this study.

The polygonal faulting zone described by (Berndt, Bünz et al. 2003) in the article “Polygonal fault systems on the mid-Norwegian margin: a long-term source for fluid flow”, differ from the Kai formation’s network of fractures on one, immediately notable point: the „pipes” originating from the PFZ (Berndt, Bünz et al. 2003) seem to be missing from the present study area.

No further fluid flow structures are present above the upward termination of the Kai formation.

One might argue that the structures could have been removed by the mass transport complex designated Unit-1, but the sediment between the slide base and the polygonal fault zone show no signs of having been similarly reworked, and still these pipes are absent.

All this suggests that the reservoir has either been completely depleted by the time the strata now hosting the PFZ was completely buried, or that the fluid has migrated along different pathways henceforth.

Another argument in favor of gas exhaustion or -absence is the lack of pockmarks either on the seafloor, or on any of the reflectors discussed in this thesis.

(Berndt, Bünz et al. 2003) (Xia, Yang et al. 2022)

Both the polygonal faulting zones and

2) Identifying the slide deposits – fitting the characteristics

According to (Bull, Cartwright et al. 2009) the common traits of mass-transport deposits are a weak amplitude signature and heavily disorganised and high frequency internal arrangement bounded by a basal shear surface and a top slide surface.

The primary purpose of this subchapter is to re-evaluate the descriptions given in Chapter V. and determine whether they can be used to identify the sedimentary units.

A. Horizon 03-02

a) Unit-1:

The massive deposit designated „Unit-1” dominates the strata between Horizons 03 and -02. Immediately above H03, the sediments are stratified and very thin, but there is a sudden elevation shift dividing the study area illustrated by the isochron map of H03.

At the northeast of the study area, a NW-SE aligned boundary marks a rapid thickening of the sediments. The material southwest of this boundary gradually thickens towards the west-northwest.

(see *Figure VI-2*)

A strong reflector can be seen on the bottom of U-1 and terminating against H02.

If Unit-1 is a landslide deposit, this would be considered the basal shear surface.

Another reflector slightly deeper mirrors the stronger amplitude signature of the presumed shear surface but its amplitude weakens when continuing out from below U-1.

For this reason, the strengthening amplitude can be attributed to increased overhead pressure from the mass transport complex.

However, at the drop described above from where Unit-1 appears, the stratified sediments underneath don't seem to be heavily affected, they only gradually thin out toward the west (might even disappear beyond the limit of the study area).

This could suggest that the mass-transport complex had insufficient kinetic energy (potential low velocity) to remove the underlying layers at once and only with the gradually increasing amount of material gained enough mass to erode into the facies below.

Regarding the material of Unit-1, most of the material has an extremely low amplitude signature, and because of this its frequency cannot be accurately determined.

It lacks extensive fragmentation, but there are a few coherent object contained within.

Where these are present, they are often laterally extensive.

As mentioned in Ch. V, Unit-1 extends beyond the boundaries of the study area to the west, south and east.

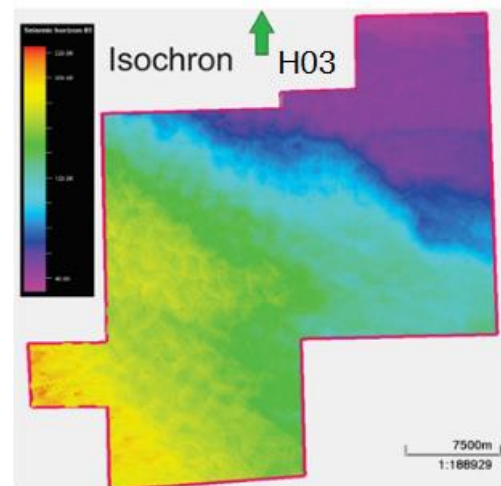


Figure VI-2 The isochron map of Horizon 03 to showcase the dimensions of Unit-1

This makes it difficult to determine its nature but the internal structure throughout more closely resembles a fine-grained debris current deposit than one resulting from a landslide.

B. Horizon 02-01

b) Unit -2

The sedimentary unit covering the southern part of the study area is aligned SE-NW, and seems to have progressed near-parallel to the general dip of Horizon 02. As mentioned in Chapter V. 2)A, some elements near the southern boundary of WIN19M02 trend almost due north, but then change direction to a northwesterly heading. All of the generated attribute maps show lineation (varying in prominence, depending on the temporal offset) following this direction. (see *Fig. VI-3*)

Overall, Unit-2 shows signs of fragmentation, especially near the bottom layer.

The material has a low amplitude signature and has been deformed by lateral pressure.

Three subunits were defined in U-2, although their differences are rather slight on the seismic sections – the attribute maps show clear distinction.

Unit-2a is less deformed than the other two, pointing to the source of lateral stress originating on the northeast.

The amplitude signature of the base layer weakens toward the northeast, while that of the top layer is strongest above U-2b, and displays local variations when covering the other two subunits.

The top surface is also more disturbed near the south, than toward the northwest.

c)

„Calm”

Even more than A01 – „Roll”, this area was considered noteworthy only compared to the heavily diversified sediments that surround it.

To signify this, „Calm” was not marked as an anomalous feature.

However, it has traits which denote its significance, rendering this decision.

The „Calm” is a field of comparatively undisturbed material extending beyond the southern boundary to the western in aligned SE-NW.

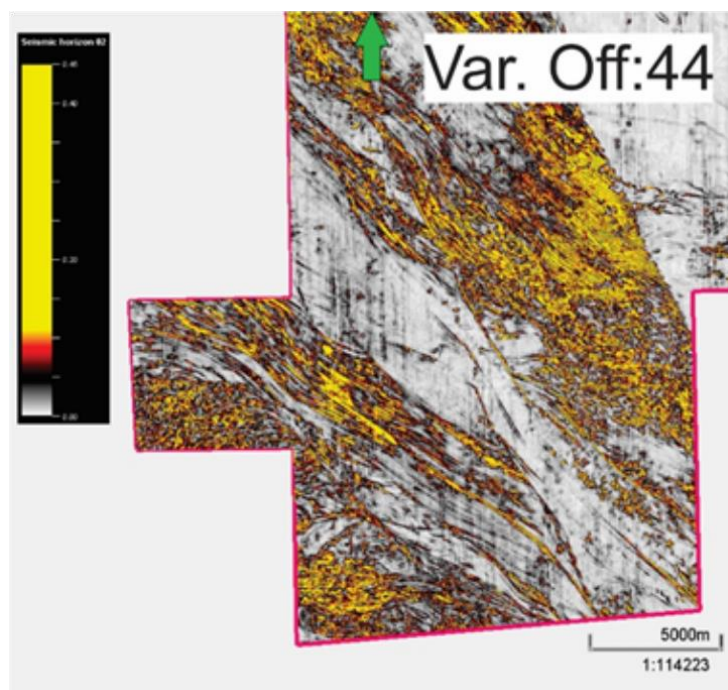


Figure VI-3 Variance map showing Unit-2, the "Calm" and Unit-3

Internally, where the seismic sections show stratification, it is concordant with the base shear surface.

At certain points the internal layers appear fragmented.

It matches the vertical extent of Unit-2, but there is a slight displacement when compared to U-3; also, some of the latter's material may have intruded into the „Calm” near the base.

At a length exceeding 15 kilometres on the dataset only, it is perhaps too large to be considered a remnant block, but it does correspond to the general transport directions of both U-2 and U-3.

It is possible that „Calm” is mostly unworked material dividing the same mass-transport complex into two parts. (Bull, Cartwright et al. 2009)

d) Unit – 3

Like U-2, Unit-3 continues to the southeast and the northwest of the study area and shows signs of lineation following this same trajectory, although slightly more north-northwest orientated, as shown on *Figure VI-3*.

Internally, U-3 is heavily fragmented, high frequency material with mid-to-weak amplitude signature.

The basal shear surface seems absent under parts of U-3, but this can be attributed to scattering stemming from the internal fragmentation.

Again, the top surface is heavily disturbed over the southern portion of U-3, but it is relatively undisturbed at the north, except over the anomalous part of the deposit (more on this at „Anomaly 10 – Bump”).

e) Unit – 4

U-4 is a wedge-shaped deposit with mostly indiscernible amplitude and frequency, surrounded by Units-3 and -5.

When observed on a SW-NE aligned Inline section it is concordant with the seafloor, and downlapping onto the basal shear surface just before connecting to Unit-3.

No discontinuities were observed in the main body of U-4, and likewise few signs of stress, or internal structures.

The base has as gradually strengthening amplitude signature towards the NW.

On a Xline section the shape of U-4 is lenticular, and the basal surface's amplitude shift is northeasterly.

At the northern boundary of U-4, there are some fragments that are

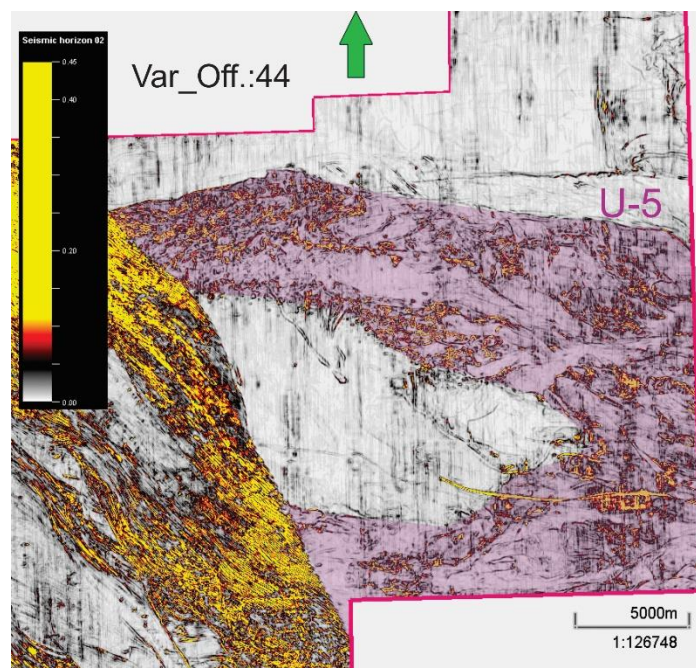


Figure VI-4 Variance map showing the marked Unit-5, and the comparatively featureless Unit-4

markedly different from the material composing the main body of Unit-4.

They more closely match the sediments belonging to U-5.

Unit – 4 is the only identified mass transport deposit visible in the recent strata of seismic block in its entirety, unless buried by surrounding deposits.

f) Unit – 5

Entering the study area from the east and the south-southeast and progressing due west and downslope until blocked from further advancement, Unit-5 surrounds Unit-4 from three sides.

Internally, U-5 is considerably fragmented, mid-to-high frequency material with initially weak, but upward strengthening amplitude signature (and yet, the top surface has comparatively weak amplitude).

The bottom layer is largely coherent with an evenly strong amplitude, but the top surface is discontinuous, with vertically displaced elements.

To the north, it is constrained by Anomalies 07 and 07-b (the variance attribute map shows the edges of the deposit very clearly) and to the west (both north and south of U-4) it terminates against Unit-3.

The extent of U-5 present in the study area is highlighted on Figure VI-4.

The southern contact zone is slightly spread out against U-3, but the northern one does not.

The probable reason for this is revealed by the isochron map – the amount of transported material is considerably less here.

g) Unit – 6

U-6 is made up of a large amount of discontinuous sediment settled atop large parts of the study area.

Comparatively strong reflectors divide the sediments of Units-3, -4 and -5 from those designated U-6, but the material of Unit-6 has a distinctly low amplitude signature.

This deposit buried the jagged, sometimes fragmented upper boundaries of the preceding sedimentary units, forming a more even surface, and a relief on Horizon 1, and a fainter one on the seafloor.

Although the portions of U-3 buried by U-6 show signs of lateral compaction, these expressions are not translated onto H01 and above.

3) Traits of chosen sedimentary structures

This subchapter serves as a second, conclusive overview of the identified sedimentary structures and determine whether their formation might hold any pertinent information concerning the evolutionary history of the study area.

A. Anomaly 01 – Roll

The Roll is a series of slightly plateau-ing layers in the center-bottom of the study area, forming an elongated rectangle with uneven edges.

The seismic sections show the underlying strata in the northern part of the structure to be unbroken in either direction, and to the south it has a very faint signature and could not be

interpreted with confidence.

No explanation was found for this change.

It was briefly considered as a kinematic indicator, but the coherent stratification does not match the description of either remnant blocks or ramps. (Bull, Cartwright et al. 2009)

Its lack of distinctive features was initially considered significant, but its subdued appearance might be mere happenstance.

The composing material might have been deposited above an upthrust block of the Kai-polygonal faulting zone.

B. Anomaly 02 – Clusters

The Clusters are a group of initially separate areas characterised by higher variance values eventually merging together with increasing distance from H03, until they become indistinguishable from their surroundings near H02.

Sediments atop the A02 instances contain slightly more coherent fragments than their surroundings.

All Clusters are located underneath Unit-3 and might be explained by differential compaction.

C. Anomaly 03 – Raindrop

A coherent block with a distinctly stronger amplitude signature than the surrounding material. It is dipping towards northwest, is roughly lenticular in this direction and there are no significant variations in its width.

The seismic sections show there are no discernible layers it might be connected to.

At the midpoint present in the study area there is a slight angle to the structure.

The characteristics of the raindrop correspond with those of translated or remnant blocks, with the former being more probable, because no effect on the depositional pattern of the surrounding material can be seen in Unit-1 (Bull, Cartwright et al. 2009)

D. Anomaly 04 – Scars

Similar to A03 but smaller, the „Scars” are a group of structures with stronger amplitude signatures and whose component layers exhibit dubious connection to surrounding material. As described in Ch. V. 1) B/b, at least A04-c has directly interfered with the depositional pattern of a different structure, one of the A02 Clusters.

All A04 instances are aligned in roughly the same northwesterly direction with the exception of Anomaly 04-e, which points due west.

The seismic sections show these structures to be equidistant from Horizon 03.

For these reasons, the Scars are determined to be remnant blocks. (Bull, Cartwright et al. 2009)

E. Anomaly 05 – Hairball

Anomaly 05 is a group of curved or angled lines noticeable on the variance map generated of Horizon 03 with an offset of 70 milliseconds.

There is no discernible system to the way the Hairball’s components are arranged.

Seismic sections show the elements of A05 to be small vertical expressions extending upward from the basal shear surface.

The description given in Chapter V. 1) B/c was subsequently re-evaluated.

Following the time-slices from a depth below Horizon 03 to the top of Unit-1 revealed more

of the A05 elements translating the pattern of the faults underneath, besides the one marked on Figure V-17.

Even though the fractures of the Kai PFZ do not extend into Unit-1, for some reason this small area was more susceptible to deformation, and therefore shows an imprint.

F. Anomaly 06 – Riverbeds

A pair of linear structures running near-parallel, heading downslope in a westerly direction from beyond the eastern boundary of WIN19M02.

Most of the characteristic of the A06 instances immediately match those attributed to longitudinal shear zones (henceforth: LSZs), but one concern that gave doubt to this conclusion was the apparent lack of scarps that are noted as a common feature.

A more thorough scrutiny of the seismic sections revealed their presence above both A06-a and -b, on the top slide surface, and thus the „Riverbeds” were firmly established as LSZs. The scarps themselves are miniscule, but they do have an imprint on either side of the first noticed and marked structures – the layers directly underneath the scarps have a slightly stronger amplitude signature resulting in an appearance of a pair of dotted, vertical lines cutting through Unit-1.

(Bull, Cartwright et al. 2009) refers to Prior et. al’s article „Depositional characteristics of a submarine debris flow” (1984), wherein they compared the zones enclosed between the longitudinal shears to chutes.

This is perhaps more obvious in the case of A06-b.

These chutes mark channels through which matter travels at a different velocity compared to material surrounding the LSZs.

G. Anomaly 07 – Cut and Anomaly 07-b – Ridge

It is clear that A07 and A07-b mark the northward termination of Unit-5.

Since U-5 seems to have progressed parallel to it, they were considered as elements of a lateral margin.

They do resemble a strike-slip fault on the variance map, and lateral pressure from the mass of U-5 might explain both the elevation shift seen in the „Cut” and the crumpled appearance of the „Ridge” – this would indicate material differences with downslope progress.

As the bottom layer is slightly elevated underneath parts of A07 and A07-b, they were also considered as ramps, but they are running parallel to the downslope direction, and are situated at the margin of Unit-5 – in all likelihood the transported mass would not have formed a ramp this way.

It also does not explain why the structures would have formed above them.

The disappearance of A07-b as it meets Unit-3 suggests it might have been partly eroded away by the progress of U-3. (Bull, Cartwright et al. 2009)

H. Anomaly 08 – Channels

There are a trio of continuous features found traversing the surveyed sediment.

They are sinuous, small channels cutting through the basal shear surface under U-4 and U-5, each the length of multiple kilometres.

The „Channels” also appear to follow each other in a sequence, but they do not align, (even allowing for the structures’ meandering).

None of them separate from the base, meaning they likewise dip downslope with it.

(Bull, Cartwright et al. 2009) attributes their formation to erosional scarring caused by translated blocks that were trapped underneath mass-transport complexes.

Indeed, at least in the case of A08-a a coherent block was found at the westward termination of this „Channel”.

All things considered, the A08 instances might be textbook examples of grooves on a basal shear surface. (Bull, Cartwright et al. 2009)

I. Anomaly 09 – Spike

This next feature is not so easily explained.

Although its appearance on a variance attribute map matches that of the A08 instances, the seismic sections reveal significant differences.

Most importantly, A09 is not restricted to the basal shear surface.

The „Spike” is elongated toward the transport direction of the main body of Unit-2, and vertically extends even beyond the entirety of U-2, both above and below it.

It is also not entirely dissimilar to longitudinal shears, but it has no „pair” and is inverted – LSZs consist of a duo of small depressions on the top layer of the mass transport complex, but A09 has a positive relief all the way to the seafloor.

As such, it is clearly not an erosive feature.

Anomaly 09 is not unique, but the selected instance is perhaps the most prominent.

The „Spike” can not be matched to the criteria of specific kinematic indicators, but considering that it does show the transport direction of its host sediment unit, A09 should not be dismissed.

One possible explanation for its presence might be lateral pressure. (Bull, Cartwright et al. 2009)

J. Anomaly 10 – Bump

Based on amplitude signatures, internal arrangement and variance- and RMS attribute maps A10 is indubitably a component of Unit-3, although it seems to have been detached from the main body.

A narrow divide betwixt the two has been described in Ch. V, 2) B/a.

There is a slight vertical displacement – towards the northwest, the „Bump” extends further from the rest of U-3.

The layer covering A10 at this area has very weak amplitude – after A10 has been exposed, the original top surface must have eroded.

However, at the southeastern terminus of the „Bump” structure, it falls short from the height of the main body.

While the isochron map shows this tendency, no elevation shift is visible on the basal surface, nor any discontinuities pointing towards faulting – the „Bump” simply seems to have a different distribution of materials than the rest of U-3.

Differential lateral pressure might explain the excess height on the north, with the aforementioned divide possibly serving as buffer, but not „thinner” part at the southeast.

The reason for this discrepancy remains undetermined.

K. Anomaly 11- Spots

The „Spots” are a group of sizeable fields contained in the main body of Unit-3.

None of them are pristine, their internal arrangement is slightly disorganised, at certain points somewhat fragmented even, but still considerably less so than the rest of U-3.

Their internal stratification even seems concordant with the basal shear surface, where visible. Above and below the „Spots” both the top and bottom surfaces of the mass-transport complex are notably less disturbed.

All of them seem elongated towards the transport direction of the main body.
The A11 instances fit the criteria for translated blocks. (Bull, Cartwright et al. 2009)

L. Anomaly 12 – Pipe

At the southernmost point of A12, (see Figure V-39) there is a small depression atop Unit-4.

On seismic sections, the „Pipe” is similar to the A08 – „Channels”, although the variance attribute map shows how different A12’s overall appearance is.

Its shape and location exclude the structure from the group of basal shear surface grooves.

As A12 continues toward the northwest, the structure divides into two „prongs”, one moving due north, and the other following the original heading.

It is reasonable to assume these elongated depressions were formed when an intact block was previously settled on top of Unit-4 began traversing the top surface and shortly after initiation, broke into two.

The northerly block travelled in a slightly erratic path.

U-4 is not otherwise significantly disturbed in the immediate vicinity.

Considering the lenticular shape of Unit-4, both objects have progressed locally downslope, despite not following the overall dipping of the study area.

Chapter V. 2) B/c mentions the presense of other blocks lending credence to the assumed development.

There is no indication of the object’s movement being linked to large-scale mass-transport.

M. Anomaly 13 – Hoofpick

Anomaly 13 is located on the southern boundary of Unit – 5, just northeast of the „Pipe”.

Examining the seismic sections revealed the physical traits of the structure are largely identical to those seen with A12.

The „Hoofpick” was formed when a small intact block became destabilised and broke apart shortly after it started to move.

Its path does not follow the general slope angle of the study area.

Once again, no connection can be established to mass-transport events.

Both A12 and A13 were measured against the criteria of kinematic indicators, (second order flow fabrics were considered) but it was eventually concluded they do not fit the mold. (Bull, Cartwright et al. 2009)

4) Summary

Six extensive deposits and thirteen sedimentary structures were identified during work on this thesis alongside one notable feature that remained unclassified (the „Calm”).

Comparison with researched data narrowed the list of relevant structures and helped identify the large sedimentary units.

Even though Horizon-03 appears fragmented, this is a result of the reflector lying atop a polygonal faulting zone – the Kai PFZ guided subsequent depositional patterns for a time

which is likely to have contributed to an instability of previous sediments lying atop Horizon 03 that may have resulted the depression U-1 settled into.

The earliest mass transport deposit in the study area is obviously Unit – 1, heading in a westerly direction following the dip of Horizon 03.

The basal shear surface is clearly present throughout the depression U-1 settled in, but there are no signs of it having significantly reworked its new environs.

The composing material has extremely low, almost transparent amplitude signature, and shows no fragmentation apart from the few intact, free blocks contained within.

For this reason, U-1 is deemed to be one of the glacial debris deposits described in Ch. III. 1) D/a – Lithostratigraphy, and Ch. VI. 1) Lithostratigraphical boundaries in the study area subchapters.

This, and the general characteristics of the strata between the Kai PFZ and Horizon 02 mark this facies as belonging to the Naust U unit.

Anomalies 03, 04 and 06 contained inside U-1 were as established as kinematic indicators. The composite image shown on Figure VI – 5 has been included to illustrate the shape and distribution of the kinematic indicators.

The attribute maps have been reused from Chapter V.

- A03 – Raindrop is identified (with some uncertainty) as a translated block aligned in a north-westerly direction
- A04 – Scars are a group of remnant blocks, since their effect on the deposition of adjacent material was noted – with the exception of the westward-pointing A04-e, all other instances of A04 are aligned NW
- A06 – Riverbeds are two longitudinal shear zones heading due west.

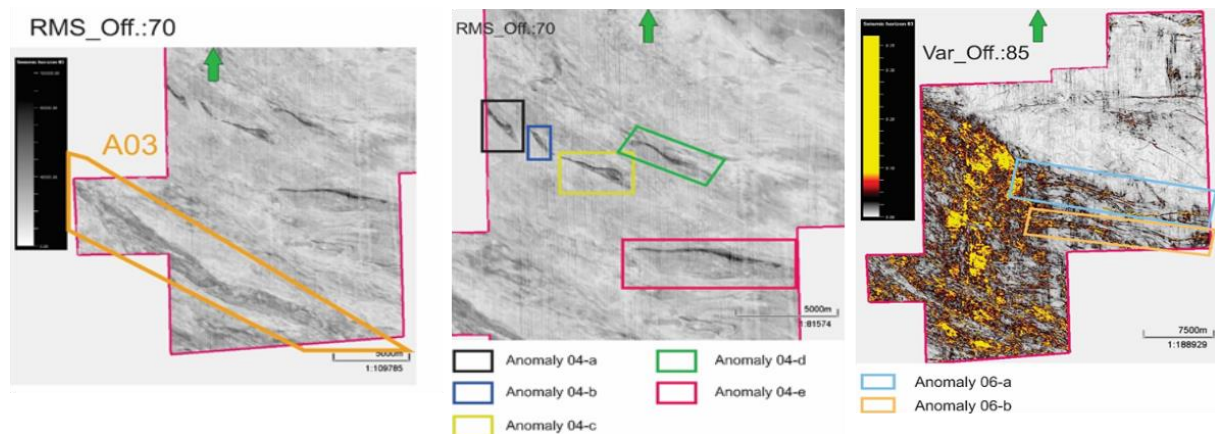


Figure VI-5 The kinematic indicators inside Unit-1 shown on attribute maps

The strata between Horizons 02 and -01 are more complicated.

Anomalies 08 and -11 are the only ones determined to be kinematic indicators – the “Calm” also would have been a guiding influence on the on the adjacent deposits.

Unit – 2 and U– 3 are concluded to be elements of the same mass-transport complex based on similar appearance on the attribute maps, heading and internal configuration.

The differences in the latter can be attributed to differential lateral compaction – with the

“Calm” lying betwixt the two, it makes sense that they would be affected differently.

U-3 also would likely have experienced added lateral pressure from the subsequent arrival of U-5.

Based on their internal arrangement, and material they match the criteria of landslide deposits and their location when matched map provided by Prof. Stefan Bünz (see *Fig VI-6* below), the U-2-3 pair are determined to be Sklinnadjupet material.

This places the strata between Horizons 02 and 01 in Naust S time.

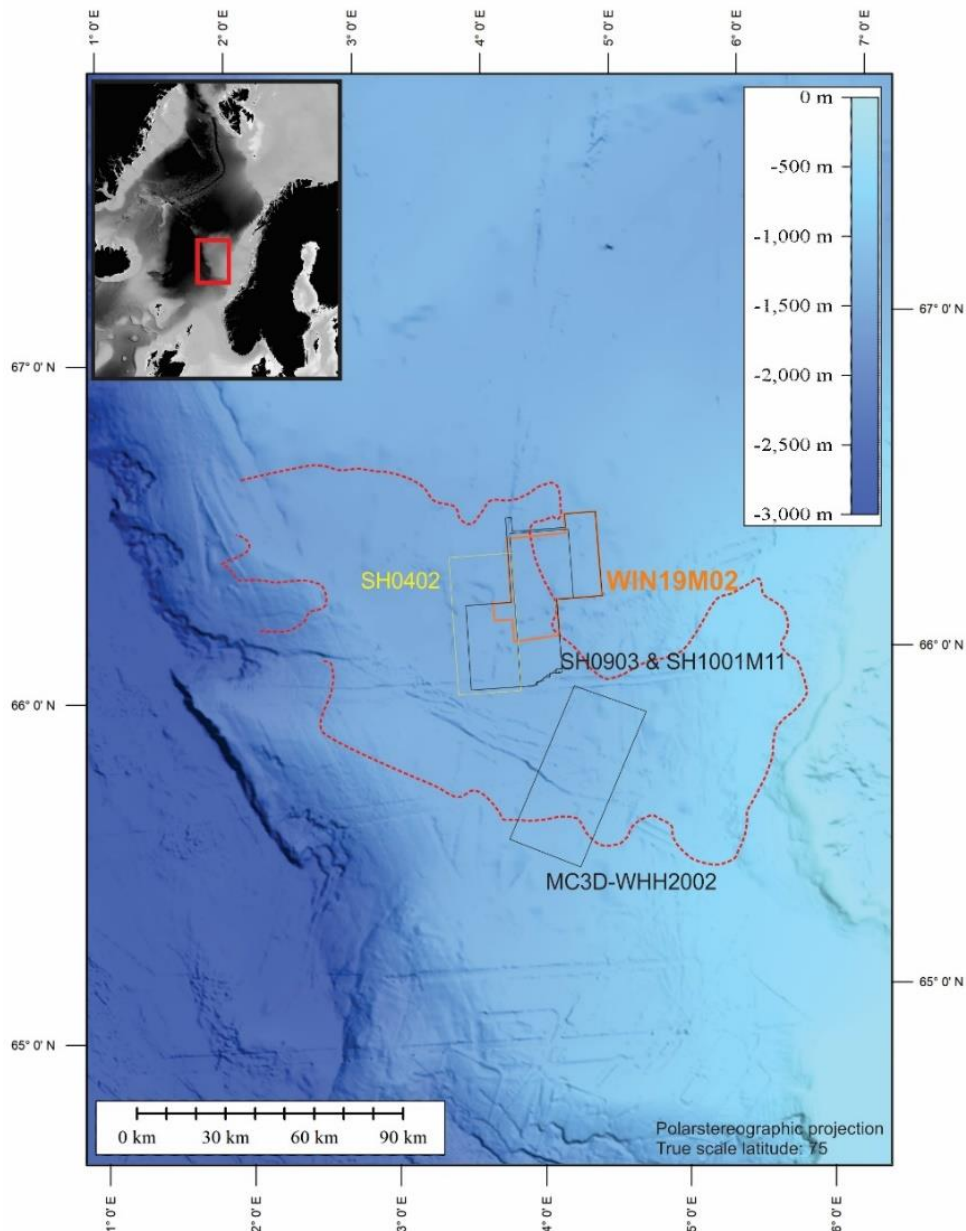


Figure VI-6 Once again, the map showing the location of the WIN19M02 seismic block in relation to the Sklinnadjupet slide

- The A11 instances are located within the main body of Unit-3. They have aligned to correspond with the heading of U-3 and since there are no

signs of the surrounding material having obstructed or reworked, these are judged to be translated blocks as well.

The instances of A08 partially underneath U-4 point towards U-4 being a mass-transport complex as well.

U-4's material resembles that of Unit-1, and its shape mark it as one of the glacigenic debris-flow lenses described by (Rise, Ottesen et al. 2006).

On the sides there are signs of having been slightly reworked by some foreign fragments indicate U-4 having migrated into the area before either U-3 or U-5.

This means that all instances of A08 arrived with U-4, regardless of their present location situated under U-5.

The sinuous westward path they take indicate this was the heading of U-4 as well.

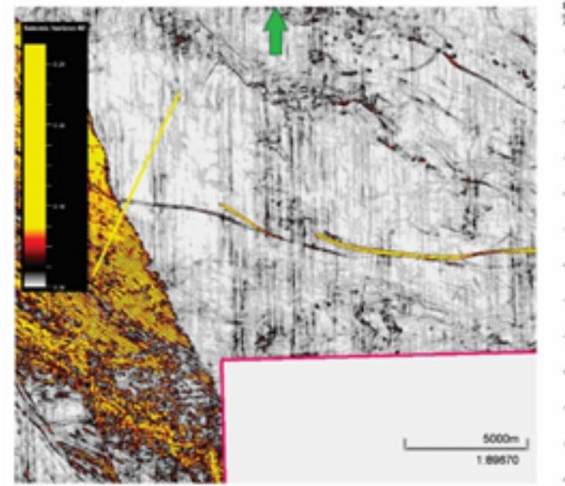


Figure VI-7 The “Channels” shown on a variance map

- The A08 – “Channels” have been described earlier as “textbook examples” of grooves on a basal shear surface

As mentioned before, Unit – 5 has surrounded U-4 on all directions. Its partial burying of U-4 and spreading out against U-3 on the south indicate Unit–5 has arrived after both.

The material of U-5 is discontinuous, and its mid-to-high frequency and relatively weak amplitude signature mark it as a landslide deposit.

No kinematic indicators have been identified in, or adjacent to U-5, but it clearly follows the general dip of Horizon 02.

Unit-6 has settled atop Units-3, -4 and -5 conclusively identifying it as the last major sedimentary unit amongst those examined.

No basal shear surface can be identified under U-6, immediately disqualifying it as a potential mass-transport complex, even though it is composed of discontinuous, low-amplitude material.

VII. Conclusion

In this thesis, a three-dimensional seismic data block was interpreted to study mass-transport deposits situated in the upper Naust strata of the Southern Vøring Margin. The major practical stages of the work process are listed below:

- The extent of the massive deposits present in the study area were subjected to morphological analysis.
- Several notable sediment structures inside or adjacent to the deposits were selected as representative examples
- The distinctive features of both the sediment structures and the deposits were documented and later matched against criteria researched

Based on the previous phases, a basic timeline of events was established:

- In Naust U times (-0.8-0.4 Ma), a glacial debris flow deposit covered most of the study area
- In the Naust S period (-0.4-0.2 Ma), first glacigenic debris migrated into the study area from the east. Second, material from the Sklinnadjupet slide arrived from the southeast, and drifted around a large block, giving the impression of two separate deposits following similar paths. Third, another, unidentified landslide deposit entered the area from the east, surrounding and partially burying the glacigenic deposit.
- Lastly, large portions of the mass-transport deposits were covered by unconsolidated material, covering much of their dramatic relief. Subsequently in Naust T times (-0.2 Ma+), the entire area was buried by fine-grained, evenly stratified sediments.
-

Although the polygonal faulting zones were identified in a manner sufficient to the needs of this work they would warrant a project of their own.

Their dimensions, material characteristics, and formation have not been examined in detail.

The deeper strata also fell beyond the scope of this thesis, but as mentioned in Chapter VI. preliminary observations revealed the presence of extensive fluid flow structures.

Additionally, some of the notable reflectors even further below are suspected to be volcanic sill intrusions.

There is plenty to discover left in the WIN19M02 dataset and it absolutely deserves further study.

This thesis might also have profited from lithological sampling and even the shallower strata it focuses on should be revisited if and when samples become available.

Unfortunately, wishes of recovered drill cores must remain a pipedream, for now.

VIII. References

Some repetitions may occur where the same reference was used for multiple chapters.

1) Chapter I:

No external references were used for Chapter I

2) Chapter II:

Knut Bjørlykke, et al. (2015). Geology of the Norwegian Continental Shelf. Petroleum Geoscience - From Sedimentary Environments to Rock Physics. K. Bjørlykke, Springer Berlin, Heidelberg: 603-637.

Mastrantonis, S. and V. Dubininkas (2022). "The next frontier: Human settlements in the marine environment." Futures **140**.

3) Chapter III:

Fjellaksel, T. (2012). 3D seismik analyse av rasavsetninger fra Sklinnadjupraset på midtre delen av Vøringmarginen. Fakultetet for Naturvitenskap og Teknologi - Institutt for Geologi. UiT - Munin, Universitetet i Tromsø - UiT. **Master's degree**: 119.

Johansen, R. (2010). 3D seismisk analyse av begravde rasavsetninger på den SV delen av Vøringmarginen. Det matematisk-naturvitenskapelige fakultet - Institutt for Geologi. UiT - Munin, Universitetet i Tromsø - UiT. **Master's degree**: 105.

Knut Bjørlykke, et al. (2015). Geology of the Norwegian Continental Shelf. Petroleum Geoscience - From Sedimentary Environments to Rock Physics. K. Bjørlykke, Springer Berlin, Heidelberg: 603-637.

Chand, S., et al. (2011). "Stratigraphic development of the south Vøring margin (Mid-Norway) since early Cenozoic time and its influence on subsurface fluid flow." Marine and Petroleum Geology **28**: 1350-1363.

Rise, L., et al. (2010). "Late Cenozoic geological development of the south Vøring margin, mid-Norway." Marine and Petroleum Geology **27**(9): 1789-1803.

Piper, D. J. W., et al. (2012). Controls on the distribution of major types of submarine landslides. Landslides - Types, Mechanisms and Modeling. J. J. Clague and D. Stead, Cambridge University Press: 95 - 107.

Shanmugam, G. (2018). Slides, Slumps, Debris Flows, Turbidity Currents, Hyperpycnal Flows, and Bottom Currents. Reference Module in Earth Systems and Environmental Sciences, Elsevier Reference Collection.

Rise, L., et al. (2006). "The Sklinnadjupet slide and its relation to the Elsterian glaciation on the mid-Norwegian margin." Marine and Petroleum Geology **23**(5): 569-583.

Bull, S., et al. (2009). "A review of kinematic indicators from mass-transport complexes using 3D seismic data." Marine and Petroleum Geology **26**(7): 1132-1151.

Berndt, C., et al. (2003). Polygonal Fault systems on the mid-Norwegian margin: a long-term source for fluid flow. Subsurface Sediment Mobilization. P. V. Rensbergen, R. R. Hillis, A. J. Maltman and C. K. Morley, Geological Society, London, Special Publications. **216**.

Cartwright, J. (2011). "Diagenetically induced shear failure of fine-grained sediments and the development of polygonal fault systems." Marine and Petroleum Geology **28**(9): 1593-1610.

Xia, Y., et al. (2022). "A Review of the Global Polygonal Faults: Are They Playing a Big Role in Fluid Migration?" Frontiers in Earth Science **9**.

Faktasider - Sokkeldirektoratet (sodir.no) - Norwegian Offshore Directorate FactPages
Wellbore: 6604/10-1 - Factpages - Norwegian Offshore Directorate (sodir.no)

4) Chapter IV

Chowdhury, K. R. (2014). Seismic Data Acquisition and Processing. Encyclopedia of Solid Earth Geophysics. H. K. Gupta, Springer Dordrecht: 1081-1097.

SEG Wiki - Society of Exploration Geophysicists.

5) Chapter V:

No external references were used for Chapter V

6) Chapter VI:

Berndt, C., et al. (2003). Polygonal Fault systems on the mid-Norwegian margin: a long-term source for fluid flow. Subsurface Sediment Mobilization. P. V. Rensbergen, R. R. Hillis, A. J. Maltman and C. K. Morley, Geological Society, London, Special Publications. **216**.

Bull, S., et al. (2009). "A review of kinematic indicators from mass-transport complexes using 3D seismic data." Marine and Petroleum Geology **26**(7): 1132-1151.

Chand, S., et al. (2011). "Stratigraphic development of the south Vøring margin (Mid-Norway) since early Cenozoic time and its influence on subsurface fluid flow." Marine and Petroleum Geology **28**: 1350-1363.

Rise, L., et al. (2006). "The Sklinnadjupet slide and its relation to the Elsterian glaciation on the mid-Norwegian margin." Marine and Petroleum Geology **23**(5): 569-583.

Rise, L., et al. (2010). "Late Cenozoic geological development of the south Vøring margin, mid-Norway." Marine and Petroleum Geology **27**(9): 1789-1803.

Xia, Y., et al. (2022). "A Review of the Global Polygonal Faults: Are They Playing a Big Role in Fluid Migration?" Frontiers in Earth Science **9**.

7) Chapter VII

No external references were used for Chapter VII

8) Illustrations

A. Chapter I:

No illustrations in this chapter

B. Chapter II:

II-1 <https://core2.gsfc.nasa.gov/research/lowman/lowman.html> by Dr. Paul D. Lowman Jr.

II-2 <https://www.submarinemap.com/>

C. Chapter III:

III-1 Map provided by Prof. Stefan Bünz

III-2 Bjørlykke Ch.25.03 with legend from Bjørlykke 25.02

III-3 Bjørlykke Ch.25.04

III-4 Bjørlykke Ch.25.10

III-5 Bjørlykke Ch.25.11

III-6 Shanmugam Fig. 16

III-7 Bull et al. – Fig. 6/B

III-8 Rise, Ottesen et al. 2006 – Fig. 1

III-9 Rise, Ottesen et al. 2006 – Fig. 10

Table 1. Shanmugam Table 1.

III-10 Bull et al. – Fig. 3

III-11 Xia, Yang et al. – Fig. 1

Table 2. Xia, Yang et al. – Table 1

III-12 Berndt et al. – Fig. 3/a

III-12 Xia, Yang et al. – Fig. 6/A

D. Chapter IV

IV-1 Chowdhury (Seismic Data Acquisition and Processing) Fig. 1.

Table 2. Data provided by Prof. Stefan Bünz

Table 3. Data provided by Prof. Stefan Bünz

E. Chapter V:

All included figures are generated for- and during work on WIN19M02 using the Petrel Software Package.

F. Chapter VI:

With the exception of Figure VI – 6, which has been provided by Prof. Stefan Bünz, all other images are reused assets from Chapter V. for- and during work on WIN19M02 using the Petrel Software Package.